DESIGN OF WAFFLE SLABS USING STRUT-AND-TIE MODEL

BY

Sunil Kumar G. Pillai

A Thesis Presented to the

DEANSHIP OF GRADUATE STUDIES

KING FAHD UNIVERSITY OF PETROLEUM & MINERALS

DHAHRAN, SAUDI ARABIA

In Partial Fulfillment of the
Requirements for the Degree of

MASTER OF SCIENCE

In

Civil Engineering

January 2011

KING FAHD UNIVERSITY OF PETROLEUM AND MINERALS
DHAHRAN 31261, SAUDI ARABIA

DEANSHIP OF GRADUATE STUDIES

This thesis, written by **SUNIL KUMAR G. PILLAI** under the direction of his Thesis advisor and approved by his Thesis committee, has been presented to and accepted by the Dean of Graduate Studies, in partial fulfillment of the requirements for the degree of **MASTER OF SCIENCE IN CIVIL ENGINEERING**.

Thesis Committee

Prof. Mohammed H. Baluch (Advisor)

Dr. Muhammad K. Rahman (Co-Advisor)

Dr. Ali H. Al-Gadhib (Member)

Prof. Husain J. Al-Gahtani (Member)

Dr. Maher A. Bader (Member)

Jan/22/2011

Dr. Nedal Ratrout
(Department Chairman)

Dr. Salam A. Zummo
(Dean of Graduate Studies)

29/1/11

Date

This thesis is dedicated to

My parents, wife and daughter

For their

Innumerable prayers, encouragement and patience

ACKNOWLEDGEMENTS

My thanks and gratitude goes first to God, for his endless blessings. Then, I would like to thank my advisor Dr. Mohammed Baluch, for his continued attention, guidance, and support. I greatly appreciate Dr Baluch for the invaluable time that he spent with me during my course as well as for the thesis work. I would like to express my sincere gratitude to Dr. M.K. Rahman, my co-advisor, for his guidance, efforts and insights throughout the study. I greatly appreciate him for his personal involvement in all phases of the thesis work. I also would like to thank the thesis committee members, Dr. Ali H. Al-Gadhib, Dr. Husain J. Al-Gahtani and Dr. Maher A. Bader, for their valuable suggestions and comments.

I am grateful to KFUPM for all the support I received during my course. I am thankful to all my professors who helped me to have a better understanding of the subject which made me more confident and helped me to complete the course and thesis work.

I am also grateful to Zamil Steel, my employer, for the flexibility in timings which made it possible to complete the course as a part time student.

TABLE OF CONTENTS

ACKNOWLEDGEMENTS ..... **IV**

TABLE OF CONTENTS ..... **V**

LIST OF TABLES ..... **XI**

LIST OF FIGURES ..... **XII**

NOMENCLATURE ..... **XV**

THESIS ABSTRACT ..... **XIX**

ملخص رسالة ..... **XX**

CHAPTER 1 1

INTRODUCTION **1**

1.1 BACKGROUND AND NEED OF THE RESEARCH 1
1.2 OBJECTIVES OF THE RESEARCH 2
1.3 SCOPE OF THE RESEARCH 3
1.4 OVERVIEW OF TYPES OF CONCRETE SLABS 4
1.5 WAFFLE SLAB SYSTEM (TWO WAY RIBBED SLAB) 7
1.6 STRUT-AND-TIE MODELING (STM) 10
1.7 ORGANIZATION OF THESIS 12
1.7.1 Section 1: Literature Review 12
1.7.2 Section 2: Validation of Strut-and-Tie Model Using ANSYS 13
1.7.3 Section 3: Develop Software STWAF 13
1.7.4 Section 4: Comparison of the STM Model to Other Design Methods 13
1.7.5 Section 5: Parametric Study of Waffle Slabs Using SWAF 13

CHAPTER 2 LITERATURE REVIEW 14

2.1 ULTIMATE STRENGTH AND EXPERIMENTAL DATA FOR WAFFLE SLABS 14
2.2 STRENGTH AND STRESS-STRAIN RELATIONSHIPS OF CONCRETE AND REINFORCEMENT 17
2.2.1 Tension Capacity of Concrete 17
2.2.2 Stress-Strain Relationships of Concrete 17
2.2.3 Compression Strength of Softened Concrete 18
2.2.4 Stress-Strain Relationships of Reinforcement 19
2.3 STRUT-AND-TIE MODELING OF CONCRETE 21
2.3.1 Bernoulli's Hypothesis and St.Venant's Principle 21
2.3.2 Strut-and-Tie Model for Deep Beams and Mode of Failure 22
2.3.3 Truss Analogy for Design of B-Region 23
2.3.4 Compression Field Theory 23
2.3.5 Modified Compression Field Theory 24
2.3.6 Components of Strut-and-Tie Model 26
2.3.6.1 Struts 26
2.3.6.2 Ties 27
2.3.6.3 Nodes 30
2.3.7 The Strut-and-Tie Method for Analysis and Design 33
2.4 CLASSICAL METHODS FOR DESIGN OF WAFFLE SLABS 38
2.4.1 Equivalent Thickness Method 38
2.4.2 Orthotropic Plate Theory 39
2.4.3 ACI Approach 40
2.4.4 Numerical Methods 41
2.5 DEFICIENCIES OF CURRENT METHODS FOR DESIGN OF WAFFLE SLABS 41
2.5.1 Equivalent Thickness Method 41
2.5.2 Orthotropic Plate Theory 41
2.5.3 ACI Approach 41
2.5.4 Numerical Methods 42

2.6 ACI PROVISIONS FOR DESIGN OF WAFFLE SLABS 42
2.6.1 General Provisions for Waffle Slab 42
2.6.2 Strength of Struts, Ties and Nodal Zones 43
2.6.2.1 Struts 43
2.6.2.2 Ties 44
2.6.2.3 Nodes 44

CHAPTER 3 STRUT-AND-TIE MODEL (STM) FOR SIMPLY SUPPORTED WAFFLE SLAB 45

3.1 DEVELOPMENT OF TRUSS MODEL FOR WAFFLE SLAB 45
3.2 PROPOSED STRUT-AND-TIE MODEL FOR WAFFLE SLAB 47
3.3 CALCULATING PROPERTIES OF MEMBERS OF THE PROPOSED MODEL 50
3.3.1 Top Chord 50
3.3.2 Bottom Chord 51
3.3.3 Vertical Members 51
3.3.4 Diagonal Members 52
3.3.5 Bracing Members 52
3.4 APPLYING LOADS TO THE PROPOSED MODEL 53
3.5 CALCULATING STRENGTH AND STRESS RATIO OF ELEMENTS OF THE MODEL 53
3.5.1 Top Chord 54
3.5.2 Bottom Chord 54
3.5.3 Vertical Members 54
3.5.4 Diagonal Members 55
3.5.5 Bracing Members 55
3.5.6 Nodes 56

CHAPTER 4 VALIDATION OF WAFFLE SLAB STM USING ANSYS 57

4.1 EXPERIMENTAL DATA USED FOR VALIDATION OF PROPOSED MODEL 57
4.1.1 Description of Waffle Slabs Used for Experiment by Abdulwahab and Khalil 57
4.1.2 Experimental Results 58
4.2 LINEAR MODEL TO FIND ALLOWABLE SAFE LOAD AS PER ACI-318 62
4.2.1 Element Type and Material Models 62
4.2.2 Application of Loads 63
4.2.2.1 Self Weight 63
4.2.2.2 Concentrated Load 63
4.2.3 Results of Linear Analysis Using STAAD 63
4.3 PREDICTING ULTIMATE LOAD CAPACITY OF SLAB USING NONLINEAR ANSYS MODEL 65
4.3.1 Material Models Used for Non-linear Truss Model 65
4.3.1.1 Concrete Used for Top Chord Members and Bracing 65
4.3.1.2 Concrete Used for Diagonal Members 67
4.3.1.3 Concrete used for Vertical Tension ties 68
4.3.1.4 Steel Used as Bottom Chord Reinforcement 68
4.3.1.5 Efficiency Factors Used for Non Linear Model 70
4.3.2 Element Type and Element Property 70
4.3.3 Application of Loads 71
4.3.4 Deflected Shape and Force Distribution 71
4.4 COMPARING RESULTS FROM STRUT-AND-TIE MODELS WITH TEST RESULTS 74
4.4.1 Strength of Slabs 74
4.4.2 Mode of Failure 77
4.4.3 Time-History Post Processing -Load Deflection Curves 81
4.4.4 Time-History Post Processing -Load Distribution between Ribs 85

CHAPTER 5 STWAF ANALYSIS AND DESIGN TOOL FOR WAFFLE SLABS 91

5.1 INTRODUCTION 91
5.1.1 Design Methodology Used in STWAF 91
5.1.2 Salient Features of STWAF 92
5.2 USER INPUTS IN STWAF 95
5.3 GENERATION OF 3D TRUSS MODEL AND ITS ANALYSIS 101
5.4 CALCULATING MAXIMUM FORCES, STRENGTH AND STRESS RATIO FOR EACH MEMBER TYPE 101
5.5 DESIGN OF ELEMENTS AND NODAL ZONES OF STRUT-AND-TIE MODEL 103
5.6 DEFLECTION OF WAFFLE SLABS 105
5.7 EXAMPLE OF STRENGTH PREDICTION PROCESS USING PROPOSED STM 107
5.7.1 Details of Waffle slab Used as Example 108
5.7.2 Trial Values Assumed for Design 108
5.7.3 Calculation for Geometry of the Truss 108
5.7.4 Calculation of Size of Elements and Nodes of the 3D Truss Model 109
5.7.4.1 Bottom Chord 109
5.7.4.2 Top Chord 109
5.7.4.3 Vertical Members 110
5.7.4.4 Diagonal Members 110
5.7.4.5 Bracing Members 111
5.7.5 Load Distribution to Nodes of Truss Model 111
5.7.6 Generation of STAAD Input and Output Files 111
5.7.7 Calculation of Strength and Stress Ratio of Elements and Nodes 112
5.7.7.1 Bottom Chord 113
5.7.7.2 Top Chord 113
5.7.7.3 Vertical Members 113
5.7.7.4 Diagonal Members 113
5.7.7.5 Bracing Members 114
5.7.8 Results and Prediction of Mode of Failure 114

CHAPTER 6 PROPOSED STM VERSUS OTHER DESIGN METHODS FOR WAFFLE SLABS 115

6.1 DETAILS OF THE 9M * 9M SLAB USED FOR COMPARISON OF DESIGN METHODS 115
6.2 DESIGN OF 9M * 9M WAFFLE SLAB BY STRUT-AND-TIE METHOD USING STWAF 117
6.3 DESIGN OF 9M * 9M WAFFLE SLAB WITH SAFE PROGRAM 124
6.4 DESIGN OF 9M * 9M WAFFLE SLAB BY ORTHOTROPIC PLATE THEORY 126
6.5 COMPARISON OF MAIN REINFORCEMENT FOR DIFFERENT METHODS 133

CHAPTER 7 PARAMETRIC STUDY OF ACI PROVISIONS FOR WAFFLE SLABS USING STWAF 134

7.1 DETAILS OF THE 10M * 10M SLAB USED FOR PARAMETRIC STUDY 134
7.2 EFFECT OF RIB SPACING 134
7.3 EFFECT OF RIB DEPTH 137
7.4 EFFECT OF RIB THICKNESS 140
7.5 EFFECT OF EFFECTIVE COVER 143

CHAPTER 8 SUMMARY, CONCLUSIONS AND RECOMMENDATIONS 147

8.1 SUMMARY 147
8.2 CONCLUSIONS 148
8.3 RECOMMENDATIONS FOR FUTURE STUDY 150

REFERENCES 151

VITA 156

LIST OF TABLES

TABLE 4.1: Geometry of Experimental Waffle Slabs 59
TABLE 4.2: Experimental Results 60
TABLE 4.3: Efficiency Factors Used for Strut-and-Tie Elements and Nodes 70
TABLE 4.4: Comparison of Results of STM Models with Test Results 75
TABLE 4.5: Mode of Failure for Slab S1 78
TABLE 4.6: Mode of Failure for Slab S2 78
TABLE 4.7: Mode of Failure for Slab S3 79
TABLE 4.8: Mode of Failure for Slab S4 79
TABLE 4.9: Mode of Failure for Slab S5 80
TABLE 4.10: Mode of Failure for Slab S6 80
TABLE 5.1: Load Distribution to Nodes of the Truss Model 112
TABLE 5.2: Forces, Strength and Stress Ratios of Elements and Nodes 114
TABLE 6.1: Comparison of Main Reinforcement for Different Methods 133
TABLE 7.1: Effect of Rib Spacing - Stress Ratios of Various Elements of the Model . 137
TABLE 7.2: Effect of Rib Depth - Stress Ratios of Various Elements of the Model 140
TABLE 7.3: Rib Thickness - Stress Ratios of Various Elements of the Truss Model ... 143
TABLE 7.4: Effective Cover - Stress Ratios of Various Elements of the Model 146

LIST OF FIGURES

Figure 1.1: Slab, Beam and Girder System 5
Figure 1.2: Flat Plate and Flat Slab 6
Figure 1.3: One-way Ribbed Slabs 6
Figure 1.4: Plastic Moulds for Waffle Slabs 8
Figure 1.5: Waffle Slab Under Construction 9
Figure 1.6: Waffle Slab After Construction 9
Figure 1.7: Strut-and-Tie Model for Deep Beam 12
Figure 2.1: Typical Stress-Strain Curve for ASTM 615 Grade 60 steel 21
Figure 2.2: Mode of Failure of Deep Beams, (MacGregor, 1997) 22
Figure 2.3: Truss Analogy (MacGregor, 1997) 24
Figure 2.4: Stress-Strain Relationships for Cracked Concrete (Collins et al. 1996) 26
Figure 2.5: Idealized Stress Fields in Struts: (a) Prismatic (b) Bottle-shaped (c) Fan-shaped (Adapted from Schliach et al. 1987). 29
Figure 2.6: Typical Stress-Strain Relationship for Concrete in Uni-axial Compression and the Idealization Used in the STM. 29
Figure 2.7: Effective Width of Tie 30
Figure 2.8: Basic Node Types: a) CCC b) CCT c) CTT d) TTT 31
Figure 2.9: Examples of Shape Idealization of a Nodal Zone with Four Struts Intersecting: a) Force Acting on the Node b) Simple Shape c) Hydrostatic Shape d) Modified Hydrostatic Shape. 32
Figure 2.10: Effective Width of Slab (ACI-318, 2008) 43
Figure 3.1: Test Slab – Finite Element Model 46
Figure 3.2: Proposed 3D strut-and-Tie Model 48
Figure 3.3: STM Model for Single Rib– Even and Odd Number of Waffle Openings 48
Figure 3.4: STM Model-Top Bracing 49
Figure 3.5: Calculating Width of Strut for Diagonal Members 53
Figure 4.1: Geometry of Waffle Slabs, Loading Arrangement, and Reinforcement Details 59
Figure 4.2: Crack Pattern for Experimental Slabs S1-S4 61

Figure 4.3: STAAD Model for Slab S2-Geometry 64
Figure 4.4: STAAD Model for Slab S2-Showing Axial Force Distribution in One Rib .. 64
Figure 4.5: Stress Strain Curve Used for Concrete in Top Chord Strut - Slab S1 67
Figure 4.6: Stress Strain Curve Used for Concrete in Diagonal Strut - Slab S1 68
Figure 4.7: Stress Strain Curve Used for Steel Reinforcement 69
Figure 4.8: ANSYS Model for Slab S1-Showing Deflected Shape 72
Figure 4.9: ANSYS Model for Slab S1-Showing Force Distribution 73
Figure 4.10: Comparison of Results - STM with Test Results -Slabs S1 to S4 (Effect of Rib Spacing) 76
Figure 4.11: Comparison of Results - STM with Test Results -Slabs S6, S2 and S5 (Effect of rib size) 76
Figure 4.12: Load-Deflection Curves for Slabs S1 82
Figure 4.13: Load-Deflection Curves for Slabs S2 82
Figure 4.14: Load-Deflection Curves for Slabs S3 83
Figure 4.15: Load-Deflection Curves for Slabs S4 83
Figure 4.16: Load-Deflection Curves for Slabs S5 84
Figure 4.17: Load-Deflection Curves for Slabs S6 84
Figure 4.18: Force in Bottom Reinforcement at Center of Ribs-Slab S1 88
Figure 4.19: Force in Bottom Reinforcement at Center of Ribs-Slab S2 88
Figure 4.20: Force in Bottom Reinforcement at Center of Ribs-Slab S3 89
Figure 4.21: Force in Bottom Reinforcement at Center of Ribs-Slab S4 89
Figure 4.22: Force in Bottom Reinforcement at Center of Ribs-Slab S5 90
Figure 4.23: Force in Bottom Reinforcement at Center of Ribs-Slab S6 90
Figure 5.1: Flow Chart for STWAF 94
Figure 5.2: Main Window of STWAF 96
Figure 5.3: General Input Window 96
Figure 5.4: Input Window for Overall Size of Waffle Slab 97
Figure 5.5: Input Window for Rib Size and Spacing 97
Figure 5.6: Window for Reinforcement Details and Depth of Compression Block 99
Figure 5.7: Window for Load Input 100
Figure 5.8: Display of Member Force for Bottom Chord in X-direction 102

Figure 5.9: Design of Bottom Reinforcement 104
Figure 5.10: Design Summary Showing Stress Ratios for All Types of Elements 104
Figure 5.11: STWAF – Deflection of Waffle Slab 106
Figure 5.12: Arrangement of Ribs- 9m * 9m slab 107
Figure 5.13: STAAD Pro Strut-and-Tie Model - 9m * 9m Slab 112
Figure 6.1: Arrangement of Ribs- 9m * 9m slab 116
Figure 6.2: Strut-and-Tie Model for 9m * 9m Slab 118
Figure 6.3: Size of struts-Strut-and-Tie method for 9m * 9m Slab 118
Figure 6.4: Properties of elements-Strut-and-Tie method for 9m * 9m Slab 119
Figure 6.5: Design of Bottom Chord-Strut-and-Tie method 119
Figure 6.6: Design of Top Chord-Strut-and-Tie method 120
Figure 6.7: Design of Diagonal Strut-Strut-and-Tie method 120
Figure 6.8: Design of Vertical Tie-Strut-and-Tie method 121
Figure 6.9: Design of Node at Bottom-Strut-and-Tie method 121
Figure 6.10: Design of Node at Top-Strut-and-Tie method 122
Figure 6.11: Design of Node for Vertical Member-Strut-and-Tie Method 122
Figure 6.12: Design Summary Strut-and-Tie method for 9mx9m Slab 123
Figure 6.13: Deflected Shape by SAFE 124
Figure 6.14: Bending Moment/meter by SAFE 125
Figure 6.15: Reinforcement in mm2/meter by SAFE 125
Figure 7.1: Effect of Rib Spacing on the Load Carrying Capacity 136
Figure 7.2: Effect of Rib Depth on the Load Carrying Capacity 139
Figure 7.3: Effect of Rib Thickness on the Load Carrying Capacity 142
Figure 7.4: Effect of Concrete Cover on the Load Carrying Capacity 145

NOMENCLATURE

ABBREVIATIONS

AASHTO	American Association of State Highway and Transportation Officials
ACI	American Concrete Institute
ASTM	American Society for Testing and Materials
CAST	Computer Aided Strut-and-Tie
CRSI	Concrete Reinforcing Steel Institute
LFRD	Load and Resistance Factor Design
MCFT	Modified Compression Field Theory
STM	Strut-and-Tie Model

ENGLISH AND GREEK SYMBOLS

a Depth of equivalent stress block defined as per ACI-318

A_{cs} Cross-sectional area of a strut

A_{nz} Cross-sectional area of nodal zone at its face, perpendicular to line of action of force

A_s Area of steel

A_{ts} Area of tensile steel reinforcement

C Compressive force in concrete

d Effective depth of a waffle slab , measured from the extreme compression fiber to the centroid of longitudinal tension reinforcement

E_c Tangent or secant modulus of elasticity of concrete

E_s Modulus of elasticity of steel

f Stress in concrete at a given strain ε

f_0 28 days cylindrical compressive stress in concrete

f_1 Average principal tensile stress in concrete

f_2 Average principal compressive stress in concrete

f_{ce} Effective compressive strength of concrete

f_{cr} Cracking strength of concrete

f_{ct} Direct tensile capacity of concrete

f_{cu} stress limit of a strut known as effective strength

f_{tc} Effective tensile strength of concrete

f_{tu} effective capacity of a tie

f_y Specified yield strength of reinforcement in tension or compression.

f'_c Specified compressive strength of concrete

f'_{ce} Softened compressive strength of concrete

F_n Nominal strength of STM element

F_{nn} Nominal compressive strength at face of nodal zone

F_{ns} Nominal compressive strength of strut

F_{nt} Nominal strength of Tie

F_u Factored force acting in STM element

h Overall depth of waffle slab

h_e Equivalent thickness of a waffle slab as per CRSI recommendation

I	Cross-sectional moment of inertia
M_n	Nominal flexural strength
P_{crack}	Test load at which the first crack appear in waffle slab test specimen
$P_{u\text{-}Test}$	Failure load reported in experiment for waffle slab test specimen
S	Rib spacing of waffle slab
t	Top slab thickness of waffle slab
V_c	Nominal shear strength provided by concrete
W	Rib thickness of waffle slab
W_s	Width of strut
W_t	Effective width of tie
α	Angle of inclination of bracing member with X-axis
β_t	Strength reduction factor for tensile strength of concrete tie
β_n	Strength reduction factor to account for effect of cracking on effective compressive strength of nodal zone
β_s	Strength reduction factor to account for effect of cracking on effective compressive strength of strut
Δ	Deflection of waffle slab at center of slab by Orthotropic plate theory
ε_0	Strain at ultimate stress
ε_1	Principal average tensile strain
ε_2	Principal average compressive strain
ε_c	Compressive strain in uniaxial compressive stress-strain curve of concrete, also compressive strain in stress-strain curve of a strut

ε_{cu} Strain at ultimate in uniaxial compressive stress-strain curve of concrete

ε_u Strain at failure

ϕ Strength reduction factor

ν Effectiveness factor

θ Angle between the strut and the adjoining tie

Ω Over-strength factor for bottom reinforcement

THESIS ABSTRACT

Full Name	**Sunil Kumar G Pillai**
Title of Study	**Design of Waffle Slabs Using Strut-and-tie Model**
Major Field	**CIVIL ENGINEERING (STRUCTURES)**
Date of Degree	**January 2011**

Multi storey buildings with waffle slabs as concrete floor and roof systems are very common in Saudi Arabia and in many parts of the world. Because of the complex geometry of intersecting ribs, the analysis and design of waffle slab is not easy. Current design methods neglect the existence of ribs and treat the slabs as solid slabs and are approximate in nature. Finite element based methods are also used for design of waffle slabs. Strut-and-tie model is being used increasingly for analysis and design of concrete structures with pronounced D-regions. With a grid of intersecting ribs, waffle slab essentially forms a D-region. This thesis presents a new approach based on strut-and-tie method for analysis and design of waffle slabs. A three dimensional strut-and-tie model is proposed for analysis and design of simply supported waffle slabs and to predict the strength and corresponding mode of failure. The result obtained from proposed method, generated in ANSYS software and analyzed using its nonlinear analysis features, is compared with experimental results from literature. The strut-and-tie model is in good agreement with experimental results for all configurations of simply supported waffle slabs, whether the mode of failure is flexural, shear or slip bond failure, and it can be employed for the design of waffle slabs. A Visual Basic based user friendly software "STWAF" has been developed for analysis of the 3D truss model using STAAD and for the design based on ACI-318-05 recommendations for waffle slabs using the proposed strut-and-tie method. Parametric studies conducted using STWAF shows that ACI code provisions for the rib dimensions and spacing of waffle slab is done in such a way that the slab fails under flexure in case of overloading for spans up to 12m.

MASTER OF SCIENCE
KING FAHD UNIVERSITY OF PETROLEUM AND MINERALS
Dhahran, Saudi Arabia
January 2011

ملخص رسالة

الاسم الكامل **سونيل كومار جي بيلاي**

عنوان الدراسة **تصميم البلاطات الخرسانية ذات الاعصاب**

وباستخدام نموذج Strut-and-tie

التخصص **الهندسة المدنية (انشاءات)**

تاريخ **يناير 2011**

المبانى المتعددة الطوابق التى يستخدم فيها البلاطات الخرسانية ذات الاعصاب كأرضية خرسانية ونظم سقف شائعة جدا في المملكة العربية السعودية وفي أجزاء كثيرة من العالم. بسبب العملية المعقدة لالضلوع المتقاطعة ، وتحليل وتصميم البلاطات الخرسانية ذات الاعصاب ليست سهلة. طرق التصميم الحالية تهمل وجود الاضلاع وتتعامل مع البلاطات على انها بلاطات مصمتة وهو افتراض تقريبى. كما تستخدم أساليب العناصر المحدودة أساس لتصميم البلاطات الخرسانية ذات الاعصاب. نموذج Strut-and-tie يتم استخدامه على نحو متزايد لتحليل وتصميم المنشآت الخرسانية وضوحا مع مد المناطق. مع شبكة متقاطعة من أضلاعه. هذه الرسالة تعرض مقاربة جديدة تستند إلى نموذج Strut-and-tie لتحليل وتصميم البلاطات الخرسانية ذات الاعصاب. نموذج ثلاثى الابعاد Strut-and-tie يتم تقديمه لتحليل و تصميم البلاطات الخرسانية ذات الاعصاب والتنبؤ بقوة التحمل وشكل الانهيار . الحصول على نتيجة من الطريقة المقترحة ، ولدت في برنامج ANSYS وتحليلها باستخدام العناصر المحدودة، وبالمقارنة مع النتائج التجريبية من الأدب. نموذج Strut-and-tie في اتفاق جيد مع النتائج التجريبية لجميع تكوينات البلاطات الخرسانية ذات الاعصاب ، ما إذا كان الانهيار هو طريقة الانحناء ، القص أو زلة فشل السندات ، وأنه يمكن أن يكون البلاطات الخرسانية ذات الاعصاب. (أ) استنادا الأساسي المستخدم البصرية البرمجيات ودية "STWAF" وقد وضعت لتحليل نموذج الجمالون ثلاثى الابعاد باستخدام STAAD لتصميم وبناء على توصيات - 318-05 المجلس الدولي للمطارات البلاطات الخرسانية ذات الاعصاب باستخدام . نموذج Strut-and-tie . الدراسات المبدئية التي أجريت باستخدام STWAF يبين أن أحكام قانون المجلس الدولي للمطارات للأبعاد الضلع والمباعدة بين الولادات الهراء بلاطة هو الحال في مثل هذه الطريقة أن فشل بلاطة تحت الثنى في حالة الحمولة الزائدة ليمتد حتى 12 متر.

ماجستير العلوم

جامعة الملك فهد للبترول والمعادن

الظهران ، المملكة العربية السعودية

يناير 2011

CHAPTER 1

INTRODUCTION

1.1 BACKGROUND AND NEED OF THE RESEARCH

Multi storey buildings with waffle slabs as concrete floor and roof systems are very common in Saudi Arabia and in many parts of the world. Because of the complex geometry of intersecting ribs, the analysis and design of waffle slab is not easy. Current design methods neglect the existence of ribs and treat the slabs as solid slabs and are approximate in nature. Finite element based methods are also used for design of waffle slabs. Strut-and-tie model is being used increasingly for analysis and design of concrete structures with pronounced D-regions. With a grid of intersecting ribs, waffle slab essentially forms a D-region. The need for this research can be summarized as follows:

1. Conventional methods for the design of waffle slabs consider behavior for waffle-slab same as flat plate or flat slab. The effect of ribs, which are the primary load carrying elements, is ignored in the analysis and its effect on rigidity of the slab is arrived based on empirical formulae.
2. Empirical methods currently being used are not predicting the mode of failure of waffle slab accurately. Instead it restrict the parameters of the waffle such as rib spacing, rib depth, rib thickness etc. to bring the slab in a desirable range where the empirical equations are more or less applicable.

3. Effect of concentrated loads is not well addressed in current methods. The behavior of the waffle slab under load depends on the bearing area and location of concentrated load and there will be a local stress concentration near the load.
4. Strut-and-tie method has been used efficiently for analysis and design of complex structures with prominent D region.
5. Waffle slab is essentially a 3-D structure due to inter connectivity of the ribs in both directions. The close spacing of the ribs make the entire waffle slab as a D-region. Strut-and-tie method is widely used for structures with D-region where the stress flow is not uniform.
6. Strut-and-tie model serve a dual purpose. They allow description of essential aspects of structural behavior and at the same time provide useful tools for detailing and dimensioning. Strut-and-tie models assist the designer in determining size, the location, the distribution, and anchorage of main reinforcement.
7. Strut-and-tie model is extensively used for members in which shear is governing. For waffle slab also many configurations, such as larger depth of rib, larger spacing of ribs and smaller rib thickness, will result in shear critical structure. The main advantage of STM method is that it can handle all types of structures whether it is bending critical or shear critical.
8. STM method is not yet proposed for waffle slabs.

1.2 OBJECTIVES OF THE RESEARCH

The main objective of this research is to develop a STM for waffle slab and to develop user-friendly software for automated design of waffle slab using STM.

The specific objectives of this study include:

- Develop a three dimensional Strut-and-tie model for simply supported waffle slab.
- Comparison of the results of the STM model with experimental results from literature. Ultimate strength and mode of failure are of key interest.
- Compare results of STM method with conventional design methods for design of waffle slab
- Verify ACI limitations on size and spacing of ribs for design of waffle slabs with respect to strength and mode of failure predicted by the proposed method.

1.3 SCOPE OF THE RESEARCH

Primary scope of the research is to develop a new approach based on strut-and-tie method for analysis and design of waffle slabs. A three dimensional strut-and-tie model is proposed for analysis and design of simply supported waffle slabs and to predict the strength and corresponding mode of failure. The proposed model, generated in ANSYS software and analyzed using its nonlinear analysis features, is compared with experimental results from literature to validate the STM method.

Scope include developing a Visual Basic based user friendly software “STWAF” for analysis and design of the 3D truss model, considering ACI-318-05 recommendations for waffle slabs, using the proposed strut-and-tie method. Scope also include conducting parametric studies using STWAF for the rib dimensions and spacing of waffle slab and compare with corresponding ACI code provisions.

1.4 OVERVIEW OF TYPES OF CONCRETE SLABS

Structural reinforced concrete floor systems are one of the most popular systems and will effectively transfer vertical and lateral loads to the vertical supports. There are many types of concrete floors. One way slab, two way slab, flat plate, flat slabs, one way ribbed slabs and two way ribbed slabs or waffle slabs are the most common types. It is a normal practice to construct beams monolithically with the slab. Figure 1.1 shows a typical arrangement of this system. The main disadvantage of this system is the large depths of members which limits the floor to floor heights.

Flat plates and flat slab construction is popular due to its architectural advantage and smaller depth of structural members. However it can be used only for small spans due to large deflections and punching shear. Since larger spans needs more slab thickness, it is not economical. For larger spans, even with drop panel and column capital, as we provide in flat slab, the shear exceeds allowable limits for concrete which result in shear reinforcement at column slab connection. Figure 1.2 shows a typical arrangement of these systems.

One-way ribbed slabs are used to make the slabs stiffer which reduce deflections and can span more. Figure 1.3 shows a typical one way ribbed slab. This is widely used in pre-cast construction as modules of single T section or double T sections. Since ribs are spanning in one direction, size of ribs will be generally high and not as economical as two way ribbed slabs. Lateral load distribution perpendicular to rib direction is poor and is not good for seismic forces, with thin slabs.

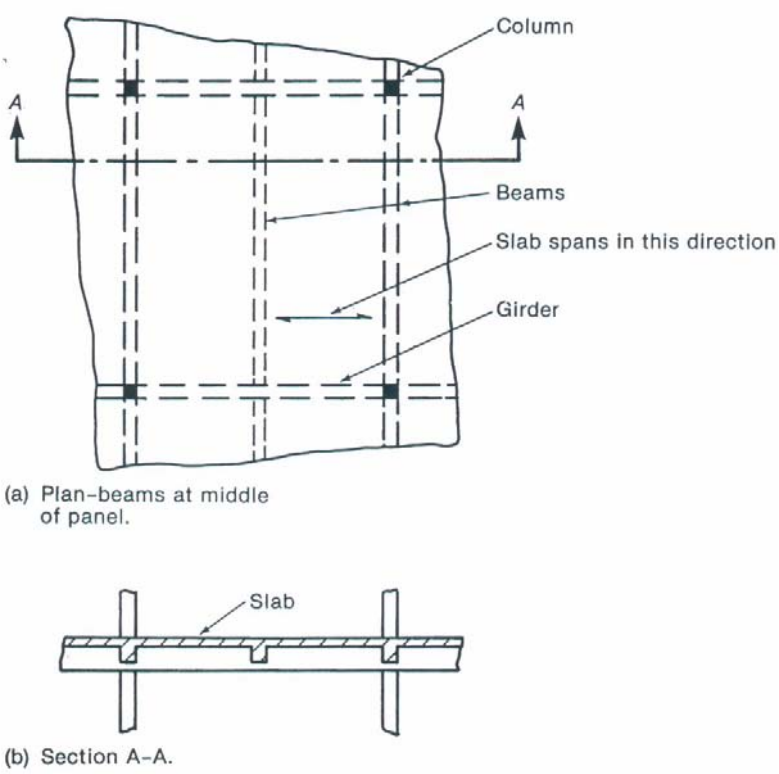

Figure 1.1: Slab, Beam and Girder System

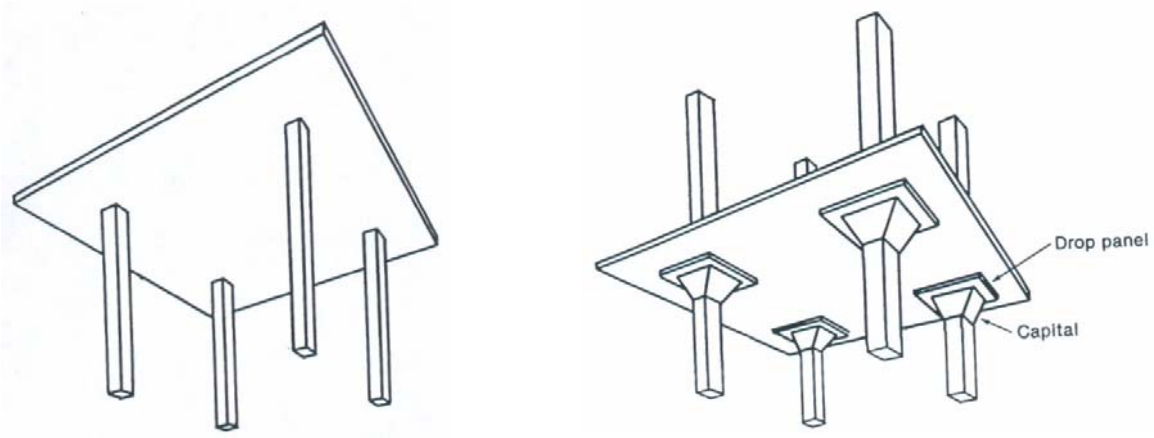

Figure 1.2: Flat Plate and Flat Slab

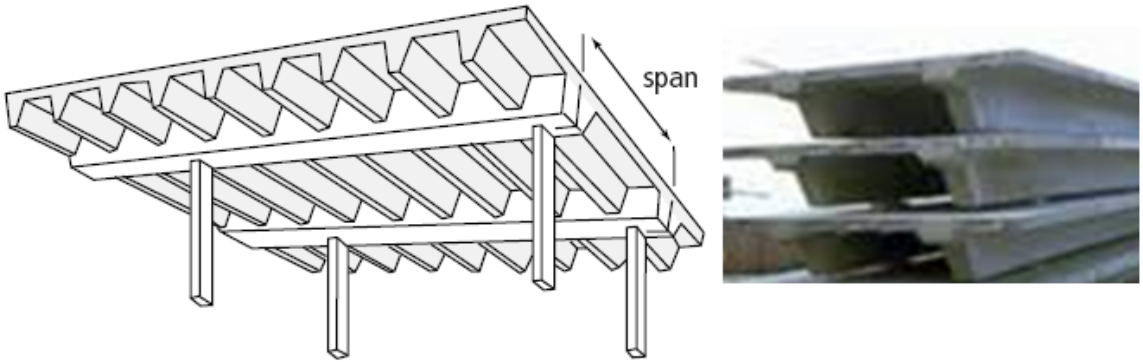

Figure 1.3: One-way Ribbed Slabs

1.5 WAFFLE SLAB SYSTEM (TWO WAY RIBBED SLAB)

Waffle slab results from the elimination of concrete below the neutral axis, which allows an economic increase on the total thickness of the slab with the creation of voids in a rhythmic arrangement. Therefore, there is a reduction on the structure self-weight and a more efficient use of materials, steel and concrete. Waffle slabs are the best option in situations, normally in the span range of six to twelve meters. The rib heights, spacing and slab thickness can be varied for optimum design. Waffle slab, also known as two-way ribbed flat slab or grid slab, is an economical and popular system in buildings and other types of structures. Its increased rigidity compared to weight makes it economical for medium span structures. Also inter connected ribs with slab on the top ensure efficient lateral distribution of loads. They exhibit higher stiffness and small deflection. Also the attractive exposed ceiling gives architectural advantage over other types of slabs. The openings between ribs at bottom of slab can be used for lighting fixtures. Waffle slab systems are commonly used in large auditoriums, parking garages, industrial facilities, marine structures and exhibition halls. Figure 1.4 shows a typical Waffle slab.

Apart from direct cost reduction in the slab, the reduction in self weight of waffle slabs and larger floor to floor heights contribute to reduction in size of columns and foundation cost in multi-story buildings. The re-usable plastic moulds and specially designed scaffolding, widely used for waffle slab construction, makes faster construction and reduces cost of form work in large scale construction.

Figure 1.4 shows a picture of plastic mould and specially designed scaffolding. Figure 1.5 shows picture of a waffle slab used for a parking garage under construction for Project Promenade (Owner : Keppel Puravankara), JP Nagar, Bangalore, India and Figure 1.6 shows picture after construction.

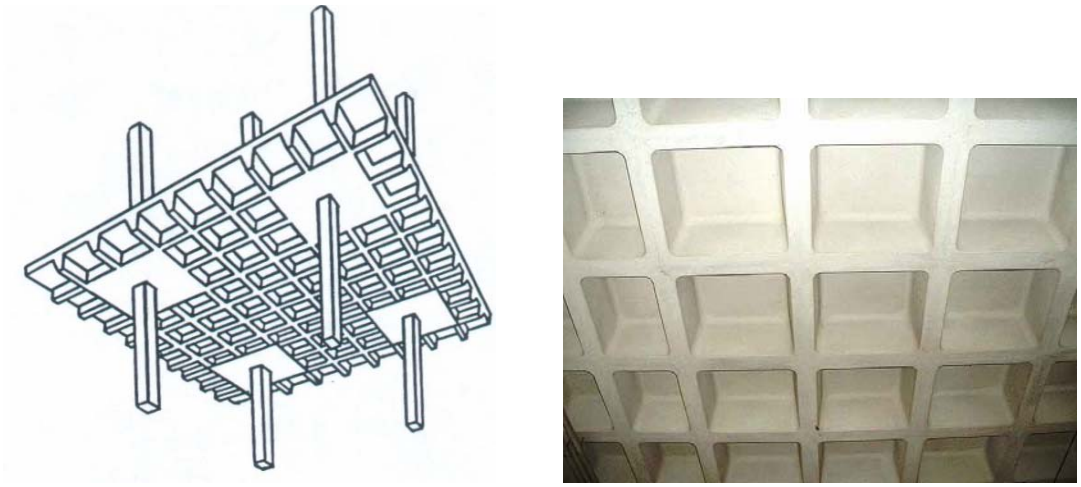

Figure 1.4: Plastic Moulds for Waffle Slabs

Figure 1.5: Waffle Slab Under Construction

Figure 1.6: Waffle Slab After Construction

Cost of plastic moulds is generally high and hence is not economical for small scale construction. The direct saving from material cost for waffle is partly nullified by the additional cost of moulds and special form work in case of small scale construction. Also for small spacing between columns as we do for residential buildings, there is not much advantage for the waffle slabs. The savings are significant and waffle slab has clear advantage over other types of slabs when we go for larger spans.

One of the reasons why designers hesitate to go for waffle slab is its complicated design procedure. The parameters of the slabs are restricted by codes and few design software's have the capability to handle the design of waffle slab. Also current design methods do not give a clear idea of the mode of failure.

1.6 STRUT-AND-TIE MODELING (STM)

Strut-and-tie Modeling is becoming an increasingly popular method for design and detailing of concrete structural members. STM is adopted in ACI 318 [1] in 2002. This method is proved to be very effective for structures with discontinuities where conventional methods fail to predict the exact behavior and ultimate load. Currently STM is widely used for a large number of structures like deep beams, corbels, pile caps etc. However the full potential of this method is not utilized yet, since it can be applied for a larger range of structures. In the current study, STM is applied for the design of waffle slabs. The whole waffle slab is a D-region due to its geometry.

In strut-and-tie modeling discrete representations of actual stress fields, resulting from the applied loads and support conditions, are considered and provides a static lower bound solution. The load carrying mechanism of a structural member is approximated by

means of struts representing the flow of compressive stresses, ties representing the flow of tensile stresses and nodal zones representing the point of intersection of struts and ties, which are subjected to multi-axial state of stress (Schlaich and Schäfer 1987) [2].

A strut-and-tie model (STM) consists of elements in pure tension or compression. Appropriate reinforcement must be provided in the portions of the structure where tension is indicated by the strut-and-tie model or where additional strength, confinement, or both, are required by the struts. By using a simple truss model, an estimation of strength of a structural element can be made and, the element can be appropriately detailed.

Even though Strut-and-tie modeling can be used for all portions of the structure, it is most useful as a design tool when applied to structures, or portions of structures, in which plane sections do not remain plane after the application of load. The behavior of such elements is not dominated by flexural deformations. The difficulty in analyzing these types of elements often arises from the inability to apply kinematic compatibility. STM disregards kinematic constraints. Overall equilibrium and equilibrium of the nodes are considered during the analysis stage. STM conforms to the lower bound theory of plasticity, which requires that only equilibrium and yield conditions be satisfied.

The capacity of a structure as estimated by a lower bound method will be less than, or at most equal to, the actual collapse load of the structure. The most appealing quality of a lower bound theory is its inherent conservatism. Strut-and-tie model is considered a rational and consistent basis for designing the cracked reinforced concrete structures. The successful application of a strut-and-tie model depends on a reliable visualization of the

path of the force flows. In a typical strut-and-tie analysis, the force distribution is visualized as compressive struts and tensile ties, respectively. Figure 1.7 provides a simple strut-and-tie model applied to a simply supported deep beam. One of the main advantages of the STM is its capacity to predict strength of shear critical structures.

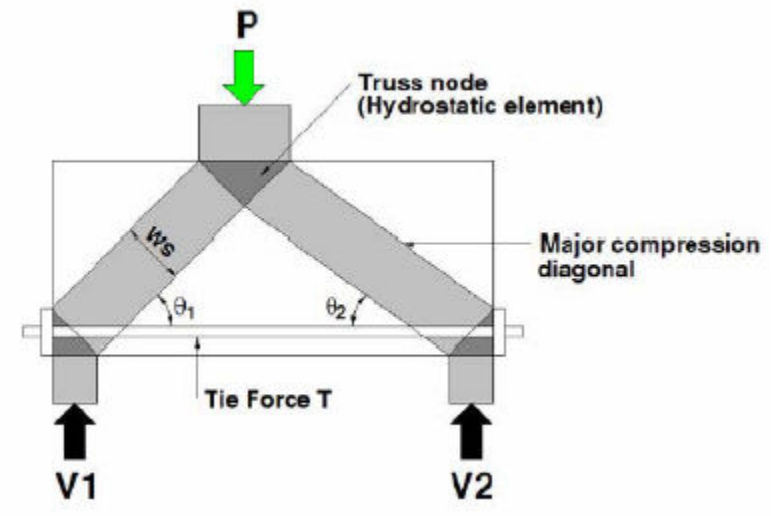

Figure 1.7: Strut-and-Tie Model for Deep Beam

1.7 ORGANIZATION OF THESIS

The research program has five major sections.

1.7.1 Section 1: Literature Review

A literature search has been conducted to obtain recent information regarding similar studies elsewhere. The literature search focused on the following areas:

- Experimental Data for simply supported waffle slabs
- Conventional methods for design of waffle slabs

- Strut-and-tie modeling of reinforced concrete elements

1.7.2 Section 2: Validation of Strut-and-Tie Model Using ANSYS

The important task in the thesis is to develop a strut-and-tie model for simply supported waffle slabs which predict the strength and mode of failure of experimental slabs from literature. The proposed strut-and-tie model is made in ANSYS [48], incorporating nonlinear material models, and a nonlinear analysis is performed for each of the experimental slabs. The results are compared with actual experimental data for strength and mode of failure.

1.7.3 Section 3: Develop Software STWAF

Geometrically waffle slab is a complicated structure and the proposed three dimensional STM consists of a large number of elements and nodes. Manual generation of the truss is time consuming and will limit the usage of the method. Hence user-friendly software dedicated for fully automatic generation of the 3D truss is developed.

1.7.4 Section 4: Comparison of the STM Model to Other Design Methods

Design of a 9m x 9m waffle slab is done with strut and tie method. The same slab is designed using the conventional design methods. The results are compared for the main bottom reinforcement at ribs keeping other parameters of the slab same.

1.7.5 Section 5: Parametric Study of Waffle Slabs Using SWAF

A parametric study is conducted using software STWAF for a 10m x 10m waffle slab and find the contribution of rib spacing, depth of ribs, thickness of ribs and concrete cover on strength and mode of failure. The ACI provisions on restriction of these parameters are compared with that predicted by STWAF.

CHAPTER 2

LITERATURE REVIEW

Literature search was done on the following areas.

1. Ultimate strength of waffle slab and experimental programs conducted for waffle slabs in the past to obtain test results.
2. Strength and stress-strain relations of concrete and steel
3. Strut-and-tie method for modelling concrete structures.
4. Design of waffle slabs by current design methods.

2.1 ULTIMATE STRENGTH AND EXPERIMENTAL DATA FOR WAFFLE SLABS

Information on the strength and behavior of reinforced concrete waffle slabs is very limited, but there have been a few theoretical and experimental investigations of waffle plates and slabs mostly in the elastic range (Timoshenko and Woinowsky-Krieger 1959 [3]; Bares and Massonnet 1966 [4]; Tebbet and Harrop 1979 [5]; Cusens and Pama 1981[6]; Kennedy and Iyengar 1982[7]).

Three load tests to destruction were made on the waffle slab roof of the Rathskeller Building in the Belgian Village exhibit at the 1964-65 New York World's Fair. Each load test was conducted at different portion of the same building to study the behavior of waffle slabs under gravity loads. The report published by

Magura and Corley, 1971[8 and 9] in ACI shows that the behavior of structure in general was in accord with existing theories. Flexural capacity was not reached in any of the test and structure failed in shear. Deflections were in good agreement with that computed from equivalent frame analysis.

Deflection characteristics of waffle panels have been studied experimentally and analytically by Xuerun Ji, Sheng-Jin Chen, Ti Huang, and Le-Wu Lu, 1986 [10]. Elastic finite element analysis was made to predict deflections. Large-scale tests have also been carried out on a limited number of slab models as part of the study to measure deflections under in plane and out of plane loading. However the study was limited up to cracking of concrete and ignored reinforcement. Based on the study they pointed out that the "equivalent thickness method", recommended by the Concrete Reinforcing Steel Institute Hand book (CRSI 1972), leads to over estimation of the torsional rigidity and under estimation of deflection under vertical loads. They recommends to reduce the equivalent thickness by 20 % to compensate the over estimation.

Tests on a large-scale model (approximately 1:3) of six panel waffle slab supported on twelve columns were conducted by Ajdukiewcz and Kliszczewicz, 1986 [11]. The results obtained from the test, location of the crack, mechanism of failure and the magnitude of destructive load are considered. Tests indicate that the main negative yield line is located comparatively far from the column face, and depends on the solid region around the column and the extension of top reinforcement. Recommendations on yield line patterns in waffle slab flat plate structures are also discussed.

Seismic load tests conducted on two story waffle plate structure by Mario E. Rodriguez, Sergio A. Santiago and Roberto Meli ,1995[12], proves the poor performance of waffle slab structure under seismic loading. They confirm that a satisfactory seismic behavior in terms of lateral stiffness and strength can be attained by the addition of bracing or structural walls.

Experimental study conducted by Hashim M.S. Abdulwahab and Mohammad H. Khalil , 2000 [13] on 1:4 scale specimens on waffle slabs with square lay-out of ribs also give useful information. They studied the impact of slab thickness, rib spacing, rib depth etc. on flexural rigidity and ultimate strength. The test results show that the first crack appeared at around 25-30 % of the ultimate strength. Also the specimens behave elastically for the first two stages, before and after the first crack appears. They applied an alternate approximate design method called "elemental disc analogy", based on "effective modulus of elasticity" for waffle slabs also. However they limited their study to simply supported waffle slabs.

A theoretical study was conducted by J Prasad, S. Chander and A.K. Ahuja (2005)[14] on "Optimum dimensions of waffle slab for medium size floors" on limited slab specimens, in the range of six to eight meter span. They used grid analysis using a FORTRAN program for analysis. The optimum dimensions for various configurations of waffle slabs were studied.

An experimental study conducted by P. F. Schwetz, F. P. S. L. Gastal and L. C. P. Silva on "Numerical and experimental study of real scale waffle slab" (2009)[15]. The objective of this work was to analyze the adequacy of a design method widely used in the modeling of waffle slabs, verifying if it represents the slab behavior

satisfactorily. A real scale waffle slab submitted to a load in a localized area was instrumented with strain gages and deflection gages for measuring specific strain and deflection in different points. The numerical analysis was made using a grid model. Tests showed a linear behavior, even though residual results could indicate cracking in some isolated sections. Numerically computed deflections presented a good estimate to test results and the experimental strains defined the presence of bending moments coincident with the forecasts of the theoretical model. However the study was limited to a stress range of the actual safe designed loads.

2.2 STRENGTH AND STRESS-STRAIN RELATIONSHIPS OF CONCRETE AND REINFORCEMENT

2.2.1 Tension Capacity of Concrete

Direct tensile strength of concrete is difficult to measure. Splitting tensile strength is generally measured to find the tensile strength of concrete. ACI 318-2008 recommends splitting tensile strength of normal weight concrete as $6.7(f'_c)^{1/2}$ in psi units, which in MPa units is $0.556(f'_c)^{1/2}$. Tensile strength of concrete is typically 8 to 15% of compressive strength.

2.2.2 Stress-Strain Relationships of Concrete

Generally all the experiments for concrete are limited to find the compressive strength of concrete, which is used for design of concrete structures. Because of various influencing factors and different conditions in experimental approaches, a general equation expressing the stress strain curve of concrete for all types of concrete has not been proposed yet.

An attempt was made to evaluate the stress strain relationship for concrete under uni-axial compression by Ali [16]. An experimental program was conducted to evaluate various parameters involved. Simple equation in the form of a polynomial was proposed as shown and was in good agreement with test results. This study does not consider tension softening since all test specimens were cylindrical specimens.

Strain at Ultimate stress,

$$\varepsilon_0 = 0.000875 \, (f_0)^{0.25} \tag{2.1}$$

Strain at failure,

$$\varepsilon_u = 0.0078 / (f_0)^{0.25} \tag{2.2}$$

Stress f, at a given strain ε is calculated by the formulae,

$$f = f_0 \, [2.1(\varepsilon/\varepsilon_0) - 1.33(\varepsilon/\varepsilon_0)^2 + 0.2(\varepsilon/\varepsilon_0)^3] \tag{2.3}$$

Where, f_0 is the 28 days cylindrical compressive strength of concrete.

An experimental study on stress-strain curve of concrete considering localized failure in compression was conducted by Watanabe [17]. One of the important factors for compressive stress strain curves of concrete is localization of failure. The stress strain curve of concrete strongly depends on the aspect ratio of concrete specimen and hence a unique stress strain curve is not adequate to express the softening behavior of concrete. To overcome the problem of localization of failure, a series of uni-axial compression tests were conducted. An equation for envelop curve involving a characteristic of compressive strength was also formulated.

2.2.3 Compression Strength of Softened Concrete

Cracked reinforced concrete can be treated as an orthotropic material with its principal axes corresponding to the directions of the principal average tensile and

compressive strains. Cracked concrete subjected to high tensile strain in the direction normal to the compression is observed to be softer than concrete in a standard cylindrical test. The phenomenon of strength and stiffness reduction is commonly referred to as compression softening. Park and Kuchma [18] conducted a study to predict shear strength of Deep beams using Strut-and-tie Model Analysis. Applying this softening effect to STM, it is recognized that the tensile straining perpendicular to the strut will reduce the capacity of concrete strut to resist compressive stresses. The softened concrete strength f'_{ce} can be determined by

$$f'_{ce} = \upsilon f'_c \tag{2.4}$$

Where, f'_c is the specified compressive strength based on cylindrical compressive test and υ is the efficiency factor of concrete.

ACI 318-2008 recommends the value of efficiency factor for bottle shaped struts without stirrup reinforcement as 0.6 for normal weight concrete. In an experimental study conducted to find the shear capacity of simply supported reinforced concrete deep beams using strut-and-tie method, Arabzadeh [19] concludes that the shear strength based on ACI strut-and-tie model is conservative.

2.2.4 Stress-Strain Relationships of Reinforcement

In the design of reinforced concrete steel structures, rebar properties do not need to be exactly known. ASTM A615 [20] only requires that yield stress of grade 60 bars need to exceed 60 ksi (414 Mpa). However for finite element analysis of the structure an actual value of yield stress, ultimate stress and stress strain relation is required to predict exact structural response.

Malvar and Crawford [21] conducted a study on Dynamic Increase Factors for Steel reinforcing bars. As part of the study, they collected the experimental data from various sources for different grades of steel for static properties of reinforcing steel. A typical stress strain curve for grade 60 bars is as shown in Figure 2.1.

Mirza and MacGregor [22] conducted extensive experimental study on reinforcing steel bars of different grades. Based on the study for US made Grade 60 (Fy = 60 ksi) bars (1356 tests), they concluded that the average yield strength is 69 ksi and Ultimate strength is 109 ksi. The average value of modulus of elasticity was 200 GPa.

ASTM A615 requires a minimum percentage elongation of 9% in 8 inches for small bars (#3 to #6), 8% for #7 and #8 bars and 7% for larger bars (#9 to #18). However for numerical applications, the value of strain at ultimate stress is of great importance to know the stiffness of the elements. Test results by Cowell [23] on ASTM A432 grade 60 re-bars indicate percentage elongation at rupture as 21% and the average strain at ultimate stress as 12%.

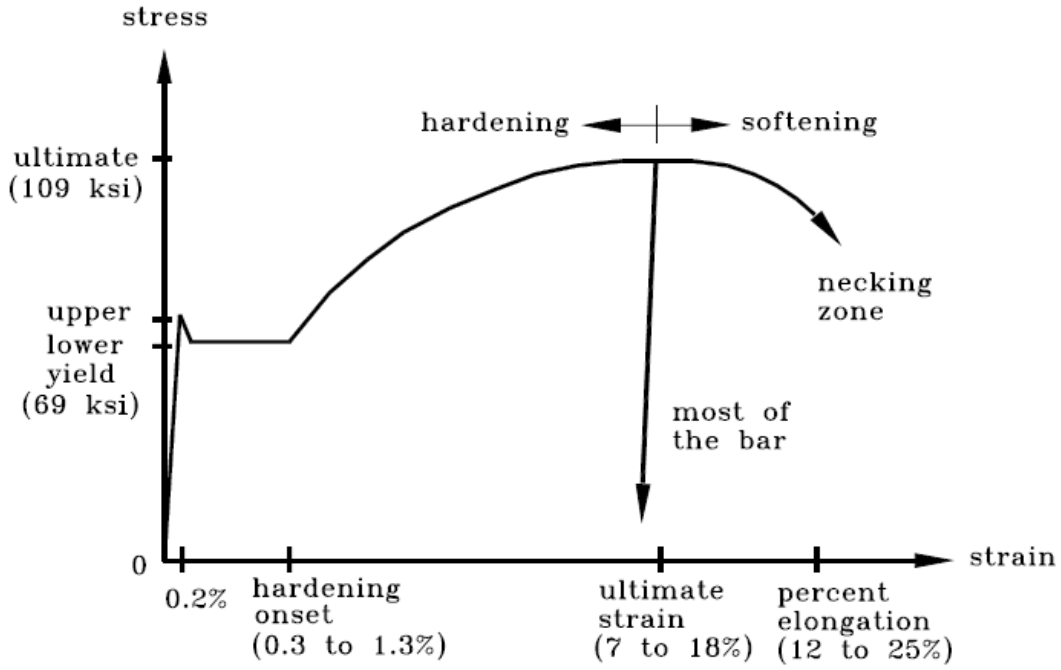

Figure 2.1: Typical Stress-Strain Curve for ASTM 615 Grade 60 steel

2.3 STRUT-AND-TIE MODELING OF CONCRETE

2.3.1 Bernoulli's Hypothesis and St.Venant's Principle

The Bernoulli hypothesis states "Plane sections remain plane after bending." This hypothesis is the basic assumption of flexural design of structural concrete by allowing linear variation in strain over the depth of the cross section. According to the Bernoulli hypothesis, any concrete structure may be subdivided into two regions. One is the B-region in which the Bernoulli hypothesis is applicable, where the B stands for beam or Bernoulli. Another is D-region in which the Bernoulli hypothesis is not applicable, where the D stands for discontinuity or disturbed.

Based on the principle of St.Venant, the dimensions of the B and D regions are obtained. St.Venant's principle states "The local distribution of forces acting on a small portion of a body subject to a stress field may be changed without changing the stress

field in the body at some distance away from the point where the distribution was made." This principle suggests that local disturbance extends about one member depth each way from concentrated loads, reaction, or sudden changes in direction or section. Also B-regions carry load by beam action and, D-regions carry load primarily by arch action involving in-plane force- MacGregor 1997 [24]

2.3.2 Strut-and-Tie Model for Deep Beams and Mode of Failure

Figure 2.2 shows a deep beam with two-point loading. Load path is well defined by the compression struts. Equilibrium at each node is ensured in the model. The type of failure modes and corresponding crack formation is also shown in Figure 2.2.

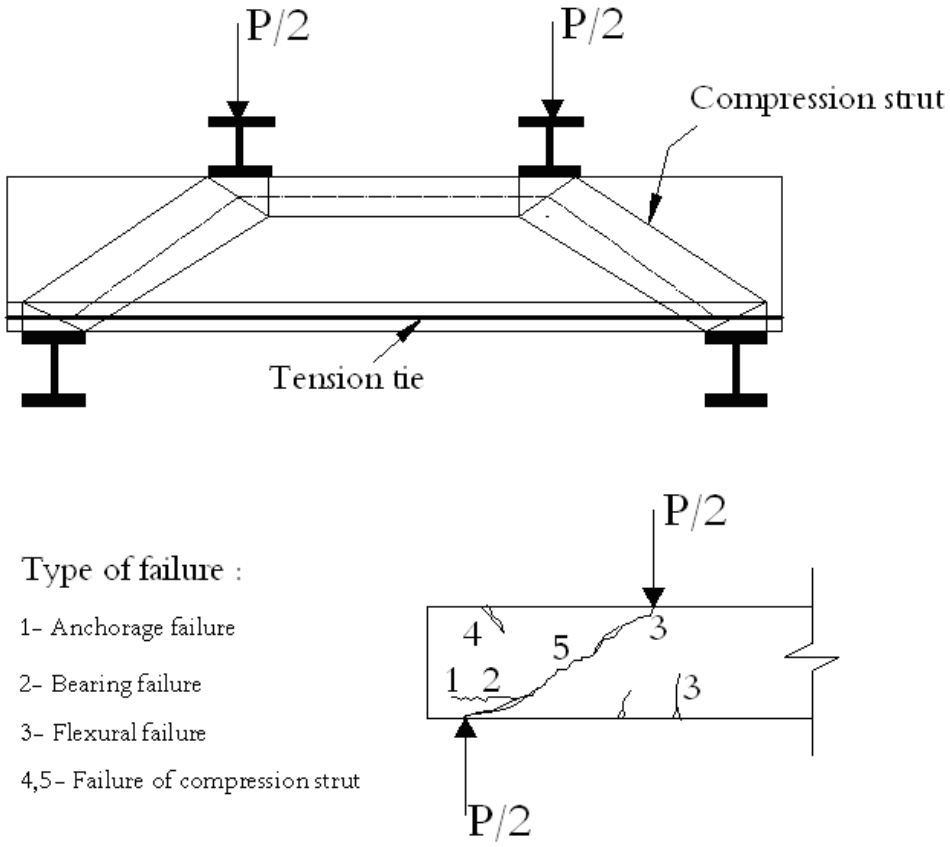

Figure 2.2: Mode of Failure of Deep Beams, (MacGregor, 1997)

2.3.3 Truss Analogy for Design of B-Region

The truss analogy is the shear design approach for reinforced concrete. The truss model introduced by Ritter in 1899 [25] has been developed and adopted by most design specifications as the standard shear design method. The general design procedure for concrete consists of selecting the concrete dimension, determining the size and the placing of reinforcement, and finally checking the serviceability (Marti, 1985) [26]. In the second step, the truss analogy is used to investigate the equilibrium of the external loads and internal force in the concrete and reinforcement. The truss model approach provides an excellent conceptual framework to show the internal forces that exist in a cracked structural concrete member.

2.3.4 Compression Field Theory

This method is based on the lower-bound theorem of plasticity which states that "If an equilibrium distribution of stresses can be found which balances the applied load and is everywhere below yield or at yield, the structure will not collapse. Since the structure can carry at least this applied load, it is a lower bound to the load-carrying capacity of the structure."

Inclined cracks in the reinforced concrete develop a vertical tension force in the vertical reinforcements, horizontal tensile forces in the horizontal reinforcements, and inclined compressive forces in the concrete between the cracks. These internal forces form the indeterminate truss.

The determinate truss system can be formed by lumping all of the stirrups cut by section A-A (Figure 2.3) into one vertical member b-c and all the diagonal concrete members cut by section B-B into one diagonal member e-f (MacGregor,1997).

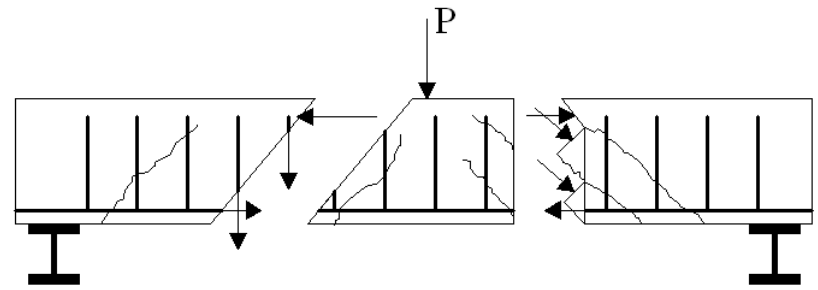

a) Internal Forces in a Cracked Beam

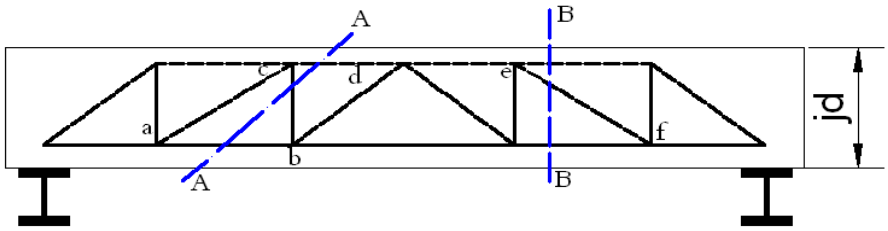

b) Pin-Jointed Truss

Figure 2.3: Truss Analogy (MacGregor, 1997)

Dashed lines and solid lines represent compressive force in the concrete and tensile force in the reinforcement respectively.

2.3.5 Modified Compression Field Theory

Tests of reinforced concrete panels subjected to pure shear demonstrated that after cracking, friction or the aggregate interlock stress in the inclined crack increase the ability of reinforced concrete to resist shear stresses (Vecciho and Collins, 1986)[27]. The modified compression field theory (MFCT) considers this shear contribution of concrete

(V_c) to the shear resistance. This design method introduced by Collins and Mitchell (1996)[28] has been adopted by the AASHTO LRFD specification.[29]

The softened compressive stress f_2 due to transverse tensile strain in the cracked concrete is expressed as a function of both the principal compressive strain ε_2 and the principal tensile strain ε_1 in the following equation (Figure 2.4).

$$f_2 = f_{2\max}\left(2\varepsilon_2/\varepsilon_c' - \left(\varepsilon_2/\varepsilon_c'\right)^2\right) \tag{2.5}$$

Where,

$$f_{2\max 2} = f_c'/(0.8+170\varepsilon_1) \le f' \tag{2.6}$$

ε_c' can be taken as 0.002

The average principal tensile stress f_1 is expressed as follows

$$f_1 = f_{cr}/\left(1+\sqrt{500\varepsilon_1}\right) \tag{2.7}$$

before yielding of reinforcement at the crack

$$f_1 = \nu_{ci}\ \tan\theta \tag{2.8}$$

after yielding of some of the reinforcement at the crack

Where, shear stress is the function of the crack width w and the aggregate size as follows:

$$\nu_{ci} = 2.16\sqrt{f_c'}/(0.3+24w/(a+0.63)) \quad \text{psi and in.} \tag{2.9}$$

Collins et al. (1996) also formulated shear contribution carried by concrete by using stress-strain relationship in the cracked concrete. It is assumed that shear stresses over the effective shear area $b_v d_v$ are uniform. The concrete contribution to the nominal shear strength can be expressed as

$$V_c = f_1 b_v d_v \cot\theta = \beta\sqrt{f'c}\, b_v d_v \qquad (2.10)$$

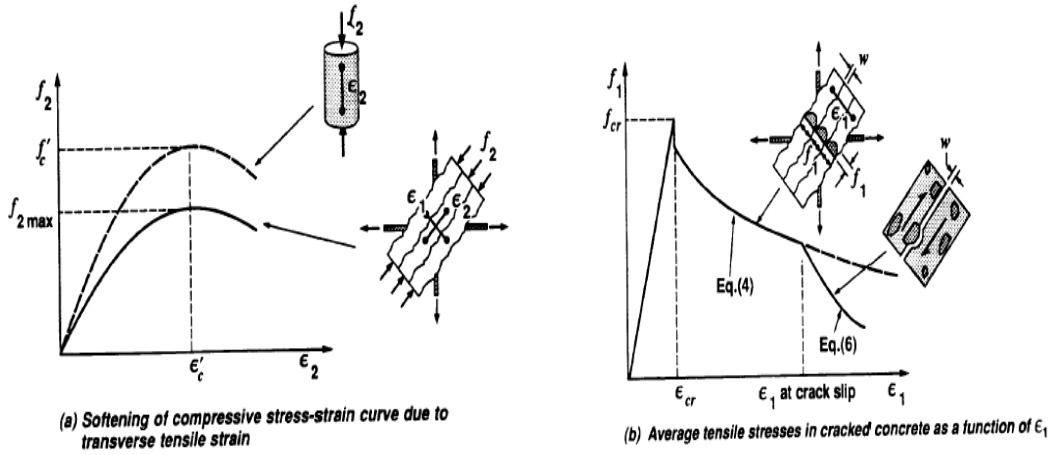

Figure 2.4: Stress-Strain Relationships for Cracked Concrete (Collins et al. 1996)

2.3.6 Components of Strut-and-Tie Model

2.3.6.1 Struts

Struts represent concrete compressive stress fields whose principal stresses are predominantly along the centerline of the struts. The shape of the strut stress field in planar D-regions may be idealized as prismatic, bottle-shaped, or fan-shaped as shown in Figure 2.5 (Schlaich et al, 1987). Struts may be strengthened by ordinary steel reinforcement, and if, so, they are termed reinforced struts.

In general, the stress limit of a strut is not the same as the uni-axial concrete compressive strength obtained from cylinder tests, f_c'. It is defined as

$$f_{cu} = \nu\, f_C{}', \qquad (2.11)$$

Where, f_{cu} = stress limit of a strut, commonly referred to as effective strength, and ν = *effectiveness factor,* also known as *efficiency factor* or *disturbance factor* (typically between 0 and 1.0).

The effectiveness factor, ν, is an empirical factor that is used to justify the application of limit analysis concept to structural concrete. It accounts for the difference in the post yielding response between the uni axial compressive stress-strain curve used for deriving the limit analysis theorem, namely the (rigid or elastic) perfectly plastic curve, and that of typical concrete as shown in Figure 2.6. If the uniform stress distribution is selected, the effective strut capacity is simply

$$f_{cu} = A_c \, f_{cu,} \tag{2.12}$$

Where, A_c is termed the effective cross-sectional area given by $A_c = w_c t$. With the same assumption, the effective capacity of reinforced concrete struts is

$$f_{cu} = A_c \, f_{cu} + A_s f_{y,} \tag{2.13}$$

Where, A_s and f_y are the cross-sectional area and the compressive yield strength of ordinary steel reinforcement, respectively.

2.3.6.2 Ties

Ties typically represent one or multiple layers of ordinary steel, in the form of flexural reinforcement, stirrups, or hoops. Ties can occasionally represent a pre-stressing steel or concrete stress field with principle tension predominant in the tie direction. The effective capacity of a tie consisting only of non-pre-stressed reinforcement is given by

$$f_{tu} = A_s f_{y,} \tag{2.14}$$

Where, A_s = area of ordinary reinforcing steel, and f_y = yield strength of ordinary steel reinforcement in tension.

The tie reinforcement is usually assumed to be enclosed and uniformly distributed in a prism of concrete (smeared reinforcement). Termed *tie effective cross-sectional area*, the cross sectional area of the concrete prism, A_t, where $A_t = w_t\ t$, where w_t is the *tie effective width* as shown in Figure 2.7. The tie capacity given in Equation 3.14 can be rewritten in terms of equivalent stress assumed to be uniformly distributed across the effective cross- sectional area as

$$f_{tu} = r_s f_{y,} \tag{2.15}$$

Where, $r_s = A_s/A_t$ is geometrical ratio of non-pre-stressed reinforcement

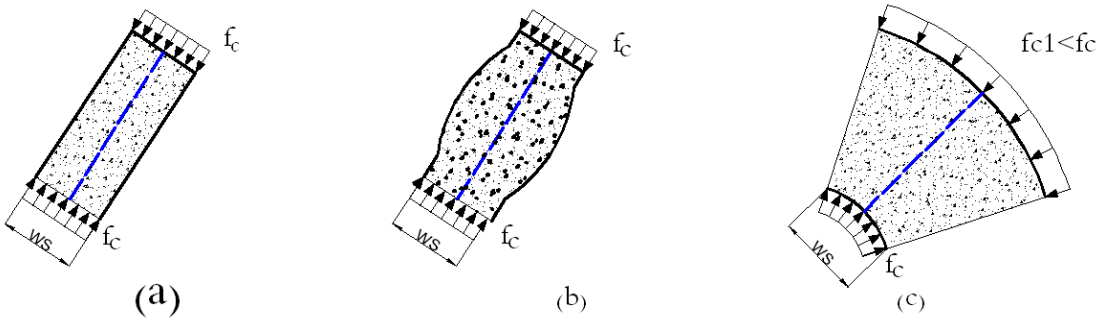

Figure 2.5: Idealized Stress Fields in Struts: (a) Prismatic (b) Bottle-shaped (c) Fan-shaped (Adapted from Schliach et al. 1987).

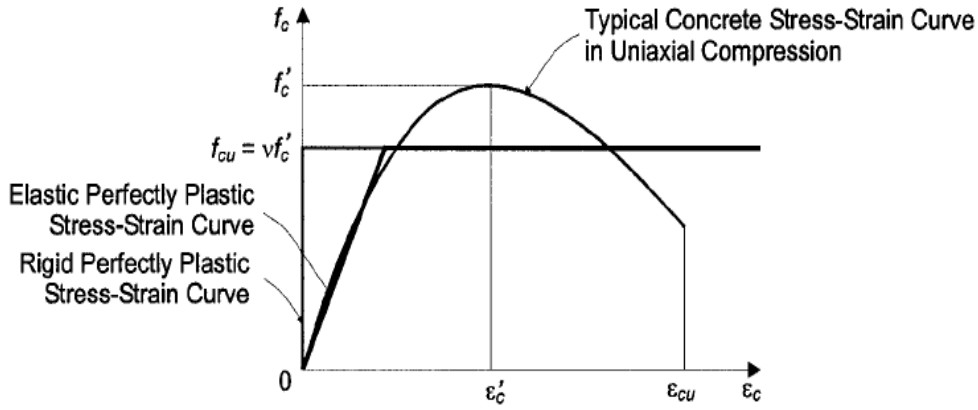

Figure 2.6: Typical Stress-Strain Relationship for Concrete in Uni-axial Compression and the Idealization Used in the STM.

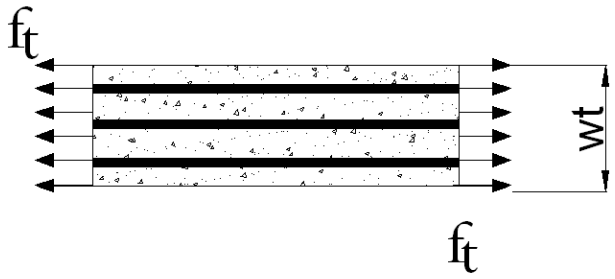

Figure 2.7: Effective Width of Tie

2.3.6.3 Nodes

Analogous to the joints in a structural steel truss, nodes represent regions in which forces are transferred between struts and ties. These regions are usually called nodal zones or nodal regions. Some literature (e.g. ACI 318-08) uses these terms slightly differently; a node refers to the meeting point of the strut axes, tie axes, and body forces acting on the node whereas a nodal zone or nodal region refers to the finite dimension of a node.

Depending on the types of forces being connected, there are four basic types of nodes with three members intersecting, namely CCC, CCT, CTT, and TTT, as illustrated in Figure 2.8, where F_c and F_t in the figure denote strut and tie forces, respectively. Originally used for nodes with three members framing the terms CCC, CCT, and TTT are extended herein for convenience to include nodes with more than three members framing as follows: CCC nodes are those in which all the framing members are struts, CCT nodes are those in which one of the framing members is a tie, CCT nodes are those in which two or more of the framing members are ties, and TTT nodes are those in which are those in which all the framing members are ties.

In 2-D design problems, the stresses in nodal zones are biaxial and are limited to the yield criterion for plane stress problems. The stress distribution in a nodal region depends on the idealized shape, which in turn depends on the effective width and direction of the strut or tie stress field entering the node. An example of this construction for a nodal zone with four struts intersecting is shown in Figure 2.9. The state of stress in these nodal zones is typically complex and difficult to determine. Variants of constructing nodal zone shapes have been proposed to simplify the stress distribution in these regions. These include the hydrostatic approach (Figure 2.9(c)) (e.g. Marti 1985 and Nielson 1998) [30] and modified hydrostatic approach (Figure 2.9 (d)) (Schlaich and Anagnostou 1990). [31] Different effective bearing strength of nodes have been proposed to account for the influencing factors, such as the number and type of intersecting truss members(struts or ties), distribution of tie reinforcement, confinement and use of fibers, level of transverse straining, volume and condition of surrounding concrete, and conditions of ties.

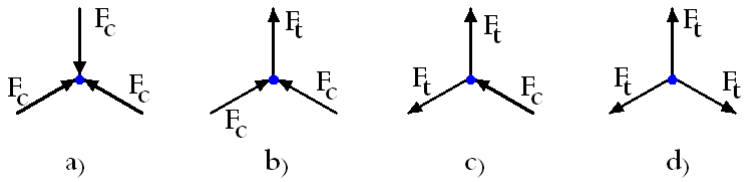

Figure 2.8: Basic Node Types: a) CCC b) CCT c) CTT d) TTT

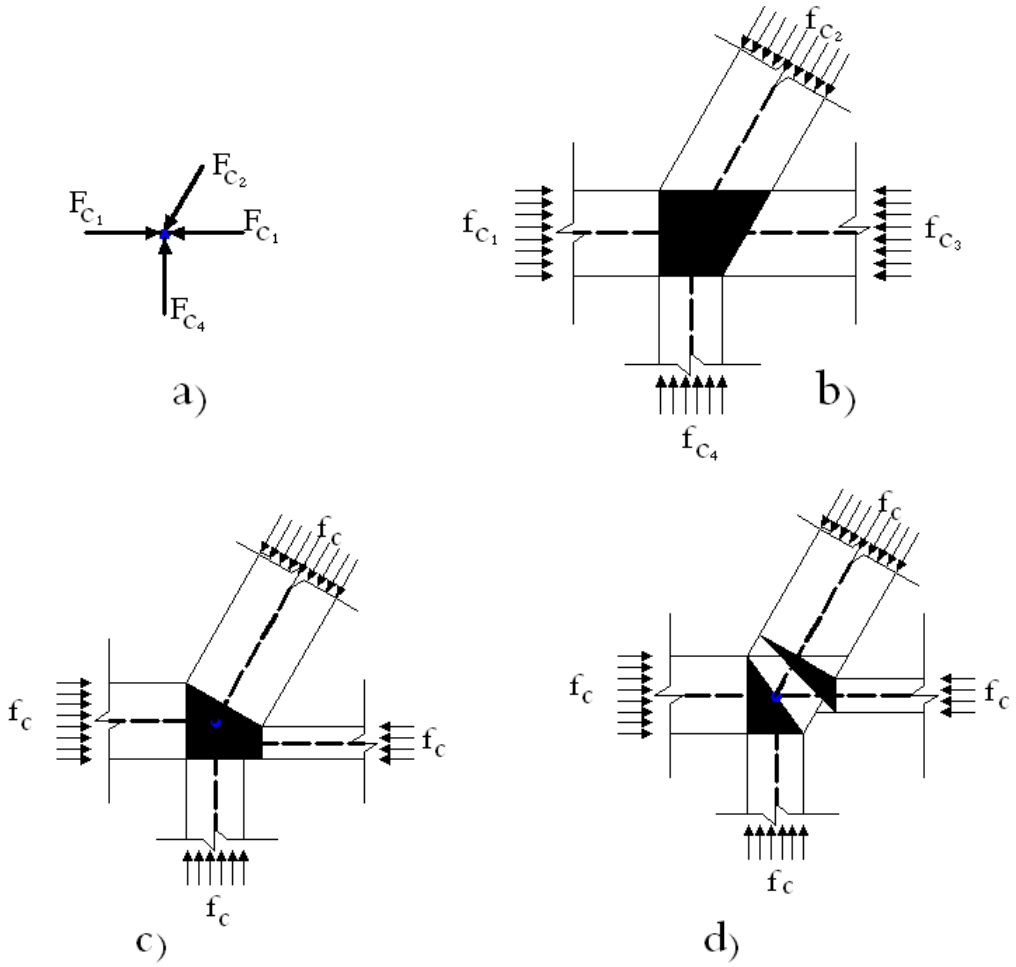

Figure 2.9: Examples of Shape Idealization of a Nodal Zone with Four Struts Intersecting: a) Force Acting on the Node b) Simple Shape c) Hydrostatic Shape d) Modified Hydrostatic Shape.

2.3.7 The Strut-and-Tie Method for Analysis and Design

The strut-and-tie models have been widely used as effective tools for designing reinforced concrete structures. The idea of a Strut-and-tie Model came from the truss analogy method introduced independently by Ritter (1899) in the early 1900s for shear design. This method employs the so-called Truss Models as its design basis. The model was used to idealize the flow of force in a cracked concrete beam. In parallel with the increasing availability of the experimental results and the development of limit analysis in the plasticity theory, the truss analogy method has been validated and improved considerably in the form of full-member or sectional design procedures. The Truss Model has also been used as the design basis for torsion.

Schlaich and Weischede (1981)[32] introduced the concept of D-regions and B-regions where D stands for discontinuity or disturbed regions and B stands for beam or Bernoulli. In D-regions, extending a distance equal to the member depth away from discontinuity such as a change in cross section or concentrated loads, the strain distribution is significantly nonlinear.

Later, Schlaich et al. (1987) generalized the application of the truss analogy concept to all parts of reinforced and pre-stressed concrete structures in the form of Strut-Tie system and suggested using the Strut-Tie system as a primary load-carrying mechanism in such regions. As a guideline for the development of a Strut-Tie model, they recommended visualizing the internal forces flow according to a linearly elastic analysis and orienting the struts and ties within 15 degrees of the elastically determined stresses.

Several theoretical and experimental studies had been carried out to analyze the shear failure of reinforced concrete beams. During the past few years, design codes ACI 318-08

and AASHTO (2005) have adopted strut-and-tie principles for the design of deep beam members.

Hwang et al. (2001) [33] have related the stress limits with the transverse strain perpendicular to the stress direction so as to consider the softening effect of concrete compressive strength. However, it may not be appropriate to apply the smeared crack model concept to the D-region, that is, the disturbed region where the conventional plane-section-remains-plane principle is not valid. Tan et al. (2001, 2003) [34, 35] have developed a direct STM for simply supported deep beams, which can consider the effects of different web reinforcement configurations (vertical, horizontal, or inclined), and pre-stressing tendons.

Nielson et al. (1978) [36] have used the theory of plasticity for computation of the inclination of compressive struts in the truss model. The reinforcement was assumed to be rigid, perfectly plastic and unable to resist lateral forces.

Bakir and Boduroglu (2005) [37] discussed the application of the softened truss and strut-and-tie models on short beams. The model has two important characteristics. The first is the non-linear association of stress and strain. The second is the softening of concrete in compression due to tensile strains in the perpendicular direction.

Young (2000) [38] presented an interactive computer graphics program for implementing the nonlinear strut-tie model approach for the practical design and analysis of disturbed regions in structural concrete. The design result showed that the nonlinear strut-tie model, combined with the graphics program, produces simple and effective solutions by providing accurate details on structural concrete.

Tjhin and Kuchma (2002) [39] developed a computer program CAST (Computer Aided Strut-and-tie) for design and analysis of reinforced and pre-stressed concrete members.

Hyo-Gyoung and Sang-Hoon (2006) [40] have introduced a method to determine strut-and-tie models in reinforced concrete (RC) structures by using evolutionary structural optimization (ESO). The introduced optimization procedure also showed the availability of determining optimal strut-and-tie models of RC structures with complicated geometry, such as corbel structures and deep beams with openings, for which the classical strut-and-tie approach has limitations in application. However, the availability of the proposed method for RC structures with complicated loadings should be checked. Further theoretical research, including the effect of material property on the optimal strut-and-tie models, as well as experimental verifications must be followed to achieve a more rational design approach.

Alshegeir and Ramirez (1992) [41] have developed an iterative computer graphics program implementing the strut-tie model approach for analysis and design of reinforced and pre-stressed concrete members. The program provides the direction of principal compressive stresses, which gives guidance in the development of strut-tie models.

Liang et al. (2006) [42] developed a strut-and-tie design methodology for three-dimensional reinforced concrete structures. The unknown strut-and-tie model is realized through the machinery of a refined evolutionary structural optimization method. Stiffness of struts and ties is computed from an evolved topology of a finite element model to solve statically indeterminate strut-and-tie problems. In addition, compressive strength for struts and nodal zones is evaluated by using Ottosen's four-parameter strength criterion.

Chun (2002) [43] developed a 3D indeterminate strut-and-tie model for the analysis of the footing system. Five different levels of stiffness were used to cover the lower and upper bounds for both cracked and un-cracked situations. By following the sequence of construction, the model predicted the stresses of the members at different stages. Finite-element solid modeling was also conducted to verify the strut-and-tie model.

Richard (1995) [44] has developed a strut-and-tie model for the punching shear behavior of a concrete slab. This model provides a quick and simple approach to punching shear behavior. It is applicable for both normal and high strength concrete under symmetric and non-symmetric loading with and without shear reinforcement.

Strut-and-tie models are discrete representations of actual stress fields resulting from the applied loads and support conditions and provide static lower bound solutions. These models actually represent the load carrying mechanism of a structural member by approximating the flow of internal forces by means of struts representing the flow of compressive stresses and ties representing the flow of tensile stresses.

Strut-and-tie model serve a dual purpose. They allow description of essential aspects of structural behavior and at the same time provide useful tools for detailing and dimensioning. Strut-and-tie models assist the designer in determining size, the location, the distribution, and anchorage of main reinforcement.

An accepted design philosophy in reinforced concrete is to produce members in which the critical section exhibit ductile behavior under extreme over load. This is done by ensuring that reinforcement yields before concrete fails and flexure controls the mode of failure.

The strut-and-tie method of design has been incorporated in ACI 318 for the design of concrete. It clearly explains the concept and gives allowable stresses in concrete struts and nodal zones.

Tiller [45] proposes a strut-and-tie model for the punching shear of concrete slabs. This model provides a quick and simple approach to punching shear behavior. It is applicable for both normal and high strength concrete under symmetric and non-symmetric loading.

STM has recently emerged as a consistent and rational method for the design of discontinuity regions in structural concrete and is being incorporated in codes of practice. While the STM provides a conceptually simple design methodology, its implementation is usually complicated by the need to perform iterative and time consuming calculations. CAST program developed by Tjhin and Kuchma (2004, 2007) [46, 47] solved many problems in this regard for two dimensional strut-and-tie problems and made it possible to explore the capabilities of STM. Although STM can be used for the design of all parts of concrete structures, it is typically applied only to design of D-regions, which include those parts which include those parts of concrete structures near abrupt changes in geometry and near concentrated forces. The STM relies on the use of strut-and-tie models as idealized flows of forces or internal load-carrying systems in the cracked body of concrete at the ultimate limit state.

Due to the wide range of structures that can be designed by the STM, there is significant uncertainty about what level of distributed reinforcement is needed to ensure that the structure is sufficiently ductile to support the loads in the manner envisaged by the designer. This added reinforcement also plays a significant role in controlling

cracking in struts and throughout the structure. By careful selection of the shape of the internal load resisting truss, the need for distributed reinforcement can be reduced. This can be accomplished by selecting the lines of action of primary struts and ties to be close to the directions of principal compressive and tensile stresses as determined by linear elastic finite element analyses.

2.4 CLASSICAL METHODS FOR DESIGN OF WAFFLE SLABS

2.4.1 Equivalent Thickness Method

The "equivalent thickness" concept that is recommended by the Concrete Reinforcing Steel institute Handbook (CRSI 1972) is an approximate method to predict the deflection of waffle slabs. Equivalent thickness is defined as the thickness of a uniform plate that has the same bending stiffness as the waffle slab. For a slab under transverse load, the equivalent thickness is obtained by averaging the gross moment of inertia.

$$h_e = \left(\frac{12I}{S}\right)^{(1/3)} \tag{2.16}$$

Where S = center-to-center distance between the ribs; and I = moment of inertia of the flanged section including one rib and the top slab of width S.

In a study of the deflection characteristics of waffle slabs, Ji et al. (1986) tested one specimen under gravity load and compared the results of the stiffness in the elastic range with those obtained by the finite-element method and the equivalent thickness concept. They concluded that the equivalent thickness method leads to overestimation of the torsional rigidity and an underestimation of the deflection. To compensate for this, they suggested that the equivalent thickness might be reduced by approximately 20%. Under

full service load (i.e., in the elastic-cracked range), they suggested that the effective stiffness might be estimated as 40% of the initial (elastic-un-cracked) stiffness.

2.4.2 Orthotropic Plate Theory

Orthotropic plate theory originally developed for an ideal elastic material, such as steel, was extended to reinforced concrete waffle slab design (Timoshenko and Woinowsky-Krieger 1959; Bares and Massonnet 1966; Cusens and Pama 1975). To predict accurately the elastic response of such structures to an applied load, it is essential for designers to use realistic estimates of the various rigidities of the structure.

For an orthotropic plate under a given load distribution and for known boundary conditions, the deflections, moments, and shears are determined by integration of the differential equation (Timoshenko and Woinowsky-Krieger 1959; Cusens and Pama 1975)

$$Dx\,(\delta^4 w/\delta x^4) + 2H\,(\delta^4 w/(\delta x^2\,\delta y^2)) + Dy\;(\delta^4 w/\delta y^4) \;= P(x, y) \qquad (2.17)$$

Where, Dx and Dy = flexural rigidities; and 2H = total torsional rigidity that is the sum of the torsional rigidities in the x-and y-directions, Dxy and Dyx, and the coupling rigidities, D1 and D2, which represent the contribution of bending to the torsion of the deck.

In the case of orthotropic plate theory, moment of inertia of ‘T’ section is calculated based on rib spacing, rib thickness, thickness of slab and overall depth. Bending and torsional rigidities are then calculated and analysis being done as a plate with uniform thickness. Based on moments and shear obtained, T-sections are designed as per code provisions.

2.4.3 ACI Approach

The empirical design methods recommended by ACI 318-2008 addresses all types of two way slabs in the same manner under vertical loads. The direct design method or equivalent frame method, applicable for two way flat plate and flat slabs, is also applicable for waffle slabs. But neither experiments nor analytical investigations have satisfactorily confirmed the appropriateness of such an approximation.

However there are significant difference in the behavior of the two types of the slabs; the increased ratio of flexural to torsional rigidities in a waffle slab results in a substantial reduction in the load that is transmitted by torsion of the slab elements. The difference is significant, when there is less number of spans in any direction.

ACI recommends two methods for the design of multi-span waffle slabs: Direct design method and Equivalent frame method. Both the methods are same as that used for two way slabs. ACI restricts rib spacing, rib thickness and rib depth for the design of waffle slab.

In Direct design method, the factored loads are calculated and slab is divided into column strip and middle strip. Moments and shear at critical sections are calculated based on coefficients. Finally design is done considering T-section. Punching shear is checked and provisions for minimum reinforcement and spacing followed.

In Equivalent frame method, the difference is that the slab is divided into two dimensional frames in each direction along column lines. Moments and shear are obtained by the analysis of the frames.

2.4.4 Numerical Methods

Finite Element modeling is a more accurate method of predicting the behavior of waffle slabs. However it needs specialized soft-wares for modeling. The cracking behavior of concrete along with ductile behavior of steel necessitates sophisticated material models, in order to trace the response of reinforced concrete structures in non-linear post cracking and post yield stages.

2.5 DEFICIENCIES OF CURRENT METHODS FOR DESIGN OF WAFFLE SLABS

2.5.1 Equivalent Thickness Method

Equivalent thickness is an approximate method, finding a thickness, by an empirical formula, which give more or less same stiffness as that of waffle slabs. It concentrates only on the deflection of the slab.

2.5.2 Orthotropic Plate Theory

Orthotropic plate theory is originally developed for ideal elastic material such as steel and plates of uniform thickness. It involves solution of differential equations and is very complicated for multi-span waffle slabs.

2.5.3 ACI Approach

ACI methods assume waffle slabs and solid slabs behave in the same manner under load. The presence of ribs and its effect is not well addressed. Increased ratio of flexural to torsional rigidity is ignored. The concept of shear and bending moment is more complex to visualize than the flow of axial stresses as we do in strut-and-tie model.

2.5.4 Numerical Methods

Even though finite element methods predict the stress distribution in the elastic range of slabs, it is difficult to obtain the ultimate strength of slab since the behavior changes drastically after cracking of concrete. It needs dedicated software to model steel and concrete separately with the nonlinearity in the material behavior well defined. Modeling of waffle slab as a finite element model is difficult due to its geometry and the inter connectivity of its ribs. Another drawback of numerical methods is that it is difficult to correlate the detailing aspect of the slab with a given stress distribution.

2.6 ACI PROVISIONS FOR DESIGN OF WAFFLE SLABS

2.6.1 General Provisions for Waffle Slab

ACI includes waffle slab in joist construction and describes waffle slab as monolithic combination of regularly spaced ribs and a top slab arranged to span in two orthogonal directions. ACI-318-08 specifies recommendations for spacing of ribs, thickness of ribs and maximum depth of ribs and slab thickness as follows:

Ribs shall be not less than 4 inch in width, and shall have a depth of not more than 3-1/2 times the minimum width of rib. Clear spacing between ribs shall not exceed 30 inch. Slab thickness shall be not less than one-twelfth the clear distance between ribs and not less than 2 inch.

Effective width of flange that can be considered as part of the rib is given by Figure 2.10 and is subjected to a maximum as center to center of ribs. Also minimum reinforcement for ribs and slabs, maximum spacing of reinforcement and minimum concrete cover are specified as per relevant sections.

2.6.2 Strength of Struts, Ties and Nodal Zones

As per ACI-318, design of struts, ties and nodal zones shall be based on

$\phi F_n \geq F_u$ where, (2.18)

F_n is the nominal strength of the respective element and F_u is the factored load.

Strength reduction factor, ϕ for all elements of Strut-and-tie models such as struts, ties, nodal zones, and bearing areas is given as 0.75.

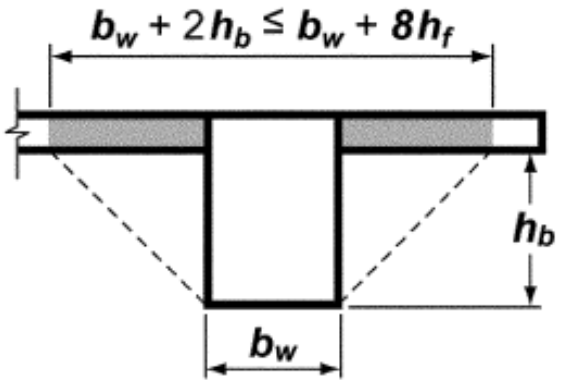

Figure 2.10: Effective Width of Slab (ACI-318, 2008)

2.6.2.1 Struts

Nominal compressive strength of strut is given by

$F_{ns} = f_{ce} * A_{cs}$ (2.19)

Where, A_{cs} is the area of cross section of the strut.

The effective compressive strength of the concrete, f_{ce}, in a strut shall be taken as

$f_{ce} = 0.85 \beta_s f'_c$ where, (2.20)

β_s = 1.0 for prismatic struts (struts of uniform cross sectional area over its length)

= 0.75 for bottle shaped struts with reinforcement provided as per ACI

= 0.60 for bottle shaped struts without reinforcement for normal weight concrete.

2.6.2.2 Ties

The nominal strength of a non pre-stressed Tie shall be taken as

$F_{nt} = A_{ts} * f_y$ where, (2.21)

A_{ts} = Area of tensile steel reinforcement

f_y = Yield strength of steel reinforcement

2.6.2.3 Nodes

Nominal compressive strength of nodal zone is given by

$F_{nn} = f_{ce} * A_{nz}$ (2.22)

Where, A_{nz} is the area of cross section of the nodal zone perpendicular to the line of action of force.

The effective compressive strength of the concrete, f_{ce}, in a nodal zone shall be taken as

$f_{ce} = 0.85 \beta_n f'_c$ where, (2.23)

β_n = 1.0 for CCC nodal zones (Node anchoring struts / bearing plate)

= 0.80 for CCT nodal zones (Node anchoring only one tie)

= 0.60 for CTT nodal zones (Node anchoring more than one tie)

CHAPTER 3

STRUT-AND-TIE MODEL (STM) FOR SIMPLY SUPPORTED WAFFLE SLAB

3.1 DEVELOPMENT OF TRUSS MODEL FOR WAFFLE SLAB

Waffle slab is modeled as a finite element model using STAAD-Pro in order to obtain the distribution of stresses and to see the effect of ribs in waffle slabs. The whole slab is modeled as an isotropic material. Stress distribution of the finite element model is shown in Figure 3.1. The slab is simply supported on all four edges. Corner lifting is allowed.

It is clear from the model that ribs play the major role in the load carrying mechanism. The local bending of slabs causes some variation in the stress distribution and hence is different from two way slabs of uniform thickness. Additional stresses at corners and more shear stresses near center of each side due to corner lifting are also evident from the model.

The whole slab can be transformed to a series of T sections in orthogonal directions which are acting together in the load carrying mechanism. The top slab helps to maintain equilibrium and maintain the relative locations of the T beams under loads. Load transfer takes place at each intersection for strain compatibility between ribs in both directions. Generally slab thickness is very less for waffle slabs and its torsional stiffness is negligible compared to the bending stiffness of the T-sections.

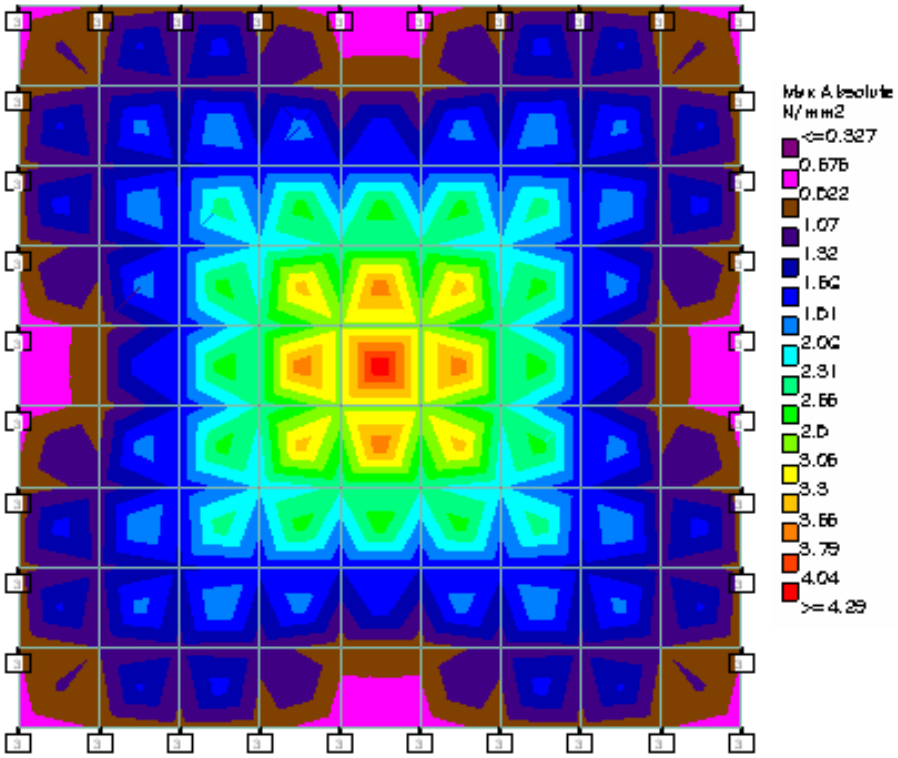

Figure 3.1: Test Slab – Finite Element Model

Waffle slab comprises a regular pattern of voids at the bottom which forms an orthogonal grid of ribs. The intersecting ribs at close interval transform the whole waffle slab as a D-region which means the conventional beam theory cannot be applied. Strut-and-tie method is generally used for structures with D-regions. Waffle slab is inherently 3-D in nature and hence 3-D strut-and-tie model is required for the analysis and design.

3.2 PROPOSED STRUT-AND-TIE MODEL FOR WAFFLE SLAB

The proposed strut-and-tie model is developed for waffle slabs, simply supported on all four edges. Corner lifting is allowed. Figure 3.2 shows the proposed model. Compression only supports provided at peripheral nodes at bottom.

In the proposed strut-and-tie model, the waffle slab is modeled as a 3-D truss. Individual ribs in each direction forms two dimensional trusses as shown in Figure 3.3. Each truss is connected with perpendicular trusses at rib intersections. Cross bracing is provided at top to simulate the action of concrete slab as shown in Figure 3.4.

Top chord consists of prismatic concrete strut which is within the top slab. Bottom chord consists of the main reinforcement at the ribs. Vertical member corresponds to ties which can be either stirrups or concrete tension ties, in case of waffle slabs without stirrup reinforcement. Inclined members consist of bottle shaped concrete struts. The intersection of struts and ties are represented by nodal zones.

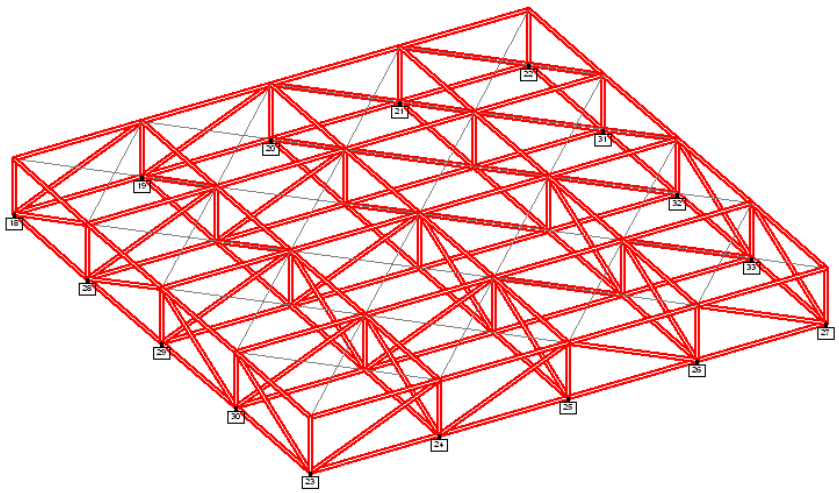

Figure 3.2: Proposed 3D strut-and-Tie Model

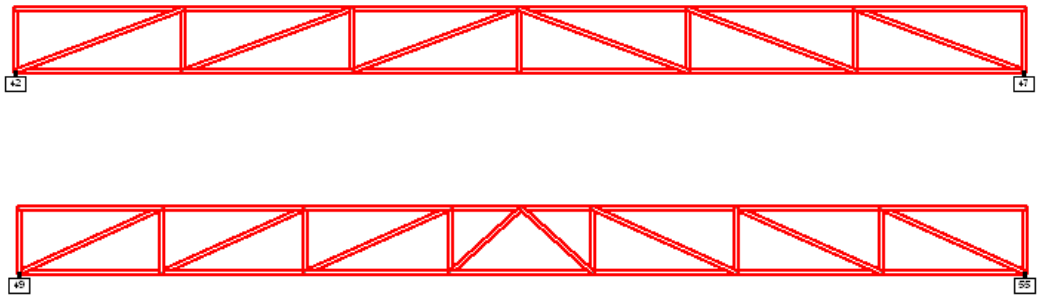

Figure 3.3: STM Model for Single Rib– Even and Odd Number of Waffle Openings

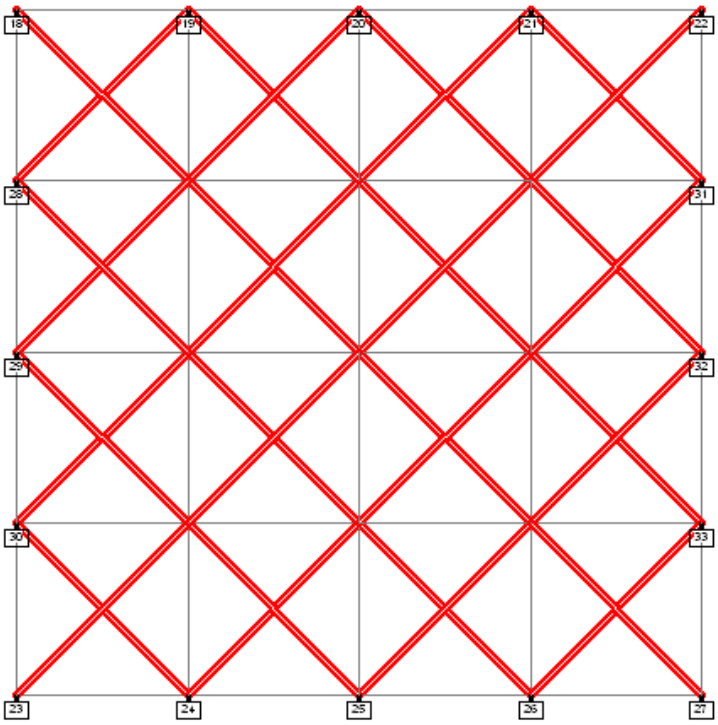

Figure 3.4: STM Model-Top Bracing

3.3 CALCULATING PROPERTIES OF MEMBERS OF THE PROPOSED MODEL

The member sizes for the proposed model are calculated as follows:

3.3.1 Top Chord

Top chord consists of prismatic concrete strut with thickness less than the slab thickness. The temperature steel provided in the slab can be ignored. Generally in slabs, the top chord does not govern and hence minimum thickness is recommended for optimization. When the thickness is reduced, the truss depth increases and hence axial forces in top chord and bottom chord reduce. However the thickness should be selected such that it is sufficient to avoid compression failure for the top struts. It can be obtained accurately by 2-3 trials. However for practical design purposes, a larger thickness like half the slab thickness can be conservatively considered since its effect of member forces is not significant.

The width of top chord is calculated based on ACI formulae for effective width of flanges that can be considered along with web for "T" sections which is minimum of the following: a) width of rib + 8 times slab thickness b) width of rib + 2 times clear height of rib below slab c) center to center spacing of rib.

Area of top chord is calculated as thickness * width. Area calculated separately for ribs in each direction if waffle spacing is different. Area of nodal zone for top chord is same as area of top strut. Modulus of elasticity of concrete is calculated as per ACI formula, based on the compressive strength of concrete, f'_c. A linear stress strain curve is used for concrete.

3.3.2 Bottom Chord

Bottom chord consists of steel reinforcement. Actual area of steel, based on number of reinforcement bars and diameter of bars, is provided in the model. An idealized bilinear stress strain curve is used for steel for calculating the ultimate load carrying capacity of the test slabs. However for design purpose, a linear stress strain curve is sufficient since stresses are not allowed beyond the yield point.

For checking allowable stress for nodal zones, the area of nodal zone is calculated as width of nodal zone * thickness of nodal zone. Width of nodal zone is two times the effective cover of bottom reinforcement. Thickness of nodal zone is same as rib thickness.

3.3.3 Vertical Members

For waffle slabs with stirrups provided in the rib, vertical member consists of stirrup reinforcement provided at the intersection of ribs. Stirrups provided in both directions can be added. Actual area of steel, based on number of stirrup legs and diameter of bars, is provided in the model. Modulus of elasticity of steel is used for slabs with stirrups.

For waffle slabs without stirrups, vertical member consists of concrete tension ties. The concrete at intersection of ribs and a portion of concrete surrounding is effective. The area of vertical member is calculated as Rib width * Rib width + Rib width * effective depth. Modulus of elasticity of concrete is used for slabs without stirrups.

3.3.4 Diagonal Members

Diagonal member consists of bottle shaped concrete strut with thickness same as rib thickness. The width of diagonal member is calculated separately at top and bottom ends of the strut separately and minimum is used for the design.

Width of diagonal member = Rib width * sin θ + chord thickness * cos θ

The calculation at bottom end is as shown in Figure 3.5. l_b is the rib thickness and w_t is the width of bottom tie. "θ " is the angle that diagonal strut makes with bottom tie. Area of diagonal member is calculated as thickness * width. Area is calculated separately for ribs in each direction if waffle spacing is different. Area of nodal zone for diagonal strut is same as area of the strut. Modulus of elasticity of concrete is considered as was considered for top strut.

3.3.5 Bracing Members

Bracing member consists of prismatic concrete strut with thickness same as slab thickness. The width of bracing member is calculated as follows:

Width of bracing member = rib width * sin α + rib width * cos α Where,

α – angle of inclination of bracing with X-axis

Area of bracing member is calculated as thickness * width. Modulus of elasticity of concrete considered for bracing also.

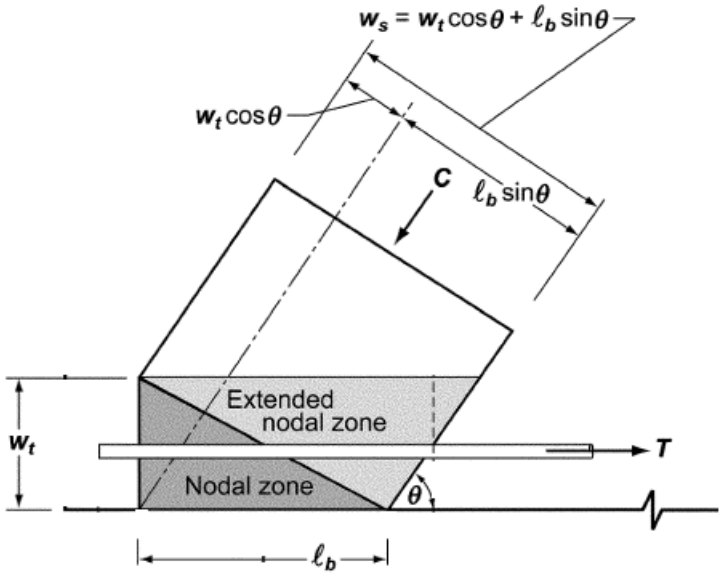

Figure 3.5: Calculating Width of Strut for Diagonal Members

3.4 APPLYING LOADS TO THE PROPOSED MODEL

All loads should be applied to the top joints of the truss. Self weight is calculated for each node at top based on tributary of the slab and length of rib. Additional dead loads and live loads to be applied based on tributary and are applied at top joints.

Suitable load factors should be considered (1.2 for dead load and 1.6 for live load as per ACI-318-2008) since the design is made for ultimate strength. Currently the model is checked for vertical gravity loads only.

3.5 CALCULATING STRENGTH AND STRESS RATIO OF ELEMENTS OF THE MODEL

Nominal strength of elements for the proposed model is calculated, as per ACI-318-08, as follows. Maximum allowable factored load is nominal strength multiplied by

strength reduction factor ϕ (= 0.75 for all elements as per ACI-318). Stress ratio is the ratio of actual force in the member / Maximum allowable factored load.

3.5.1 Top Chord

Top chord is a prismatic concrete strut and nominal strength is calculates as

$F_{ns} = f_{ce} * A_{cs}$ where, A_{cs} is the area of cross section of the strut.

The effective compressive strength of the concrete, f_{ce}, in a strut shall be taken as

$f_{ce} = 0.85 \beta_s f'_c$ where,

$\beta_s = 1.0$

3.5.2 Bottom Chord

Bottom chord is steel reinforcement and nominal strength is calculated as

$F_{nt} = \Omega A_{ts} f_y$ where,

A_{ts} = Area of tensile steel reinforcement

f_y = Yield strength of steel reinforcement

Ω = Over strength factor of 1.25

Over strength factor considered for the bottom reinforcement, considering sharing of loads between ribs as is done in other methods with strips.

3.5.3 Vertical Members

For waffle slabs with stirrups provided in the rib, vertical member is stirrup reinforcement and nominal strength is calculates as

$F_{nt} = A_{ts} * f_y$ where,

A_{ts} = Area of tensile steel reinforcement (stirrups)

f_y = Yield strength of steel reinforcement

For waffle slabs without stirrups, vertical member is concrete tension ties and nominal strength is calculates as follows

$F_{nt} = f_{te} * A_{ct}$

Where, A_{ct} is the area of cross section of the concrete tie.

The effective tensile strength of the concrete, f_{te}, in the concrete tension tie shall be taken as

$f_{te} = \beta_t f_{ct}$ where,

$\beta_t = 0.6$ (Considered for concrete tension tie)

Direct tension capacity of concrete, f_{ct} , is considered as $0.33 (f'_c)^{1/2}$ (Mpa) and $4 (f'_c)^{1/2}$ in psi.

3.5.4 Diagonal Members

Diagonal member consists of a bottle shaped concrete strut and nominal strength is calculates as follows

$F_{ns} = f_{ce} * A_{cs}$ where, A_{cs} is the area of cross section of the strut.

The effective compressive strength of the concrete, f_{ce}, in a strut shall be taken as

$f_{ce} = 0.85 \beta_s f'_c$ where,

β_s = 0.75 with stirrups provided in the ribs

= 0.60 without stirrups in the ribs

3.5.5 Bracing Members

Bracing member is a prismatic concrete strut and nominal strength is calculates as

$F_{ns} = f_{ce} * A_{cs}$ where, A_{cs} is the area of cross section of the strut.

The effective compressive strength of the concrete, f_{ce}, in a strut shall be taken as

$f_{ce} = 0.85 \beta_s f'_c$ where,

β_s = 1.0

3.5.6 Nodes

All top nodes are CCT nodal zones since only one tie (vertical member) is anchored by these nodes. All bottom nodes are CTT nodal zones since two ties (vertical member and bottom tie) are anchored by these nodes. Nominal compressive strengths of nodal zones are calculated as follows:

$F_{nn} = f_{ce} * A_{nz}$ where, A_{nz} is the area of cross section of the nodal zone perpendicular to the line of action of force.

The effective compressive strength of the concrete, f_{ce}, in a nodal zone shall be taken as

$f_{ce} = 0.85 \beta_n f'_c$ where,

β_n = 0.80 for CCT nodal zones (Top nodes)

= 0.60 for CTT nodal zones (Bottom nodes)

CHAPTER 4

VALIDATION OF WAFFLE SLAB STM USING ANSYS

4.1 EXPERIMENTAL DATA USED FOR VALIDATION OF PROPOSED MODEL

4.1.1 Description of Waffle Slabs Used for Experiment by Abdulwahab and Khalil

An experimental study of reinforced concrete waffle slabs with a square layout of ribs was conducted by Abdulwahab and Khalil [13]. Tests to failure were carried out on Six large-scale (1/4-in. scale) models with varied rib spacing and rib depth. The test program was designed to investigate the effect of the rib spacing and the rib depth on the flexural rigidity and strength of waffle slabs. In all tests, the slabs were simply supported along the edges, at spans of 1500mm. Slabs were subjected to a central ‘‘patch’’ load over an area of 300 * 300 mm as shown in Figure 4.1.

Concrete for the specimens was normal weight, with a mix proportion of 1:1.5:3 of ordinary Portland cement: fine aggregate of maximum size of 4.75 mm: course aggregate of maximum size of 6.7 mm with a water: cement ratio of 0.47. It was designed to achieve a concrete cylinder compressive strength of about 30 MPa at 28 days.

Flexural reinforcement consisted of 8-mm-diameter smooth steel bars with yield strength of 398 MPa. The bars were placed in the ribs with a clear cover of 8 mm. As temperature and crack control reinforcement, wire mesh with an average diameter of 0.7 mm and mesh size of 25 mm was used. It was placed at the middle of the topping of the waffle slabs (10 mm from the top).

The load was applied in a series of increments of 2.5–5kN, and the deflections and strain measurements were recorded. After cracking, the crack location and development was also recorded. The loading was continued to destruction to determine the mechanism of failure. Figure 4.1 and Table 4.1 shows geometry of waffle slabs, loading arrangement, and reinforcement details.

4.1.2 Experimental Results

Table 4.2 shows cracking, ultimate loads and mode of failure for tested specimens S1 to S6. Flexural cracking was observed at about 25–30% of the ultimate load. Waffle slabs S4 to S1 in order, which have the same thickness and rib reinforcement but vary in the number of ribs from 5 (S4) to 11 (S1), the load capacity increased and deflections reduced as the rib spacing is reduced. Also the mode of failure is noted to change from shear failure to flexural failure. Figure 4.2 shows crack patterns at bottom of the slab for specimens S1 to S4.

For waffle slabs S6, S2 and S5 in order, have the same number of bays and reinforcement but vary in the size of the ribs. The load capacity increased and deflections reduced as we increase the rib size. However the mode of failure changed from flexural failure to shear failure.

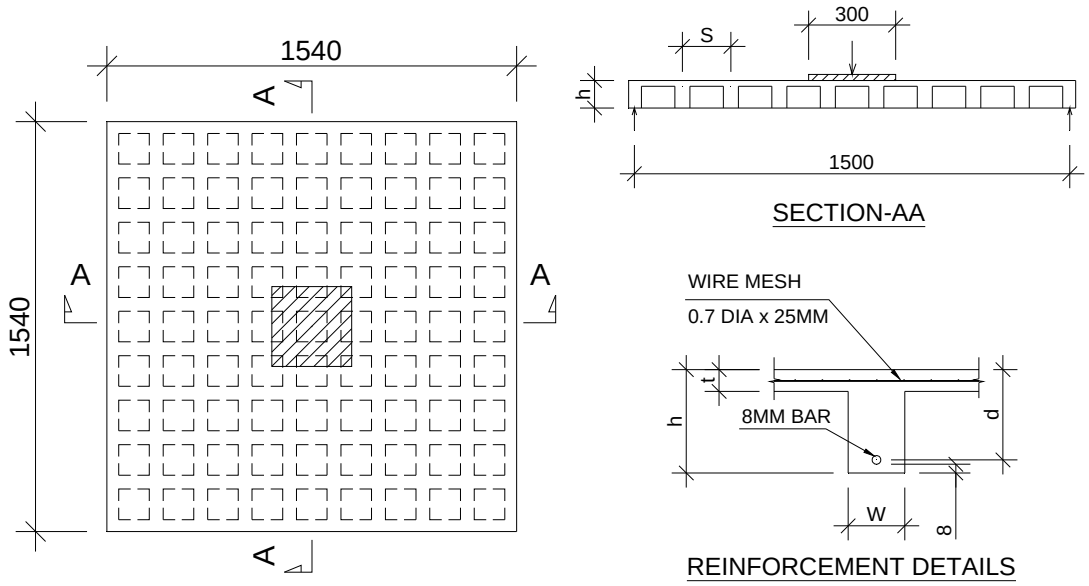

Figure 4.1: Geometry of Waffle Slabs, Loading Arrangement, and Reinforcement Details

S – Rib spacing

h – Overall Depth

t – Top slab thickness

d – Effective depth

W – Rib width

f'_c – Concrete compressive strength

TABLE 4.1: Geometry of Experimental Waffle Slabs

Specimen	f'_c Mpa	S mm	t mm	W mm	h mm
S1	31.3	136	20	52	95
S2	32.0	167	20	52	95
S3	31.4	214	20	52	95
S4	28.9	300	20	52	95
S5	29.9	167	20	57	125
S6	29.1	167	20	47	65

TABLE 4.2: Experimental Results

Specimen	P_{crack} kN	$P_{u\text{-}Test}$ kN	Mode of Failure
S1	30	105	Flexural failure; cracks extended toward corners
S2	20	81	Flexural failure; cracks extended toward corners
S3	20	65	Mainly flexural failure; cracks extended toward corners and edges; some shear cracks
S4	20	48	Sudden punching shear failure; flexural and shear cracks were formed
S5	40	120	Sudden punching shear failure with slip-bond failure
S6	20	48	Flexural failure; cracks extended toward corners

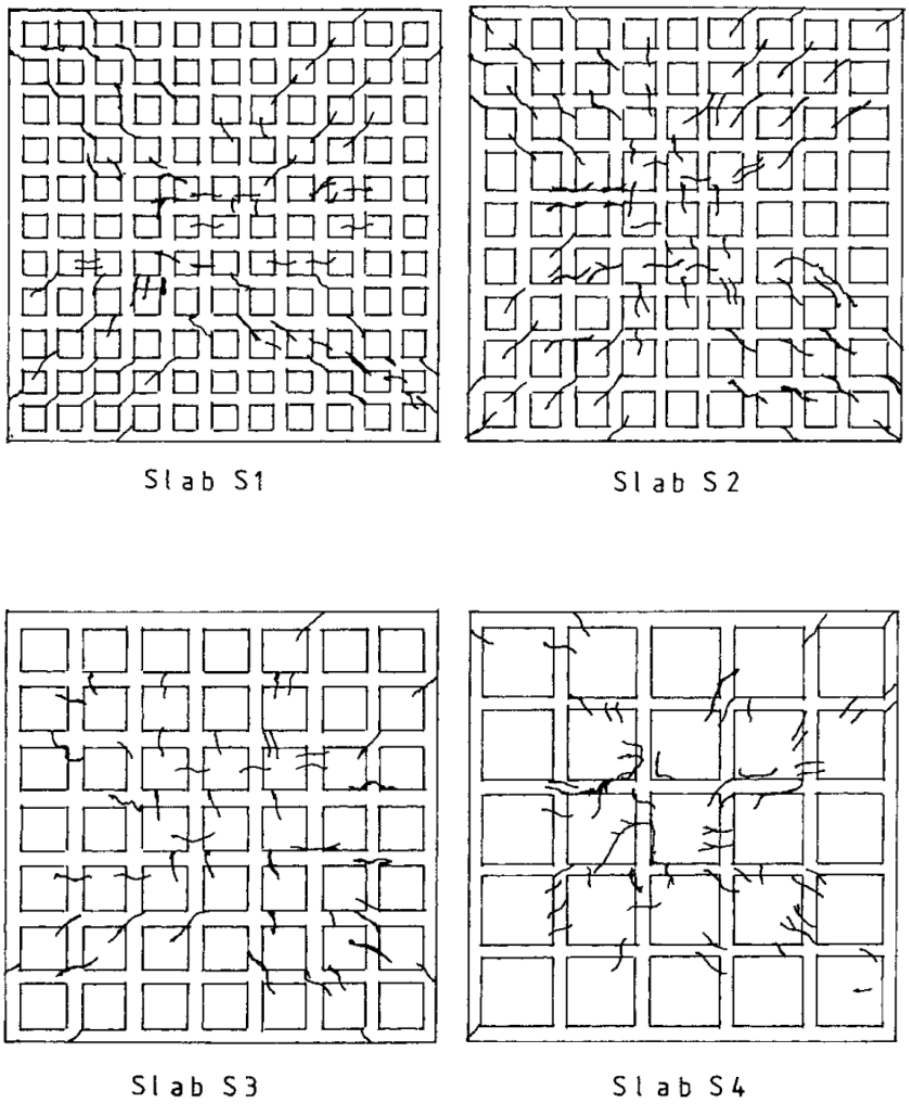

Figure 4.2: Crack Pattern for Experimental Slabs S1-S4

4.2 LINEAR MODEL TO FIND ALLOWABLE SAFE LOAD AS PER ACI-318

Linear strut-and-tie models, for the experimental slabs of Reference [13], are constructed using STAAD Pro to find the proposed safe load carrying capacity as per ACI. All slabs were modeled with linear material models and a static analysis performed. This gives an indication of the factor of safety involved in the design.

4.2.1 Element Type and Material Models

Since all the members are subjected to axial loads only, they are specified as truss members in STAAD. All elements are modeled as prismatic elements and area of each strut-and-tie element is calculated and input in the model.

Both steel and concrete are considered as linear elastic materials as per ACI. At stress levels limited by ACI provisions, this approximation is reasonable and gives conservative results.

Modulus of elasticity of concrete is calculated as

$$E_c = 57000(f'_c)^{1/2}$$

Where, f'_c is the 28 days compressive strength of concrete in psi which is measured separately for each specimen. Poisson's ratio of concrete is considered as 0.20.

For steel, modulus of elasticity, E_s is takes as 200000 Mpa. Yield strength of steel is considered as 398 Mpa. Poisson's ratio of concrete is considered as 0.3.

4.2.2 Application of Loads

4.2.2.1 Self Weight

Self weight is calculated and applied as structural nodal loads at top nodes of the model.

4.2.2.2 Concentrated Load

To stimulate the load at center over an area of 300X300, equal concentrated loads applied on the four central nodes at top. The value of the load is incrementally increased till one of the elements of the truss model reached its safe capacity as per ACI. Strength reduction factors and over strength factors are applied to find the proposed ultimate load.

4.2.3 Results of Linear Analysis Using STAAD

Figure 4.3 shows the geometry of truss model in STAAD. Figure 4.4 shows the force distribution of one of the ribs at the center of the truss model at safe ultimate load of one of the slabs (S2). The middle two ribs in both directions are loaded more and the bottom reinforcement in these ribs reaching the ultimate stress at the failure load. The mode of failure is bending failure since all other elements of the truss model except the bottom reinforcement do not reach their allowable capacity.

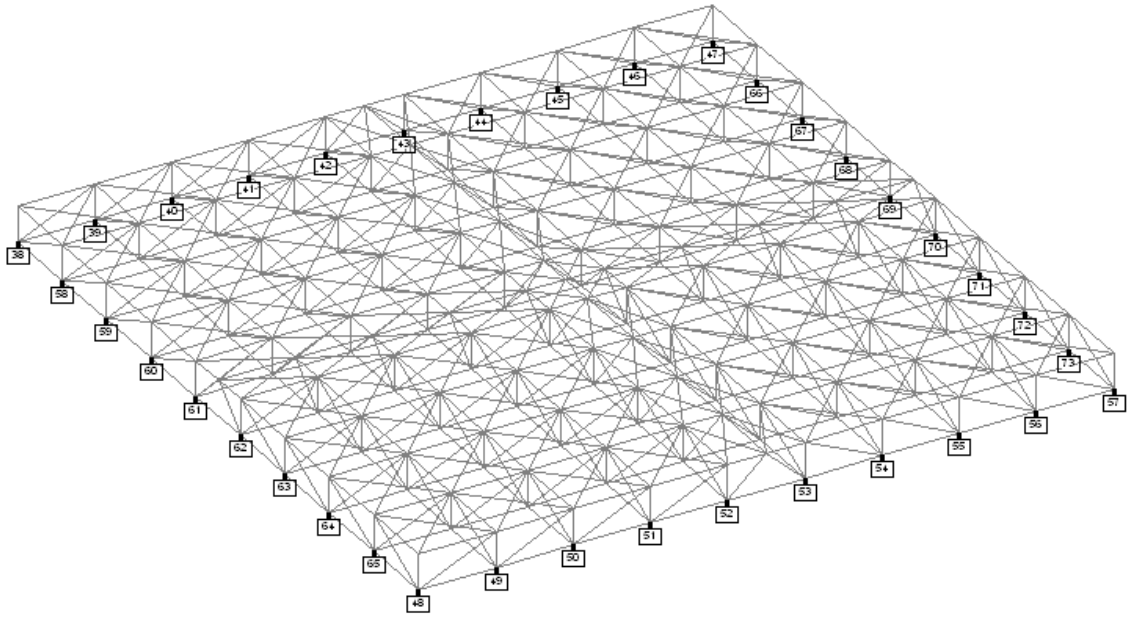

Figure 4.3: STAAD Model for Slab S2-Geometry

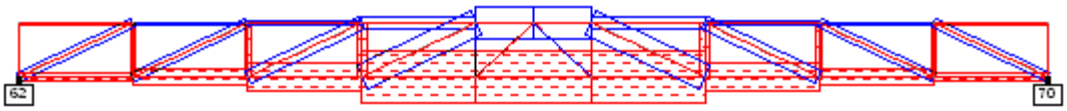

Figure 4.4: STAAD Model for Slab S2-Showing Axial Force Distribution in One Rib

4.3 PREDICTING ULTIMATE LOAD CAPACITY OF SLAB USING NONLINEAR ANSYS MODEL

Nonlinear strut-and-tie models, for all the six experimental slabs, were constructed using ANSYS software. The square slabs used in the experiments are simply supported on four edges with corner lifting allowed. A load higher than the expected failure load is applied. ANSYS analysis engine give converging solutions only up to failure load. It gives the failure load as factor of the total load applied. Then the actual failure load is applied instead of the higher load and stresses in various elements of the truss are plotted using time-history post processing in ANSYS. The mode of failure can be predicted by finding the type of element which reached the ultimate stress at this failure load.

4.3.1 Material Models Used for Non-linear Truss Model

For nonlinear strut-and-tie model, the basic constituents of reinforced concrete, namely concrete and steel are modeled as nonlinear materials, since the slabs are loaded up to failure. As the load is increased in the waffle slab, the stress in each element increases. The distribution of loads on each element of the truss will be proportional to its strain and its relative stiffness. However in a non-linear material model, since the modulus of elasticity of both steel and concrete varies as the stress level is increased, the relative stiffness of various elements in a model varies as the load is increased. This results in redistribution of forces after each load increment.

4.3.1.1 Concrete Used for Top Chord Members and Bracing

Top chord members are prismatic struts and are in the compression zone of the simply supported slab. This allows the concrete in these struts to reach its ultimate compressive strength without any reduction for tension softening.

The compressive strength of concrete used for each specimen is the only measured quantity during testing of the experimental waffle slabs. The study conducted by Ali [16] suggests the following equations to establish the stress strain curve of a concrete specimen.

Strain at ultimate stress,

$$\varepsilon_0 = 0.000875 \, (f'_c)^{0.25}$$

Strain at failure,

$$\varepsilon_u = 0.0078 / (f'_c)^{0.25}$$

Stress f, at a given strain ε is calculated by the formulae,

$$f = f'_c \, [2.1(\varepsilon/\varepsilon_0) - 1.33(\varepsilon/\varepsilon_0)^2 + 0.2(\varepsilon/\varepsilon_0)^3]$$

Stress strain curves are separately plotted for each slab specimen since the compressive strength is varying. The same curves are used in ANSYS models as multi-linear curves. Stress strain curve for concrete in top chord of slab specimen S1 is as shown in Figure 4.5. Poisson's ratio of concrete is considered as 0.20.

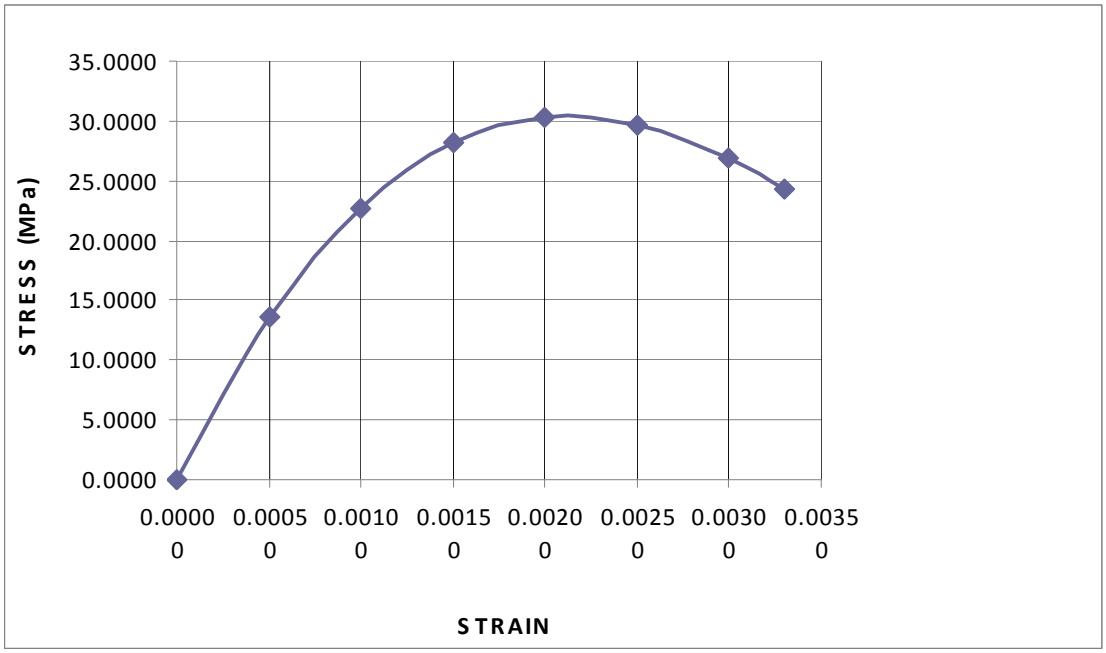

Figure 4.5: Stress Strain Curve Used for Concrete in Top Chord Strut - Slab S1

Bracing members are modeled for the stability of the 3-D truss and maintain relative locations of the nodes at deformed shape. The forces on these members are negligible compared to forces in other truss members and are not governing. Hence concrete models used for top chord members are used for the bracing members also.

4.3.1.2 Concrete Used for Diagonal Members

Diagonal members are bottle shaped struts and the transverse tensile strains in the concrete will develop cracks which results in reducing the compressive strength of concrete near ultimate stage. An efficiency factor of 0.7 is used to account for the tension softening. Stress strain curve for concrete in diagonal member of slab specimen S1 is as shown in Figure 4.6. Poisson's ratio of concrete is considered as 0.20.

4.3.1.3 Concrete used for Vertical Tension ties

For the experimental slabs, since there is no stirrup reinforcements provided, the concrete at intersection of ribs act as vertical tie. The direct tension capacity of concrete is considered as 0.33 * $(f'_c)^{½}$ Mpa. (4 * $(f'_c)^{½}$ psi). A linear stress strain curve is used for concrete in tension. Poisson's ratio of concrete is considered as 0.20.

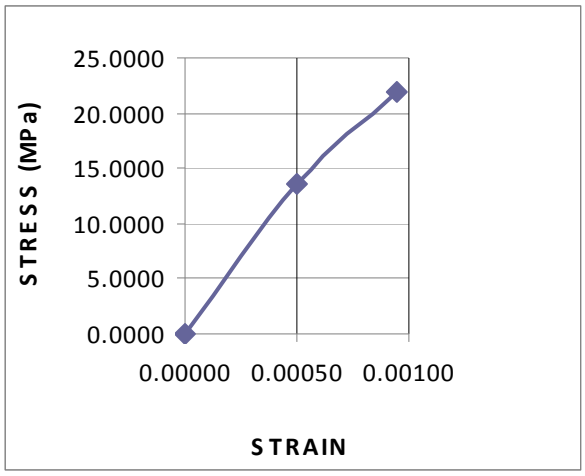

Figure 4.6: Stress Strain Curve Used for Concrete in Diagonal Strut - Slab S1

4.3.1.4 Steel Used as Bottom Chord Reinforcement

The steel used for the main reinforcement of the experimental slabs are with nominal yield strength of 398 Mpa. This is of the range of grade 60 steel (414 Mpa). Based on the experimental study conducted by Mirza and MacGregor [22] on Grade 60 (Fy = 60 ksi) bars, they concluded that the average yield strength is 69 ksi and ultimate strength is 109 ksi. This in the order of 1.15 Fy for actual yield stress and 1.8 Fy for ultimate strength. Also they found the average strain at ultimate stress as 0.12 and average strain at rupture as 0.21.

For the steel used as bottom reinforcement, the actual yield strength is considered as 457.7 MPa and ultimate strength as 716.4 MPa. The average strain at ultimate stress and rupture are considered as 0.12 and 0.21, respectively.

The following stress strain curve as shown in Figure 4.7 is used for reinforcement in the nonlinear model for all specimens. Poisson's ratio of steel is considered as 0.3.

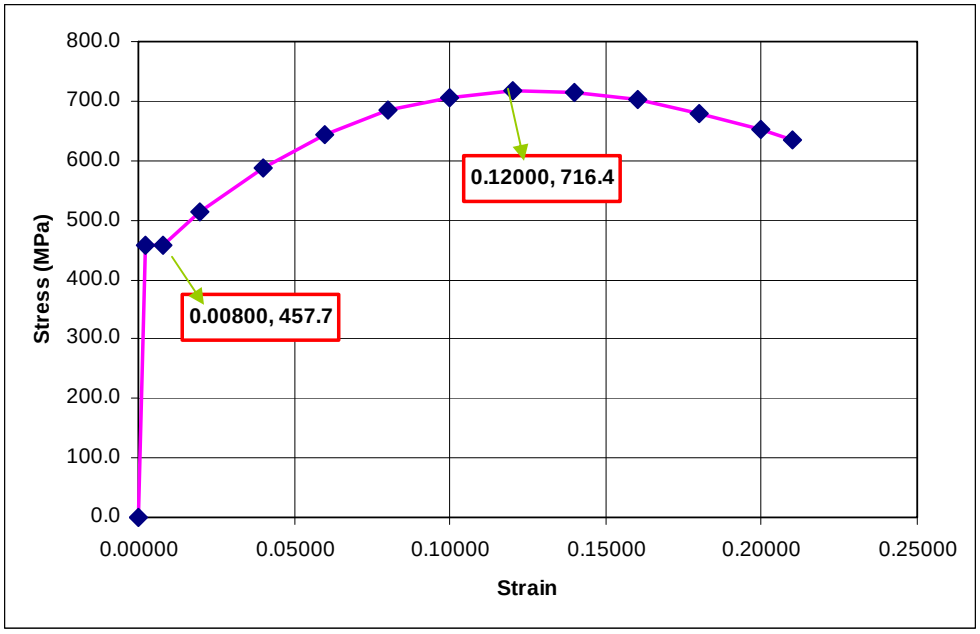

Figure 4.7: Stress Strain Curve Used for Steel Reinforcement

Material model used for reinforcement is multi-linear model with modulus of elasticity, E_s = 200000 MPa up to yield point. For the nonlinear parts of the curve at strain hardening and beyond ultimate strength is plotted based on a 3rd degree curve derived from curve fitting as follows:

$y = 0.2x^3-1.33x^2+2.13x$ where,

$y = (\sigma-457.7)/(716.4-457.7)$

$x = (\varepsilon - 0.008)/(0.12 - 0.008)$

For any value of strain ε, beyond the perfect plastic region, the corresponding stress σ can be evaluated using the above equation.

4.3.1.5 Efficiency Factors Used for Non Linear Model

Table 4.3 shows the efficiency factors considered for nonlinear material models of struts and nodal zones which are used to calculate ultimate strength.

TABLE 4.3: Efficiency Factors Used for Strut-and-Tie Elements and Nodes

Element / Node	Efficiency Factor
Node for Bottom Tie-CTT	0.70
Top strut - Prismatic strut	1.00
Top strut-Node -CCT	0.80
Diagonal strut - Bottle shaped	0.70
Diagonal strut- Node Top - CCT	0.80
Diagonal strut- Node Bottom - CTT	0.70

4.3.2 Element Type and Element Property

Since all the members are subjected to axial loads only, Link-8 elements which are dedicated to 3-D axial elements in ANSYS used for modeling for all elements.

Area of each strut-and-tie element is calculated and input in the model as “real constants” in ANSYS. Separate real constants are defined for each type of elements such as top chord, bottom chord, vertical members, diagonal members and bracing members.

Material models are defined as multi-linear models as mentioned earlier for each type of elements. Each member of the truss model is assigned with corresponding element type, real constant and material model.

4.3.3 Application of Loads

Self weight is calculated and applied as structural nodal loads at top nodes of the model. To stimulate the test load at center over an area of 300mm * 300mm, the load is divided into 4 equal concentrated loads and applied on the four central nodes at top.

4.3.4 Deflected Shape and Force Distribution

Figure 4.8 shows the deflected shape of the truss model at ultimate failure load of one of the slabs, S1. The deflected shape shows maximum deflection at center as expected and corner lifting is evident.

Figure 4.9 shows the force distribution of the truss model at ultimate failure load the slab S1. The middle two ribs in both directions are loaded more and the bottom reinforcement in these ribs reaching the ultimate capacity at the failure load.

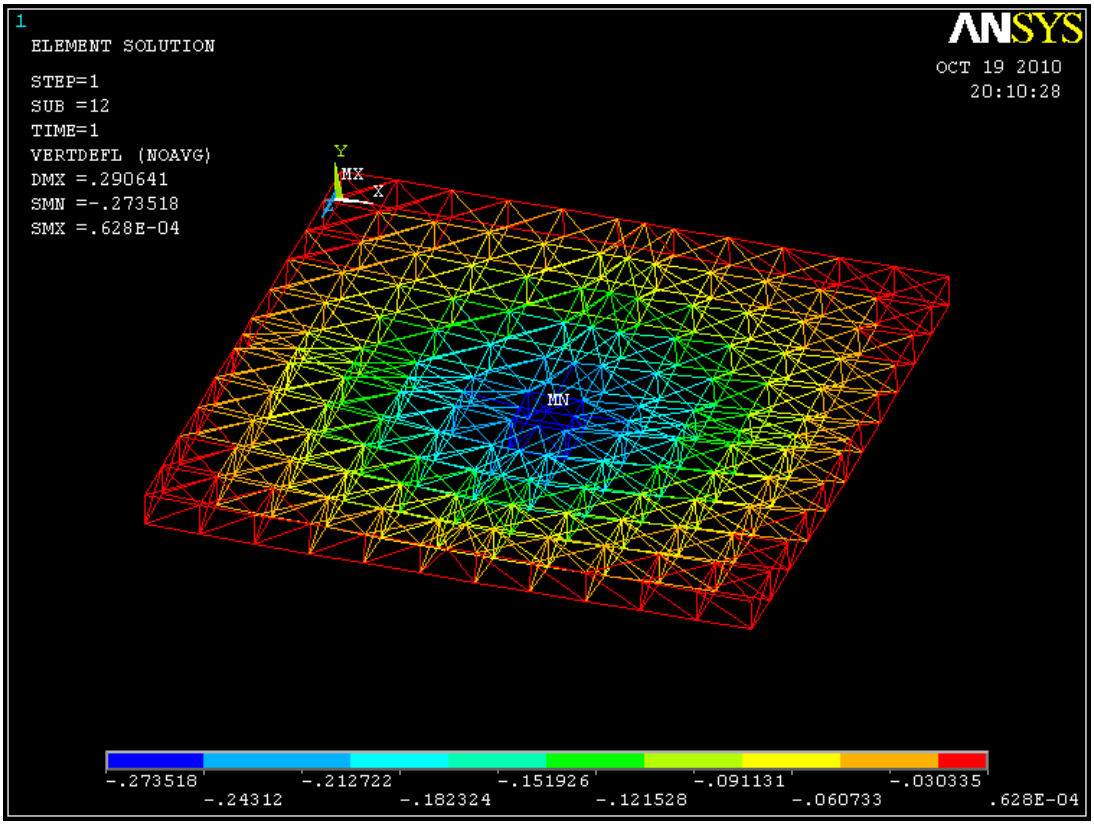

Figure 4.8: ANSYS Model for Slab S1-Showing Deflected Shape

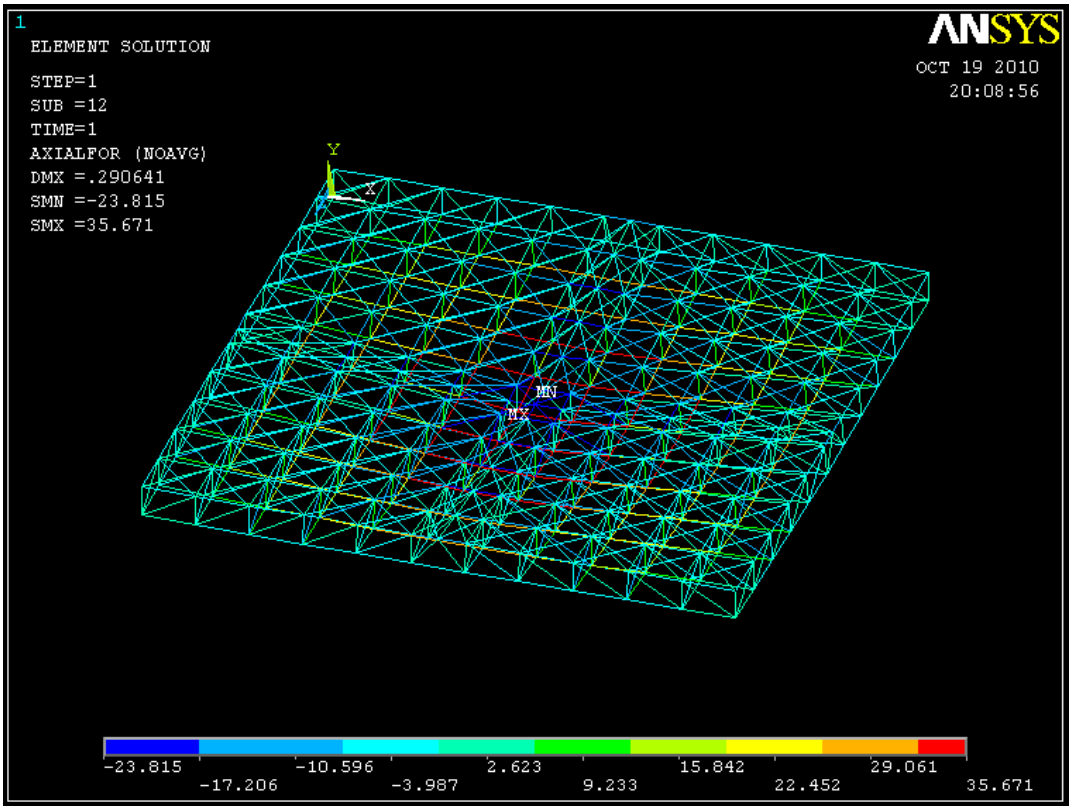

Figure 4.9: ANSYS Model for Slab S1-Showing Force Distribution

4.4 COMPARING RESULTS FROM STRUT-AND-TIE MODELS WITH TEST RESULTS

4.4.1 Strength of Slabs

Table 4.4 shows details of the slabs and a comparison between proposed load as per ACI strut-and-tie recommendations (Load-ACI) , predicted load capacity as per non-linear ANSYS model (Load-NL) and actual capacity of the slab under test (Test load). The predicted loads as per Nonlinear Strut-and-tie models are in good agreement with the actual test loads.

Waffle slabs S1 to S4, which have the same thickness and rib reinforcement but vary in the number of ribs from 5 (S4) to 11 (S1), the load capacity increased as expected, similar to test results as the spacing of ribs is reduced. Figure 4.10 shows the comparison of allowable loads proposed as per ACI, predicted ultimate loads as per nonlinear model and test results of slabs S1-S4. These curves show the effect of rib spacing on the additional live load carrying capacity.

Waffle slabs S6, S2 and S5 in order, have the same number of bays and reinforcement but vary in the size of the ribs. The load capacity increased as the rib size is increased, as expected similar to test results. Figure 4.11 shows the comparison of allowable loads proposed as per ACI, predicted ultimate loads as per nonlinear model and test results of slabs S6, S2 and S5. These curves show the effect of rib size.

TABLE 4.4: Comparison of Results of STM Models with Test Results

Slab	f'_c	Overall Depth mm	Rib Width mm	Rib Spacing mm	STM Load-ACI Pu in kN	STM Load-NL kN	TEST Load kN	Percentage Difference ##	Factor of Safety
S1	31.3	95.0	52.0	136.4	**35.2**	**92.2**	**105.0**	**12.2**	**2.98**
S2	32.0	95.0	52.0	166.7	**31.0**	**79.1**	**81.0**	**2.3**	**2.61**
S3	31.4	95.0	52.0	214.3	**27.2**	**65.0**	**65.0**	**0.0**	**2.39**
S4	28.9	95.0	52.0	300.0	**23.6**	**47.8**	**48.0**	**0.4**	**2.03**
S5	29.9	125.0	57.0	166.7	**43.0**	**109.6**	**120.0**	**8.7**	**2.79**
S6	29.1	65.0	47.0	166.7	**19.0**	**47.7**	**48.0**	**0.7**	**2.53**

- Percentage difference between Test and ANSYS Strut-and-tie model.

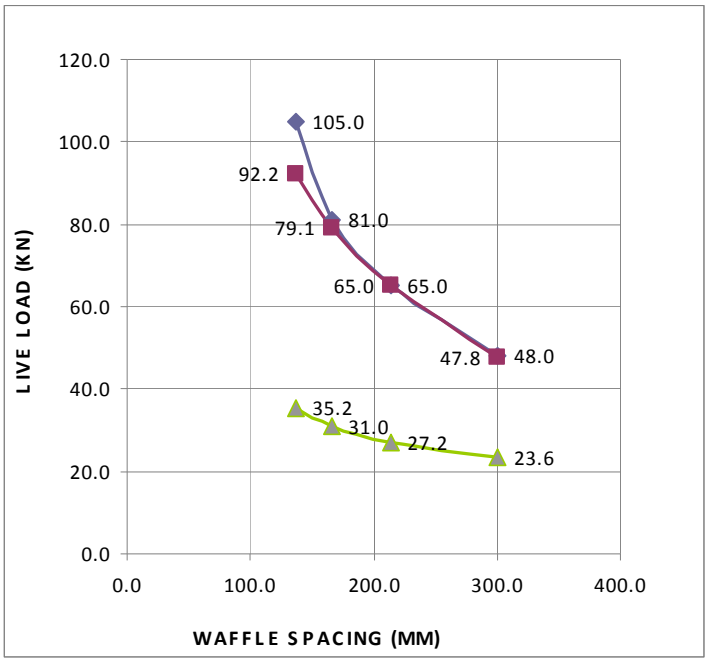

Figure 4.10: Comparison of Results - STM with Test Results -Slabs S1 to S4 (Effect of Rib Spacing)

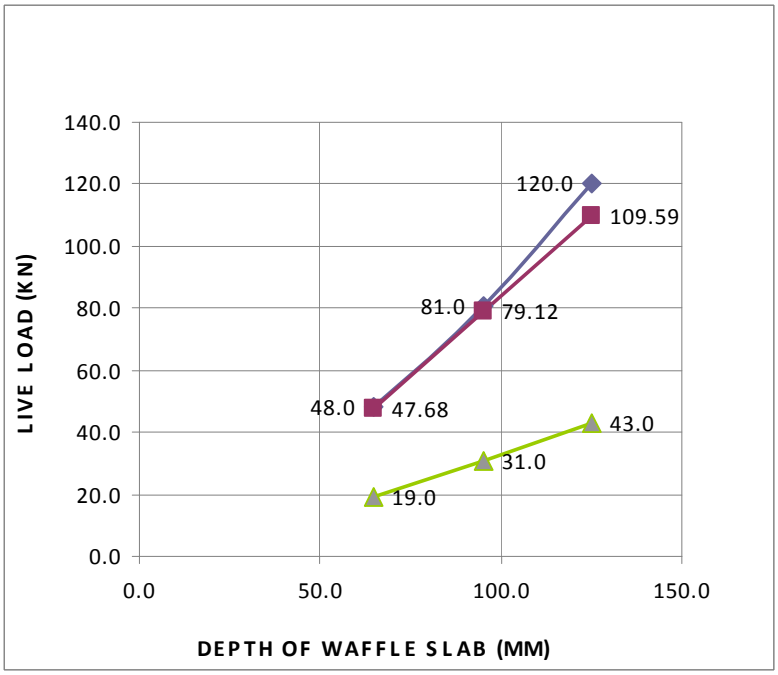

Figure 4.11: Comparison of Results - STM with Test Results -Slabs S6, S2 and S5 (Effect of rib size)

4.4.2 Mode of Failure

Mode of failure was predicted for experimental slabs S1 to S6 based on the non-linear strut-and-tie model. Maximum force in each type of member is noted from the nonlinear model under failure load. The ultimate capacity of each type of member and nodal zone is evaluated. The ratio of the actual force to ultimate capacity will give the stress ratio. Critical member or nodal zone responsible for failure is the one with stress ratio 1.0. All other members will have stress ratio less than 1.0. Tables 4.5 to 4.10 show the forces in each type of member and nodal zone, its ultimate strength and stress ratio for slabs S1 to S6 respectively.

The type of member which is critical will predict the mode of failure. If the bottom reinforcement is critical, the mode of failure is flexural failure. If the diagonal strut near the support fails first, it is a flexural shear failure. If the diagonal strut near the concentrated load fails first, it is a sudden punching shear failure. The bottom nodal zone failure causes slip-bond failure.

Generally top chord failure will not occur unless a very small depth of compression block is considered. This should be avoided by increasing the depth of compression block and slab thickness if required. A vertical member failure is due to the shear forces and is not recommended as well. Sufficient stirrup reinforcement to be provided in case this is the failure mode.

As the waffle spacing is increased from S1 to S4, the mode of failure changes from flexural to shear, as in the experimental results. For the slabs S1 and S2, failure of reinforcement governs the strength as per the nonlinear model which indicates flexural failure, as noted in the experimental results.

TABLE 4.5: Mode of Failure for Slab S1

Member	Area mm^2	Strength (kN)	Forces (kN)	Ratio	Mode of Failure
Diagonal Strut near Load	1794	-39.31	-23.25	0.59	
Nodal Zone for Diagonal-Top	1794	-44.92	-23.25	0.52	
Nodal Zone for Diagonal-Bottom	2426	-53.15	-23.25	0.44	
Top Strut	1364	-42.68	-22.08	0.52	
Nodal Zone for Top Strut	1364	-34.15	-22.08	0.65	
Bottom Tie	50.26	36.00	36.00	**1.00**	**Flexural**
Nodal Zone for Bottom Tie	1248	27.34	20.20	0.74	
Vertical Tie	10816	20.11	11.54	0.57	

Expected mode of failure: **Flexural Failure**

TABLE 4.6: Mode of Failure for Slab S2

Member	Area mm^2	Strength (kN)	Forces (kN)	Ratio	Mode of Failure
Diagonal Strut near Load	1617	-36.22	-23.42	0.65	
Nodal Zone for Diagonal-Top	1617	-41.40	-23.42	0.57	
Nodal Zone for Diagonal-Bottom	2277	-50.99	-23.42	0.46	
Top Strut	1667	-53.33	-23.66	0.44	
Nodal Zone for Top Strut	1667	-42.67	-23.66	0.55	
Bottom Tie	50.26	36.00	36.00	**1.00**	**Flexural**
Nodal Zone for Bottom Tie	1248	27.96	21.15	0.76	
Vertical Tie	10816	20.34	9.91	0.49	

Expected mode of failure: **Flexural Failure**

TABLE 4.7: Mode of Failure for Slab S3

Member	Area mm2	Strength (kN)	Forces (kN)	Ratio	Mode of Failure
Diagonal Strut near Load	1414	-31.07	-30.03	**0.97**	Punching Shear
Nodal Zone for Diagonal-Top	1414	-35.51	-30.03	0.85	
Nodal Zone for Diagonal-Bottom	2098	-46.11	-30.03	0.65	
Top Strut	2020	-63.43	-20.82	0.33	
Nodal Zone for Top Strut	2020	-50.74	-20.82	0.41	
Bottom Tie	50.26	36.00	36.00	**1.00**	**Flexural**
Nodal Zone for Bottom Tie	1248	27.43	16.36	0.60	
Vertical Tie	10816	20.14	10.01	0.50	

Expected mode of failure: **Flexural Failure with punching shear cracks**

TABLE 4.8: Mode of Failure for Slab S4

Member	Area mm^2	Strength (kN)	Forces (kN)	Ratio	Mode of Failure
Diagonal Strut near Load	1184	-23.95	-23.94	**1.00**	Punching Shear
Nodal Zone for Diagonal-Top	1184	-27.37	-23.94	0.87	
Nodal Zone for Diagonal-Bottom	1888	-38.20	-23.94	0.63	
Top Strut	2020	-58.38	-18.41	0.32	
Nodal Zone for Top Strut	2020	-46.70	-18.41	0.39	
Bottom Tie	50.26	36.00	32.80	0.91	
Nodal Zone for Bottom Tie	1248	25.25	23.20	0.92	
Vertical Tie	10816	19.33	6.03	0.31	

Expected mode of failure: **Sudden Punching Shear Failure near Load**

TABLE 4.9: Mode of Failure for Slab S5

Member	Area Mm^2	Strength (kN)	Forces (kN)	Ratio	Mode of Failure
Diagonal Strut near Load	2245	-46.99	-25.27	0.54	
Nodal Zone for Diagonal-Top	2245	-53.70	-25.27	0.47	
Nodal Zone for Diagonal-Bottom	2915	-61.01	-25.27	0.41	
Top Strut	1667	-49.83	-23.28	0.47	
Nodal Zone for Top Strut	1667	-39.87	-23.28	0.58	
Bottom Tie	50.26	36.00	36.00	**1.00**	**Flexural**
Nodal Zone for Bottom Tie	1368	28.63	20.90	0.73	
Vertical Tie	15561	28.28	13.73	0.49	

Expected mode of failure: **Flexural Failure**

TABLE 4.10: Mode of Failure for Slab S6

Member	Area mm^2	Strength (kN)	Forces (kN)	Ratio	Mode of Failure
Diagonal Strut near Load	1063	-21.65	-21.63	**0.999**	Punching Shear
Nodal Zone for Diagonal-Top	1063	-24.75	-21.63	0.874	
Nodal Zone for Diagonal-Bottom	1695	-34.53	-21.63	0.626	
Top Strut	1370	-39.87	-22.60	0.567	
Nodal Zone for Top Strut	1370	-31.89	-22.60	0.709	
Bottom Tie	50.26	36.00	36.00	**1.000**	**Flexural**
Nodal Zone for Bottom Tie	1128	22.98	20.83	0.907	
Vertical Tie	6721	12.05	5.98	0.496	

Expected mode of failure: **Flexural Failure with Shear cracks**

For slabs S3, flexural failure is the predicted failure mode as obtained in actual test. Also the diagonal strut is reaches a stress ratio of 0.97 which indicates occurrence of shear cracks as obtained in the actual test.

For slab S4, failure of diagonal bottle shaped strut near the load limit the load carrying capacity of the slab, which is a clear indication of a sudden punching shear failure as obtained in experimental result.

The predicted mode of failure for slabs S5 is flexural failure as per nonlinear strut-and-tie model. However the actual failure during test was reported as sudden failure due to slip bond failure. Also in this slab, the second highest stress ratio was for bottom nodal zone which represent slip bond failure. The difference may be due to higher strength of actual reinforcement, more cover for reinforcement or a local failure occurred during the test due to removal of some portion of concrete surrounding the reinforcement during crack propagation.

For slabs S6, flexural failure is the predicted failure mode as obtained in actual test. However the diagonal strut is reaching a stress ratio of 0.99 which indicates occurrence of shear cracks as well which was not reported in the literature.

4.4.3 Time-History Post Processing -Load Deflection Curves

Using the time history post processing in ANSYS, load deflection curves are plotted for experimental slabs S1 to S6. The sudden drop in the stiffness beyond 50 % of the ultimate capacity gives a good indication of the safe range of loading and justifies the factor of safety provided by ACI strut-and-tie provisions. Figure 4.12 to 4.17 shows load –deflection curves for slabs S1 to S6 respectively. The value shows deflection in meters and time shows the factor of failure load.

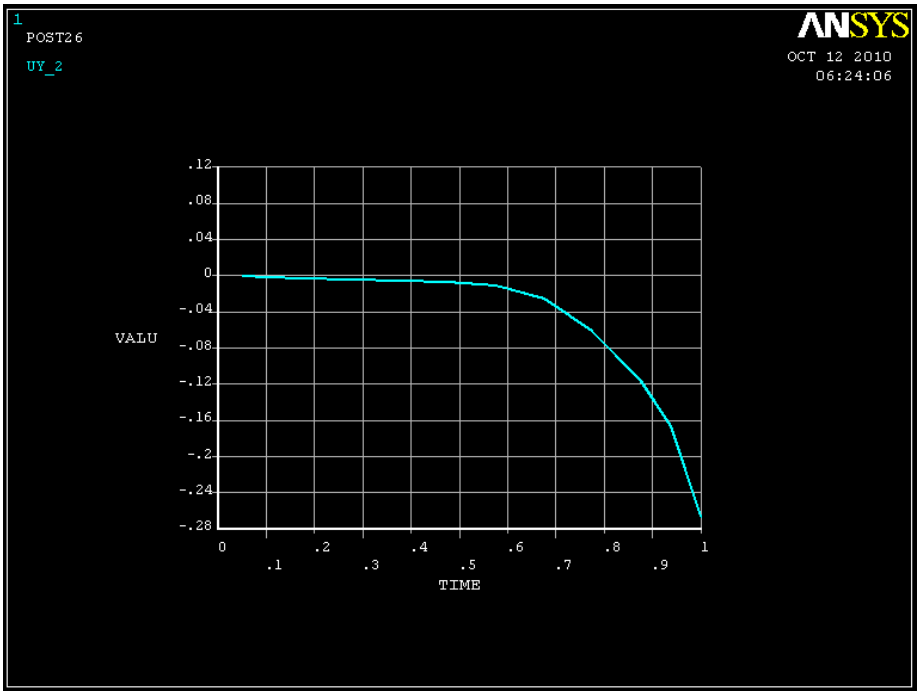

Figure 4.12: Load-Deflection Curves for Slabs S1

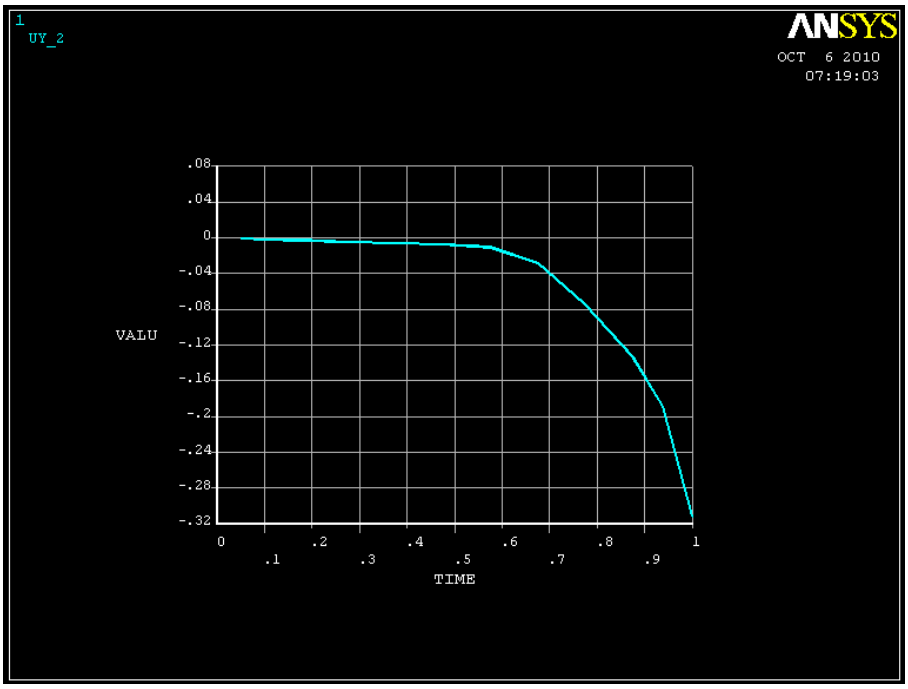

Figure 4.13: Load-Deflection Curves for Slabs S2

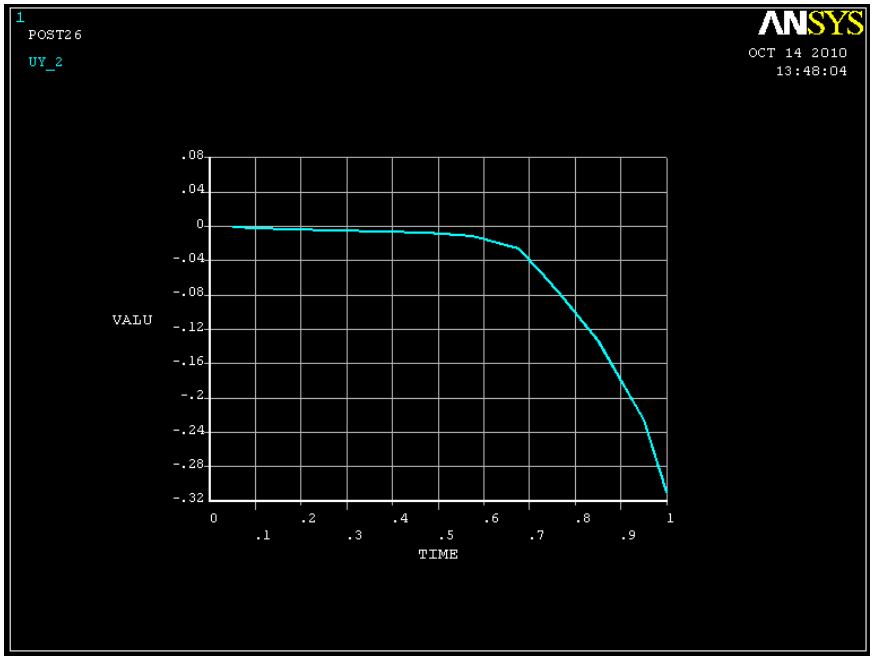

Figure 4.14: Load-Deflection Curves for Slabs S3

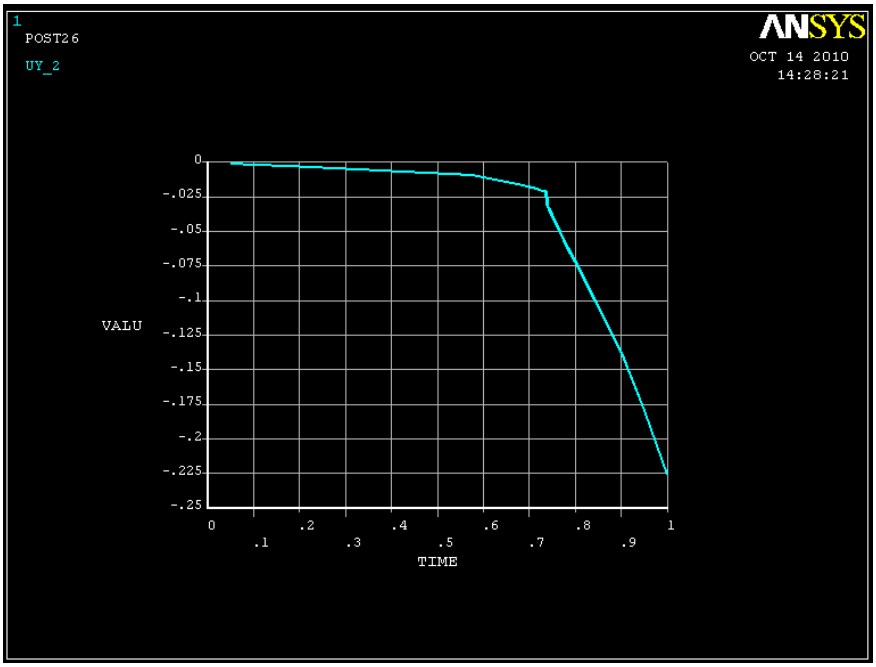

Figure 4.15: Load-Deflection Curves for Slabs S4

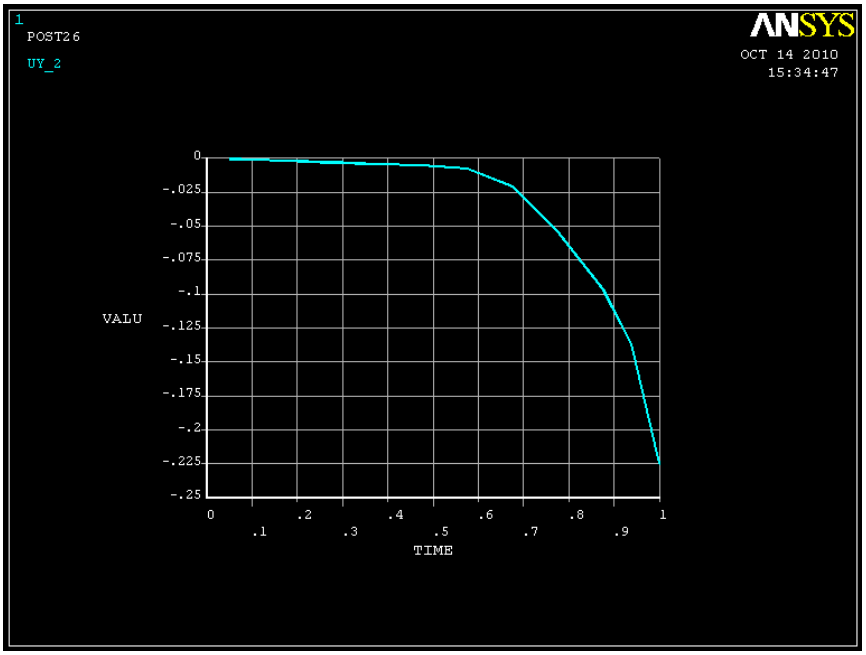

Figure 4.16: Load-Deflection Curves for Slabs S5

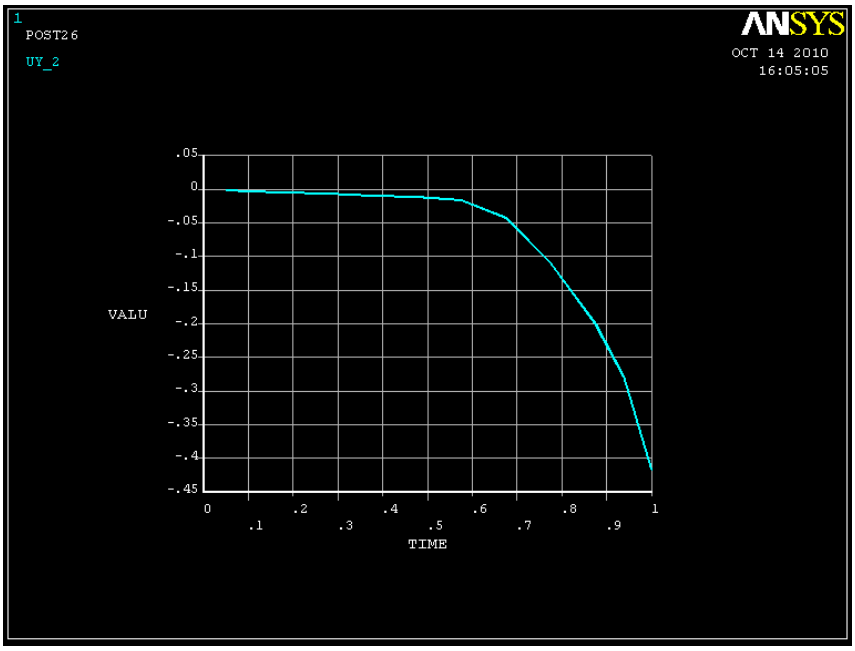

Figure 4.17: Load-Deflection Curves for Slabs S6

A sudden drop in stiffness of slab S4 is noted which has larger rib spacing and mode of failure is shear failure. As the ribs are spaced closer, better redistribution of forces take place after yielding of reinforcement and the load deflection curve will be a smooth curve.

4.4.4 Time-History Post Processing -Load Distribution between Ribs

The time history post processing in ANSYS gives a good insight on the load carrying mechanism and distribution of forces during each load increment. The force at bottom reinforcement at center of each rib is plotted. It clearly shows the yield point of reinforcement in each rib and the redistribution of forces after the yield point. Also the distribution of forces till the first yielding of the middle rib is more or less proportional to its distance from support, with center rib carrying the maximum forces. However after yielding of main reinforcement, since the stiffness of the ribs drops significantly, the ribs which are away from the center start taking a major contribution of the additional load and finally at ultimate stages, the variation of forces shared by ribs reduces to a minimum.

Figure 4.18 to 4.23 shows force in bottom reinforcement at center of rib for each rib for slabs S1 to S6 respectively. Rib1 is the rib near center and Rib2 the next and so on.

Yield capacity of the reinforcement is 23 kN and its ultimate capacity is 36 kN. Figure 4.18 shows force in bottom reinforcement at center of rib for slab S1. As the load increases, the axial forces in bottom reinforcement of ribs increase for all the ribs. However since the axial force in reinforcement of the rib near center of the slab (Rib-1) is more and it is evident that it carries more load. The distribution to other ribs is proportional to its distance from center up to yielding of the first rib.

The yielding of reinforcement in Rib 1 takes place at about 47% of the predicted capacity. Since the stiffness of reinforcement drastically reduced after yielding, the further increase in load is mainly shared by other ribs which are not yet yielded. This is clear from the drastic reduction in slope for the curve for Rib 1 and increase in slope for other ribs.

The yielding of reinforcement in Rib 2 takes place at about 58% of the predicted capacity. Further increase in load is mainly shared by other ribs which are not yet yielded. This is clear from the drastic reduction in slope for the curve for Rib 2 and increase in slope for ribs 3 to 5.

Rib 3 and Rib4 of slab S1 reached the yield point almost at the same time at around 67% of the predicted capacity. At this point the only rib left is Rib5 without yielding and which is away from the center concentrated load. The overall stiffness of the slab also reduces drastically at this point. Since load needs to be transferred to the exterior ribs and to supports, rib 1 to 4 share more load till the reinforcement in Rib 1 reaches its ultimate strength which is the limit of strength for slab also.

Figure 4.18 clearly shows the redistribution of forces between ribs after yielding and at the time of failure, force in reinforcement for ribs 2 to 4 are very close to ultimate. Even in rib 5 which is away from the center, the force in reinforcement is yielded and reached around 73% of the ultimate capacity.

Figures 4.19, 4.20 and 4.21 show the force in bottom reinforcement at center of ribs for slabs S2, S3 and S4 respectively. The difference is that due to increase in rib spacing, the number of ribs is less. Since the number of ribs are less and spaced apart, there is not

much scope for redistribution and resulted in a lower failure load as obtained by experimental results as we increase rib spacing to a larger value.

Since the mode of failure is shear failure for slab S4, even the reinforcement at middle rib directly under the load itself is not reached its ultimate capacity. The axial stress in the diagonal member radiating away from the concentrated load reached its ultimate strength at failure load, which indicates a sudden punching shear failure as obtained in experiment.

For slabs S6, S2 and S5 in order, the number of ribs is same due to the same rib spacing and load distribution to ribs is more or less same as can be seen in Figures 4.23, 4.19 and 4.23, respectively. However the capacity of the slab increased as the rib size is increased, matching the experimental results.

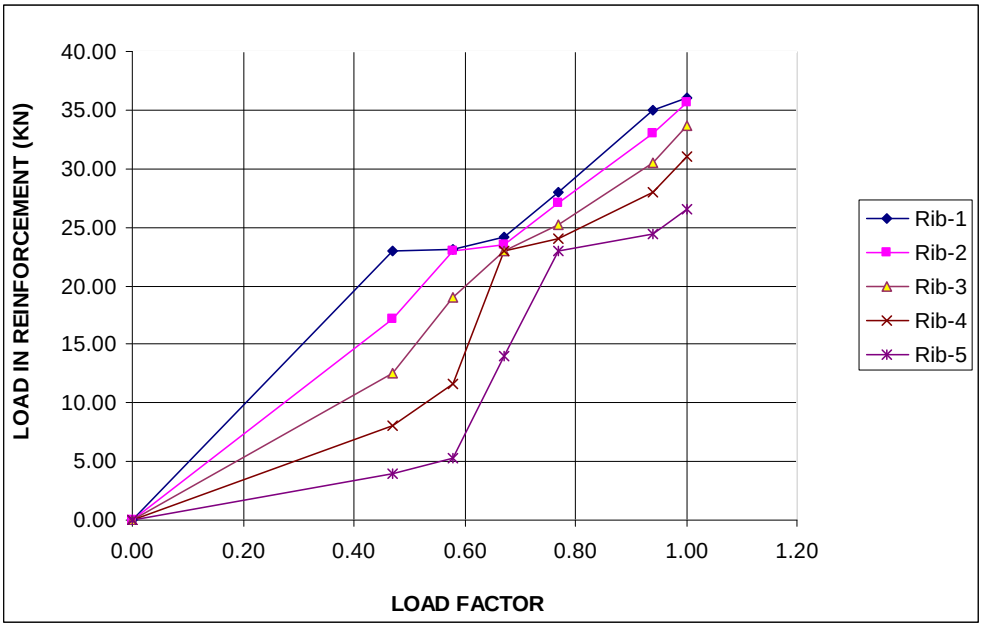

Figure 4.18: Force in Bottom Reinforcement at Center of Ribs-Slab S1

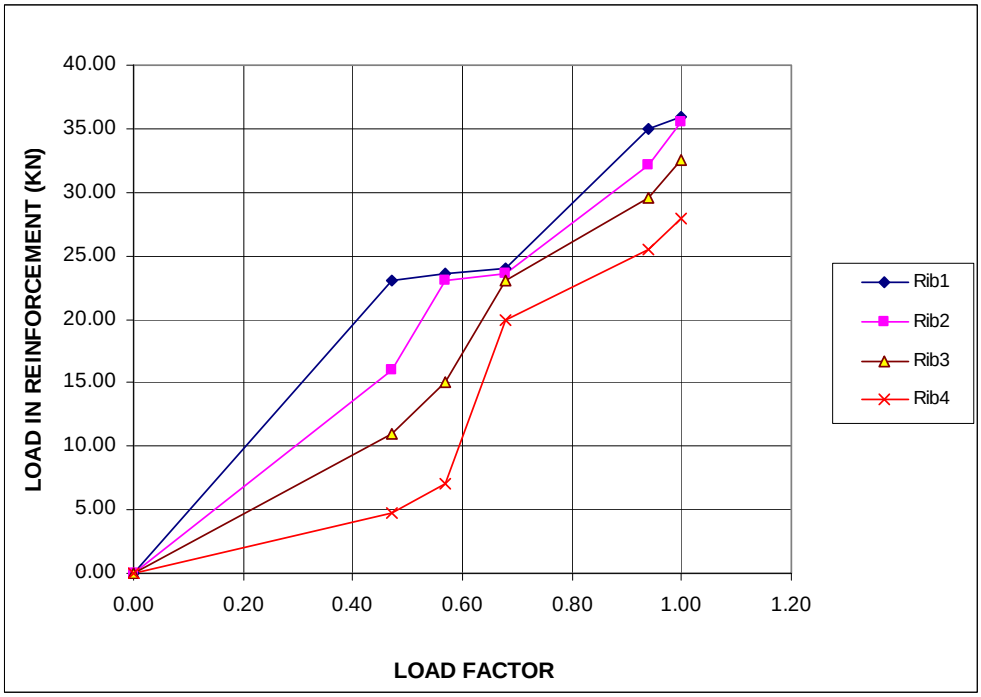

Figure 4.19: Force in Bottom Reinforcement at Center of Ribs-Slab S2

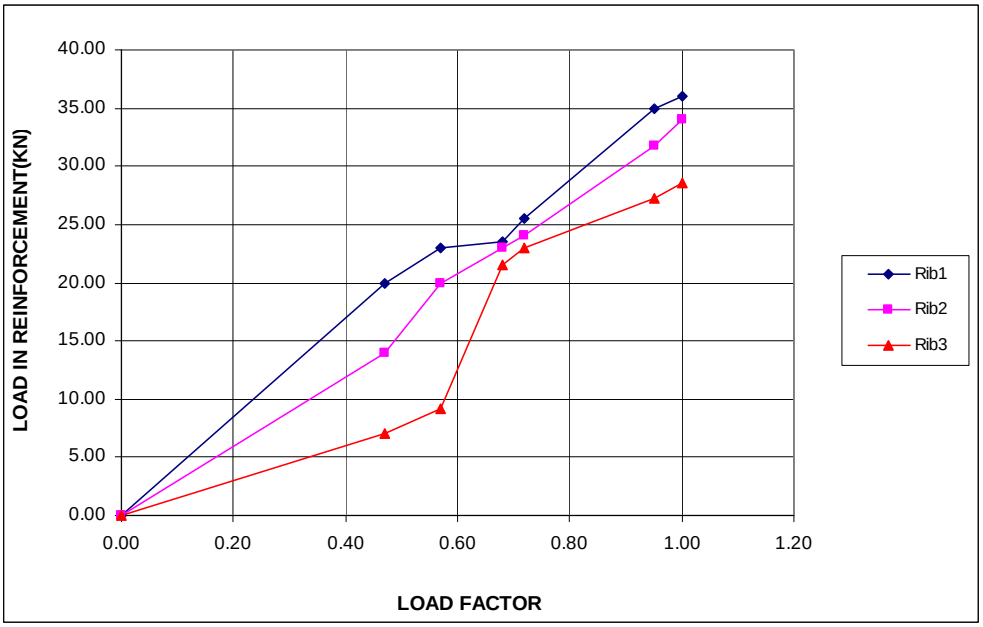

Figure 4.20: Force in Bottom Reinforcement at Center of Ribs-Slab S3

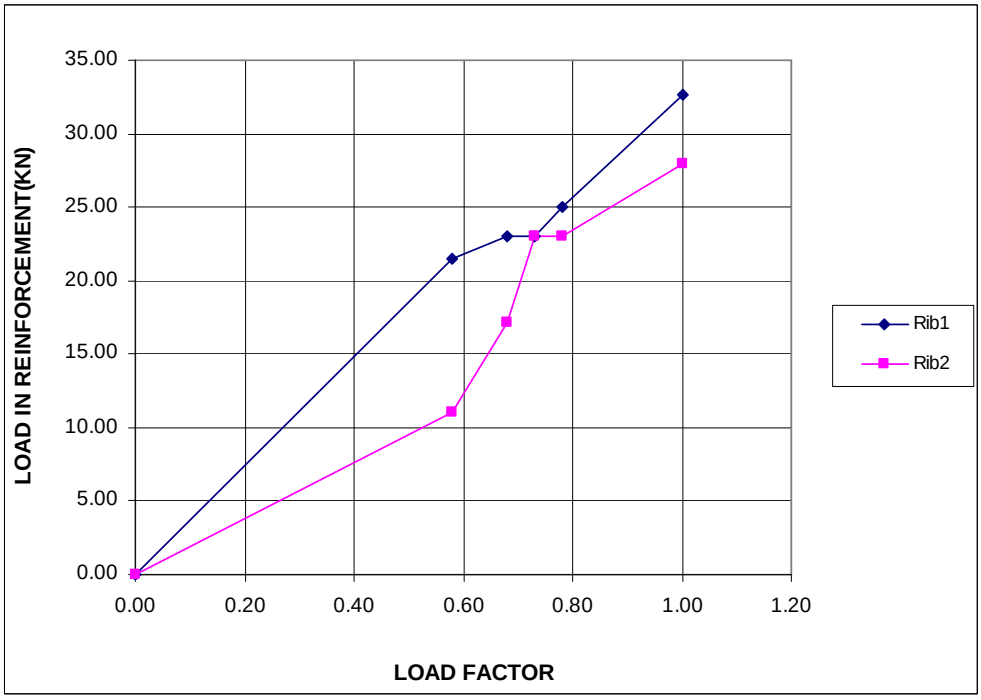

Figure 4.21: Force in Bottom Reinforcement at Center of Ribs-Slab S4

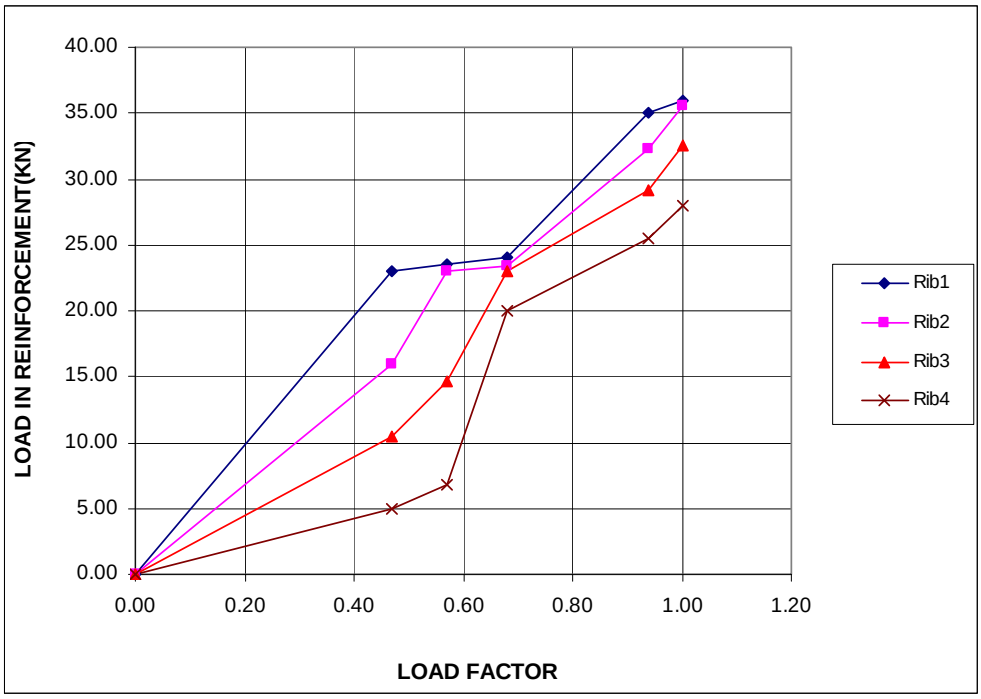

Figure 4.22: Force in Bottom Reinforcement at Center of Ribs-Slab S5

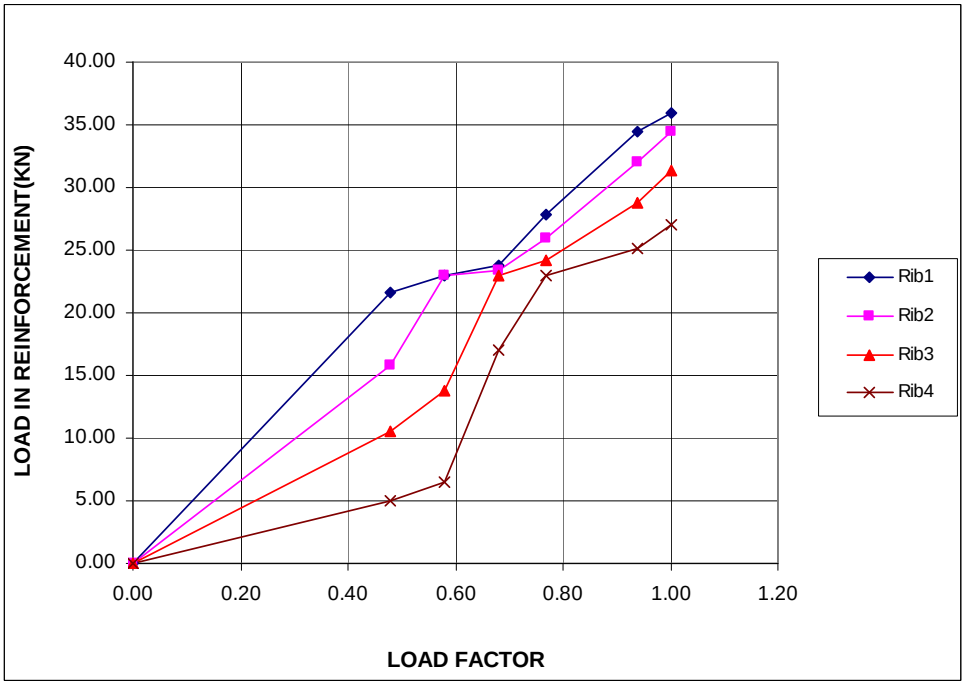

Figure 4.23: Force in Bottom Reinforcement at Center of Ribs-Slab S6

CHAPTER 5

STWAF ANALYSIS AND DESIGN TOOL FOR WAFFLE SLABS

5.1 INTRODUCTION

Geometrically waffle slab is a complicated structure and the proposed three dimensional strut-and-tie models consist of a large number of elements and nodes. Manual generation of the truss is time consuming and will limit the usage of the method. Hence user-friendly software dedicated for fully automatic generation of the 3D truss is developed.

Software "STWAF" (Strut-and-tie for Waffle slab) is developed in this thesis for simply supported waffle slabs supported on four edges. Figure 5.1 shows the flow chart of STWAF showing the working procedure for design of a waffle slab.

5.1.1 Design Methodology Used in STWAF

STWAF is a design tool developed using visual basic and is capable of interacting with user for the input and output. Based on user input, on the dimensions of waffle slab and loading, STWAF automatically generates a 3D truss model. Loads are factored as per ACI. The properties of the elements of the truss model are calculated based on strut-and-tie design principles as per ACI-318 recommendations. Basically it generates a STAAD input file for the proposed 3D truss. Then user can do analysis of the truss with STAAD Pro analysis engine from STWAF environment. STWAF interacts with STAAD output to extract member forces which are used in design of elements and nodal zones of the 3D strut-and-tie model.

Maximum force for each type of elements is calculated by STWAF from the output of the analysis. Nominal strength of each type of element is calculated as per ACI-318-2008 based on cross sectional area, material properties and effective stress factors. Safe ultimate loads are calculated by multiplying by strength reduction factor. Stress ratio for each type of element is calculated as ratio of maximum force under factored loads in the element to the safe ultimate load. Similarly stress ratios for nodal zones are also calculated.

For a safe design, all stress ratios should be less than 1.0. Also by comparing the stress ratios of each type of element, the mode of failure can be predicted. The data can be revised partly or completely, till all elements are safe and desired mode of failure is obtained for the slab.

5.1.2 Salient Features of STWAF

The main features of STWAF can be summarized as follows:

- User friendly input.
- ACI-318 Strut-and-tie provisions are incorporated in calculating sizes of struts, ties and nodal zones.
- Fully automated generation of 3D truss.
- STWAF automatically interacts with STAAD Pro to generate STAAD model.
- User interference is allowed on generated 3D truss model to apply additional concentrated loads, if any.
- Analysis using STAAD Pro analysis engine.

- User can view analysis results directly from STAAD Pro graphic environment, even though it is not needed for practical design.
- STWAF automatically extracts member forces from STAAD output for the design of strut-and-tie elements and nodal zones.
- The member force for each type of element is displayed and maximum governing force is reported.
- ACI-318 strut-and-tie provisions are incorporated in calculating strength of struts, ties and nodal zones.
- Design of each type element and nodal zone can be obtained from STWAF.
- A summary of stress ratios is reported for the ease of optimization process.
- The stress ratios of different types of elements and nodal zones indicate the expected mode of failure.
- The whole design process is faster and will result in fully optimized design with known mode of failure under overloading.
- Detailing aspects of the slab like min concrete cover, minimum thickness of ribs etc. can be obtained by few trials.
- STWAF allows the designer with relatively small effort to gain a better understanding of the likely performance of the structure and then to make design changes to improve performance under ultimate loads.

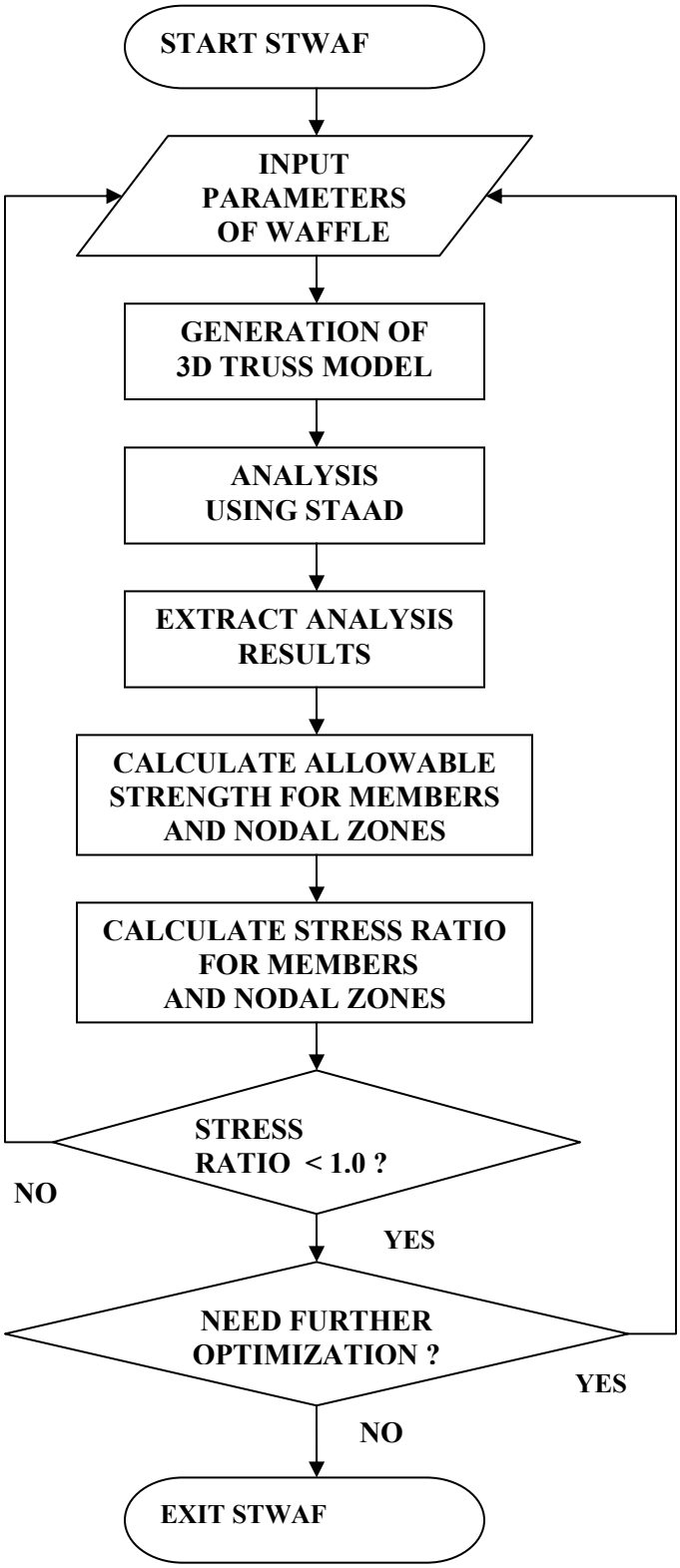

Figure 5.1: Flow Chart for STWAF

5.2 USER INPUTS IN STWAF

The main window of the program contain drop down menu which gives access to all windows for user inter face as shown in Figure 5.2.

The inputs are divided into different windows and are arranged in order for easy access as shown in Figure 5.3 to 5.7. The material properties are specified in general input window as shown in Figure 5.3. Dimensions of the waffle slab like slab thickness, overall depth and span in X and Y directions are provided in second window as shown in Figure 5.4.

Rib thickness and number of waffle openings in X and Y directions are specified in next window as shown in Figure 5.5. The clear depth of ribs below slab and center to center spacing of ribs will be calculated and displayed by the program. The rib thickness is considered same for all ribs in X and Y directions. Rib spacing need not be same in each direction and is calculated based on span and number of waffle openings.

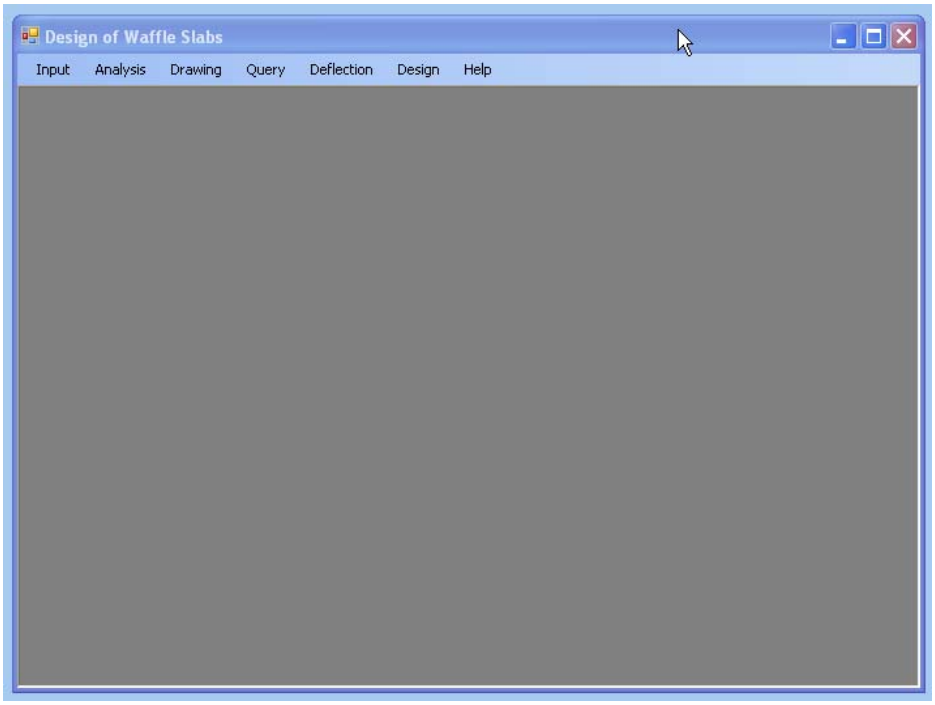

Figure 5.2: Main Window of STWAF

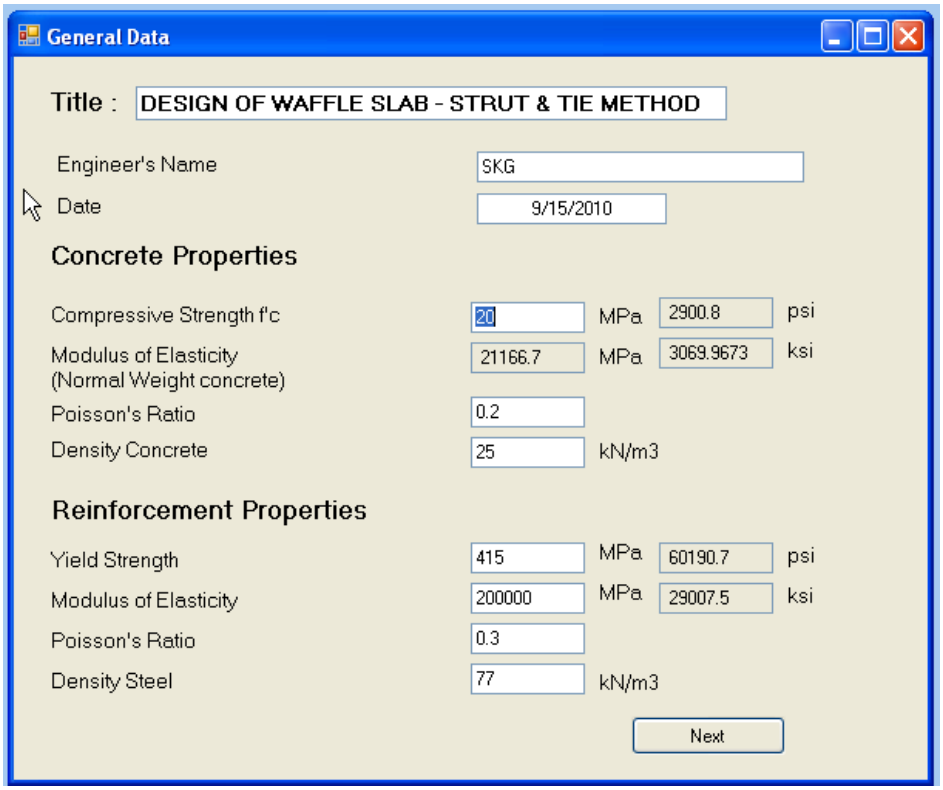

Figure 5.3: General Input Window

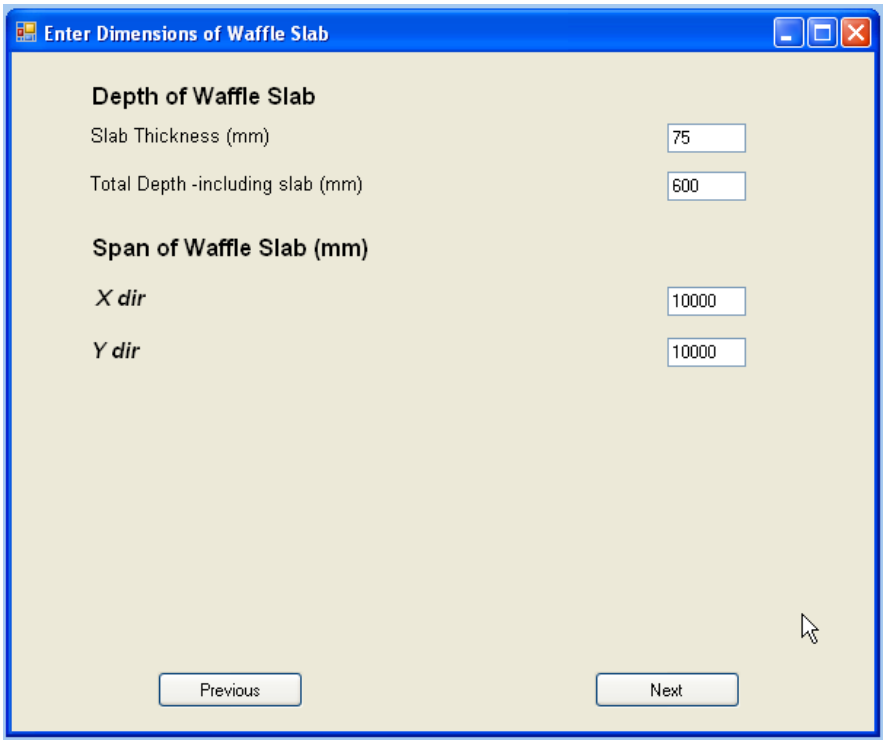

Figure 5.4: Input Window for Overall Size of Waffle Slab

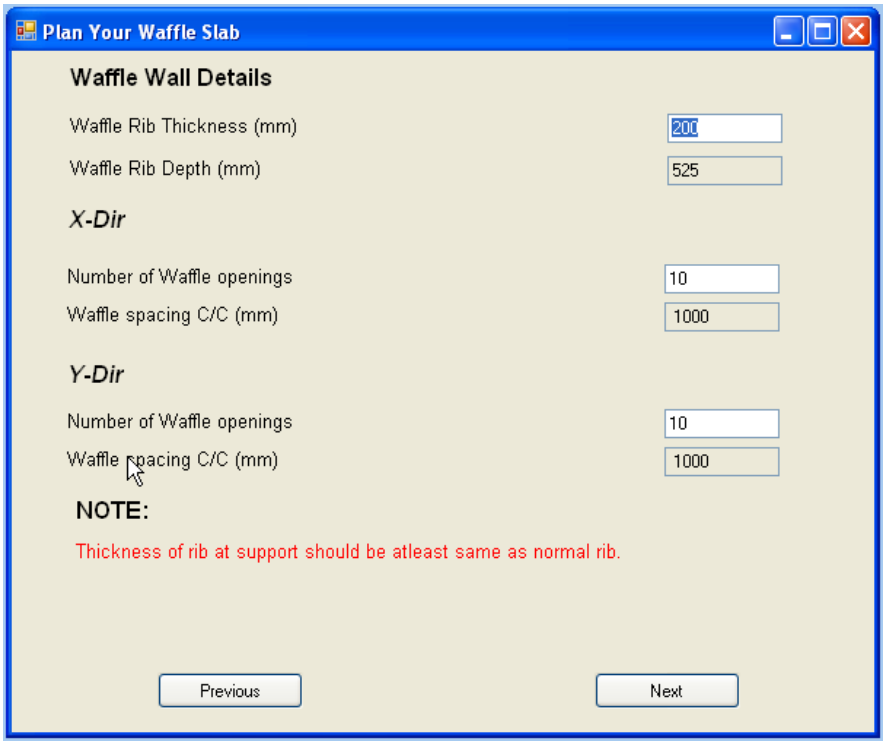

Figure 5.5: Input Window for Rib Size and Spacing

Reinforcement details and depth of compression block is specified in next window as shown in Figure 5.6. The diameter and number of bars can be specified in each rib for both directions separately. The area of reinforcement will be calculated and displayed automatically.

For conventional methods, the slab is divided in to middle strip and column strip and bending moment is calculated for the entire width of each strip. This bending moment is equally distributed to all the ribs in the strip, which allows redistribution of forces. An over strength factor is specified in STWAF for the bottom reinforcement and its default value is 1.25. The user is able to edit this factor and can reduce it, in case he needs to be conservative.

STWAF can handle waffle slabs with and without stirrup reinforcement. However the default design is kept with reinforcement since it is a normal practice to provide stirrups in the ribs. The diameter and number of stirrup legs in one rib can be specified. Same stirrups are considered in both directions in current version of STWAF. The area of reinforcement will be calculated and displayed automatically.

Effective cover of reinforcement is to be specified which is the sum of clear cover and diameter of main reinforcement. The same effective cover is considered in both X and Y directions to maintain the same depth for the entire 3D truss.

Depth of compression block to be specified which should be less than the slab thickness. The thickness of top chord will be considered as this depth and a minimum thickness is recommended for optimization. When this is reduced, the truss depth increases and hence axial forces in top chord and bottom chord reduce. However the depth should be selected such that it is sufficient to avoid compression failure for the top

struts. It can be obtained accurately by 2-3 trials. However for practical design purposes, a larger depth like half the slab thickness can be conservatively considered since its effect on truss depth is very less thereafter.

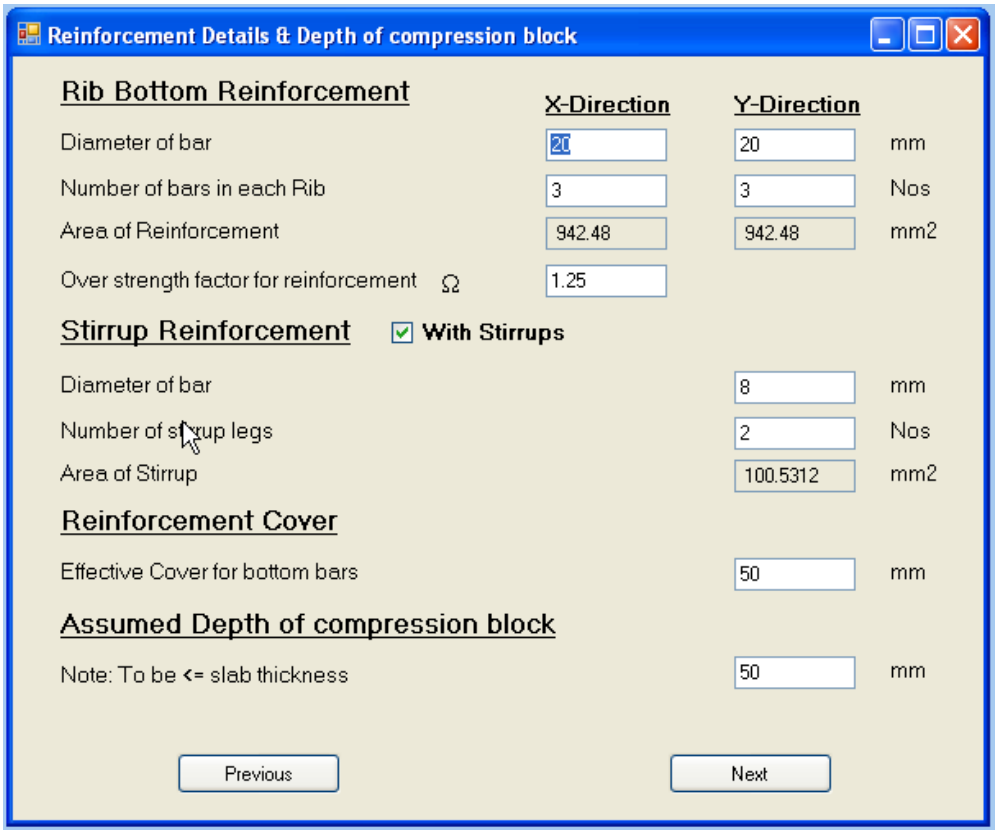

Figure 5.6: Window for Reinforcement Details and Depth of Compression Block

Current version of STWAF supports uniformly distributed loads as shown in Figure 5.7. The program is capable of calculating its self weight. However if the user wants to input it as a uniformly distributed load (UDL) including weight of finishes etc, it is possible as well. It is also possible to generate its self weight by program and give additional dead load as uniformly distributed dead load. Live load is given as UDL. Load factors will be considered by program as per ACI and displayed separately for deflection and strength.

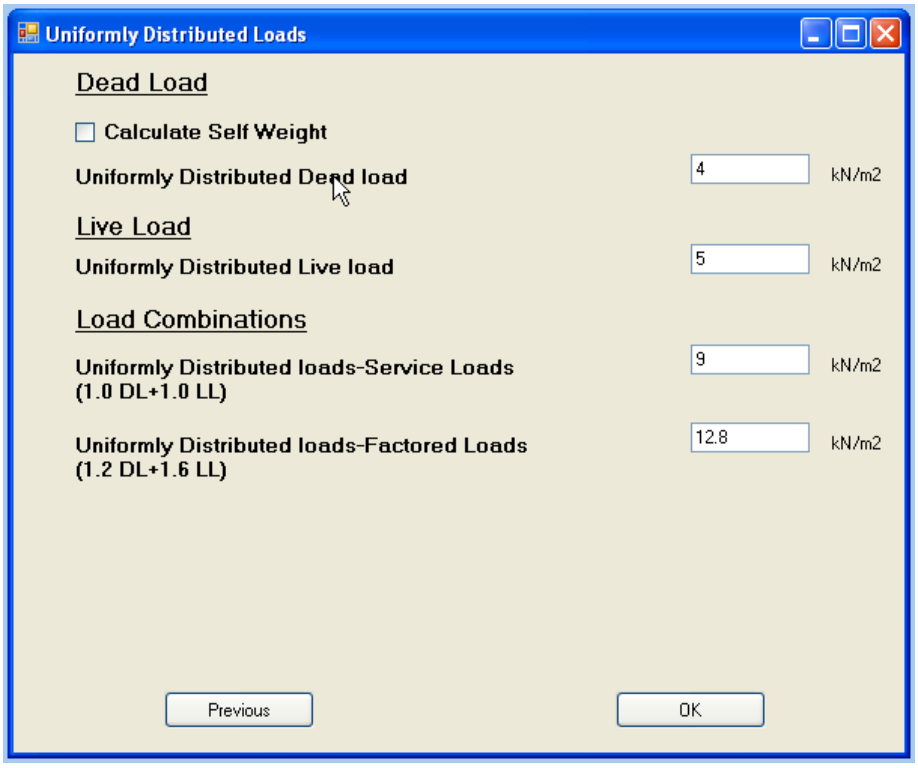

Figure 5.7: Window for Load Input

5.3 GENERATION OF 3D TRUSS MODEL AND ITS ANALYSIS

STAAD Pro analysis engine is used by STWAF for the linear analysis of the 3D truss. Once the input is over, user can go to Analysis menu and click “Run STAAD” command. This generates STAAD input file for the 3D truss and opens STAAD Pro environment automatically, provided the STAAD Pro is installed in the System. Then user can run analysis from STAAD Pro.

User can use all features of STAAD Pro to view input and output. Even some additional concentrated loads can be added in the model but will be the responsibility of the user on the accuracy of the load and its location. Also it should be in compatible units of the existing loads.

Once analysis is over, user can close STAAD Pro. STWAF interacts with STAAD output file automatically to extract member forces.

5.4 CALCULATING MAXIMUM FORCES, STRENGTH AND STRESS RATIO FOR EACH MEMBER TYPE

Maximum force for each type of elements is calculated by STWAF from the output of the analysis. The axial force for each type of element and maximum force can be displayed from the program from Analysis menu similar to the one shown in Figure 5.8, which is made for bottom chord members in X direction and is used for calculating reinforcement for ribs in X direction. Similarly forces in all types of elements can be displayed.

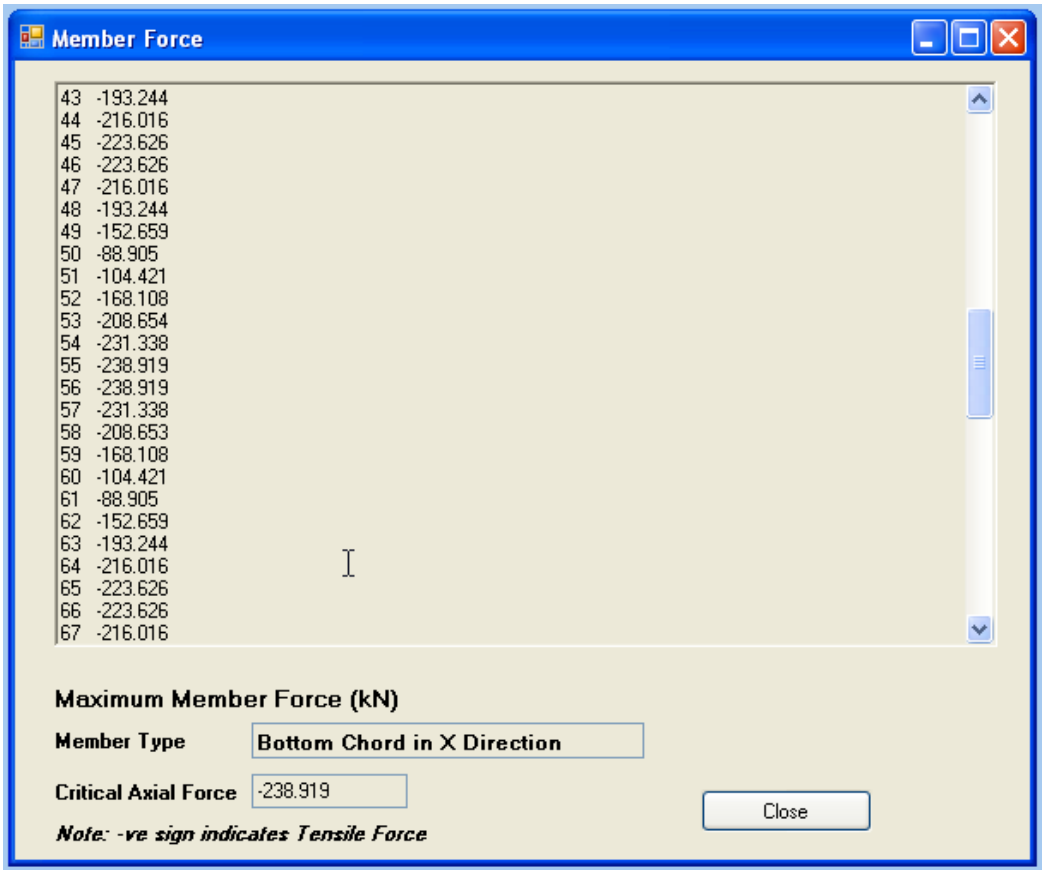

Figure 5.8: Display of Member Force for Bottom Chord in X-direction

5.5 DESIGN OF ELEMENTS AND NODAL ZONES OF STRUT-AND-TIE MODEL

Nominal strength of each type of element is calculated as per ACI-318-2008 based on cross sectional area, material properties and effective stress factors. Safe ultimate loads are calculated by multiplying by strength reduction factor. In case of bottom reinforcement, an additional over strength factor is used to distribute the stress to more ribs. A dimensionless parameter termed stress ratio is introduced, given by ratio of maximum force under factored loads in the element to its safe strength. Similarly stress ratios for nodal zones are also calculated.

Figure 5.9 shows design of bottom chord, which is the main reinforcement. Design of reinforcement in X and Y directions are shown in same window. Similarly design of other elements and nodal zones can be displayed. Typical outputs of SWAF for design of various elements and nodal zones are shown in Chapter 6.

A stress ratio greater than 1.0 indicates that the member or nodal zone is not having the sufficient strength, as obtained by the code provisions, to resist the external load. For a given external load and material properties, the size of member has to be increased to keep all stress ratios less than 1.0 for safe design.

For ease of optimization the summary of design is displayed in a separate window. Stress ratios for all elements and nodal zones are displayed in this window as shown in Figure 5.10.

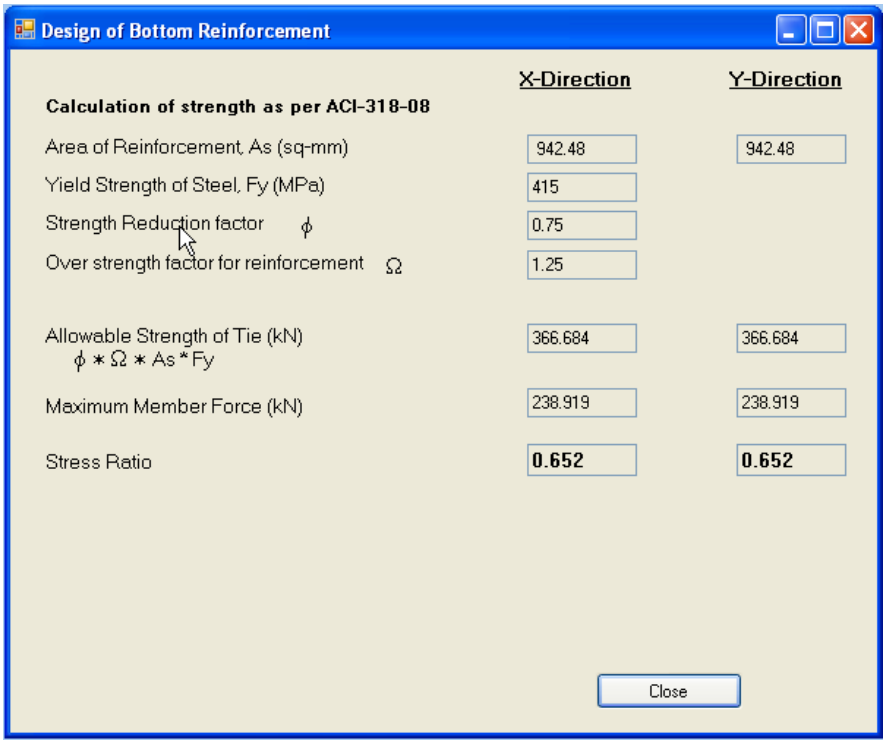

Figure 5.9: Design of Bottom Reinforcement

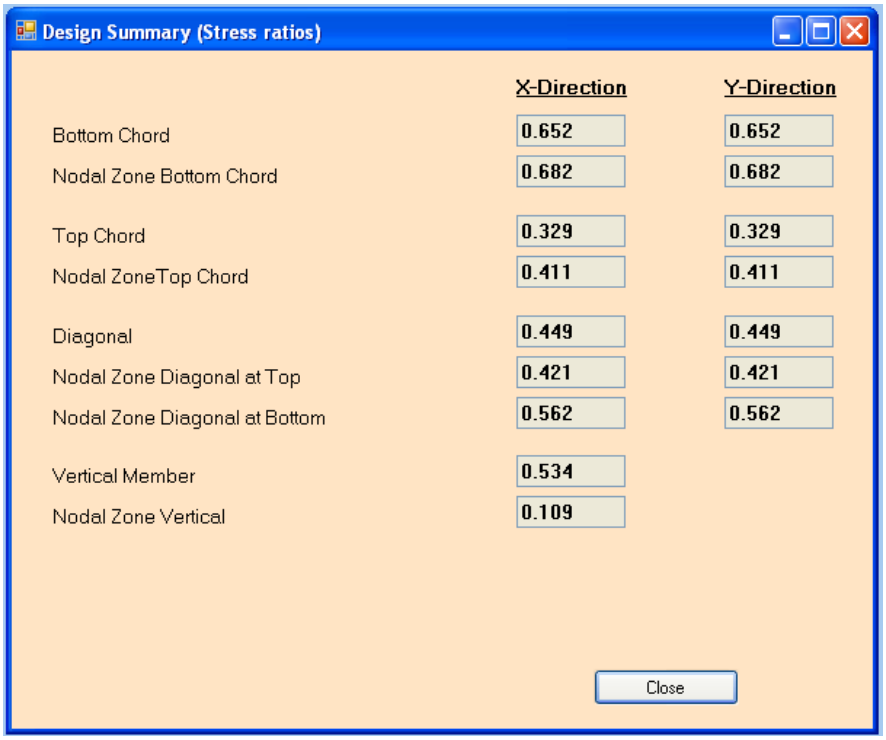

Figure 5.10: Design Summary Showing Stress Ratios for All Types of Elements

Also by comparing the stress ratios of each type of element, the mode of failure can be predicted. The data can be revised partly or completely, till all elements are safe and desired mode of failure is obtained for the slab.

5.6 DEFLECTION OF WAFFLE SLABS

Strut-and-tie method is used to predict the ultimate strength of waffle slab. The deflection calculated using strut-and-tie is always more than actual deflection due to many factors. The cracked concrete surrounding the reinforcement is contributing to the stiffness even though its contribution on the strength is negligible. Also Strut-and-tie model consider only the mechanism of the waffle slab at the failure load and ignores the load path. To overcome this deficiency, in STWAF, a separate module is added to calculate the deflection of simply supported waffle slabs using orthotropic plate theory as shown in Figure 5.11. This helps to check serviceability requirements as well.

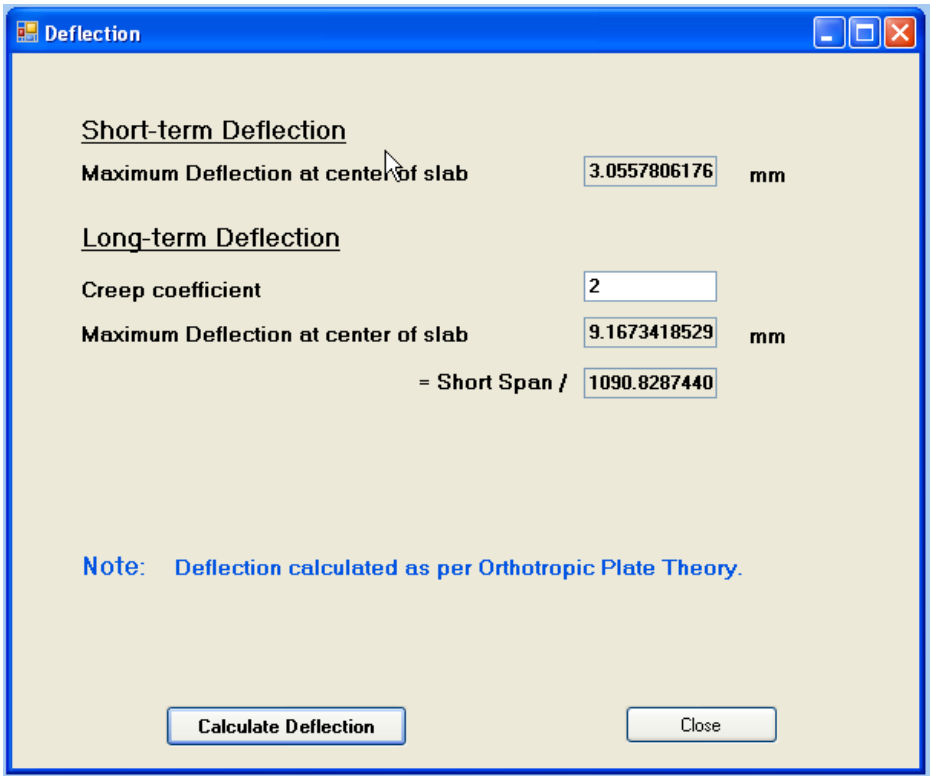

Figure 5.11: STWAF – Deflection of Waffle Slab

5.7 EXAMPLE OF STRENGTH PREDICTION PROCESS USING PROPOSED STM

Design of a 9m * 9m simply supported slab, as shown in Figure 5.12, was done using Strut-and-Tie method to illustrate the procedure adopted by STWAF for generation of 3D-truss model and to calculate strength and stress ratio of various elements of the strut-and-tie model. The analysis of the truss is done using STAAD Pro.

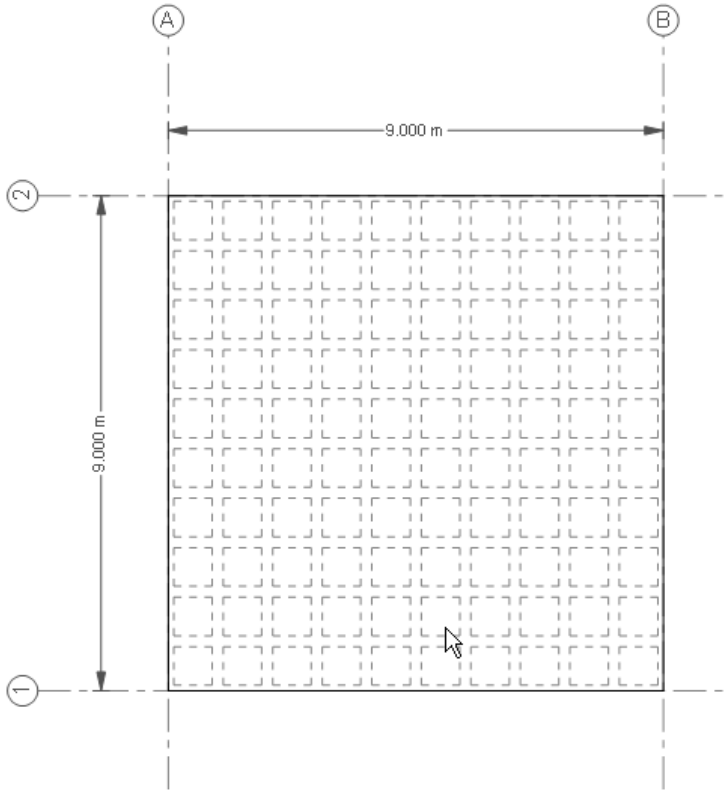

Figure 5.12: Arrangement of Ribs- 9m * 9m slab

5.7.1 Details of Waffle slab Used as Example

Span of Waffle in X and Z direction	=	9000	mm
Yield strength of Reinforcement, fy	=	415	Mpa
Compressive strength of concrete, f'_c	=	20	Mpa
Density of concrete	=	25	kN/m^3
Spacing of ribs in each direction, S	=	900	mm
Top slab Thickness, t	=	60	mm
Waffle Rib thickness, W	=	200	mm
Overall depth of waffle slab including top slab, h	=	500	mm
Effective cover of bottom reinforcement	=	50	mm
Live load	=	7	kN/m^2

5.7.2 Trial Values Assumed for Design

Depth of compression block (< slab thickness), a	=	25	mm
Diameter of bottom reinforcement	=	20	mm
Number of bars at bottom	=	2	Nos
Area of bottom reinforcement	=	628.32	mm^2
Diameter of stirrup reinforcement	=	8	mm
Number of legs per stirrup	=	2	Nos
Area per stirrup	=	100.531	mm^2

5.7.3 Calculation for Geometry of the Truss

Depth of truss = h-(a/2)-effective cover

= 438 mm

Co-ordinates in X and Z directions are based on the rib spacing and in Y direction based on depth of truss.

5.7.4 Calculation of Size of Elements and Nodes of the 3D Truss Model

Since slab is square and same rib spacing provided in X and Z directions, elements sizes are same in both directions

5.7.4.1 Bottom Chord

Bottom chord consists of reinforcement and area is same as the area of reinforcement.

Area of Bottom chord = Area of bottom reinforcement = 628.32 mm^2

Width of Nodal zone at bottom = 2 * Effective cover

= 100 mm

Thickness of nodal zone = Rib thickness

= 200 mm

Area of bottom chord nodal zone = 20000 mm^2

5.7.4.2 Top Chord

Top chord is a concrete prismatic strut

Width of top chord is the minimum of the following:

a) Rib thickness + 8 * Thickness of top slab = 680 mm

b) Rib thickness + 2 * Projection of rib below slab = 1080 mm

c) Center to center spacing of ribs = 900 mm

Width of top chord = 680 mm

Depth of top chord = Depth of compression block (a)

= 25 mm

Area of top chord = 17000 mm^2

Area of top chord nodal zone = Area of top chord

= 17000 mm^2

5.7.4.3 Vertical Members

Vertical members consists of stirrup reinforcement and area is sum of the area of stirrups in X and Y directions

Area of Vertical = 201.06 mm^2

Area of Nodal zone = Rib thickness X * Rib thickness Y

= 200 * 200 = 40000 mm^2

5.7.4.4 Diagonal Members

Diagonal members are concrete bottle shaped struts

Thickness of diagonal member = Rib thickness

= 200 mm

Width of diagonal member to be calculated at top and bottom and minimum is considered.

Angle of diagonal strut with bottom reinforcement,

θ = 25.94 degree

Width of diagonal member at top

= Rib width * Sin θ + Top chord thickness * Cos θ

= 110.0 mm

Width of diagonal member at bottom

= Rib width * Sin θ + Bottom chord nodal zone width * Cos θ

= 177.4 mm

Width of diagonal = 110.0 mm

Area of diagonal member = 21992 mm^2

Area of diagonal at nodal zone = Area of diagonal

= 21992 mm^2

5.7.4.5 Bracing Members

Bracing members are concrete prismatic struts

Depth of bracing member = Slab thickness

= 60 mm

Width of bracing member to be calculated as follows

Angle of bracing strut with X axis α = 45.00 degree

Width of bracing member

= Rib thickness * Sin α + Rib thickness * Cos α

= 282.8 mm

Area of Bracing member = 16971 mm^2

5.7.5 Load Distribution to Nodes of Truss Model

Dead load is calculated based on tributary of slab and length of rib in each direction. Live load is calculated based on tributary. All loads are applied to nodes at top as shown in Table 5.1.

5.7.6 Generation of STAAD Input and Output Files

Figure 5.13 shows the generated truss model in STAAD Pro. Factored loads are used for design of various elements and nodal zones. Load combinations used as per ACI 318-08 as, 1.2 Dead load + 1.6 Live load

The analysis is carried out to obtain the member forces, which is used to check the stress ratios of the various elements and nodal zones of the truss.

TABLE 5.1: Load Distribution to Nodes of the Truss Model

Load	Interior node	Edge node	Corner Node
	kN	kN	kN
Dead Load	4.735	3.358	2.284
Live Load	5.670	2.835	1.418

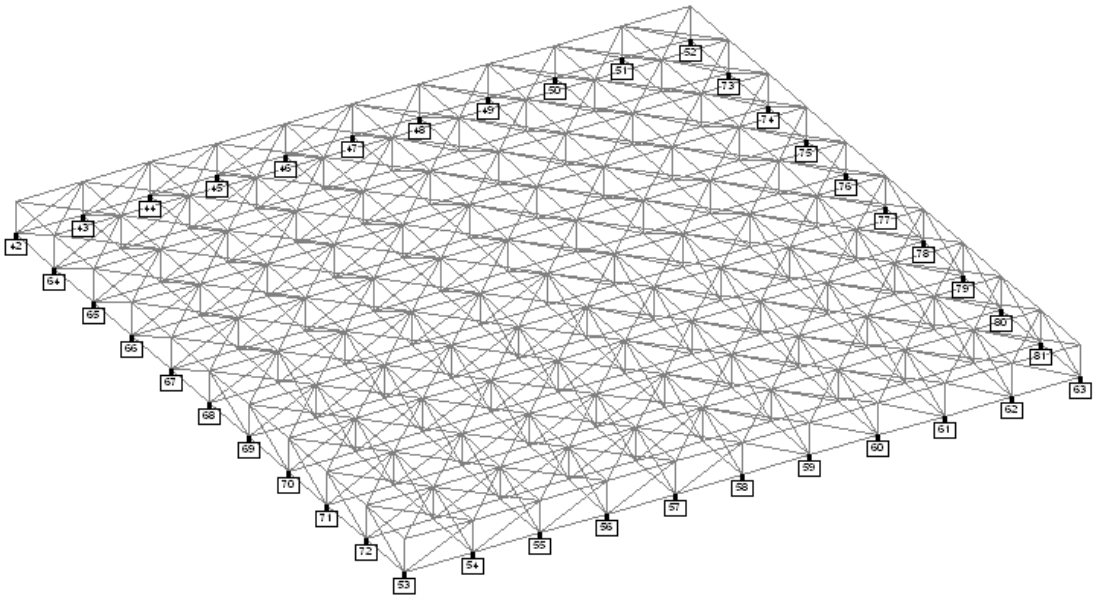

Figure 5.13: STAAD Pro Strut-and-Tie Model - 9m * 9m Slab

5.7.7 Calculation of Strength and Stress Ratio of Elements and Nodes

Allowable strength of Struts, Ties and Nodal zones are calculated based on ACI -318 Strut-and-tie provisions. Strength reduction Factor ϕ is considered as 0.75 for all elements and nodal zones as per ACI.

5.7.7.1 Bottom Chord

Area of reinforcement As	=	628.32 mm2
Over strength factor for Tie Ω	=	1.25
Capacity of Tie	=	ϕ * Ω * fy * As
= 244.5 kN		
βn for Bottom Nodal Zone (CTT)	=	0.60
Capacity of Nodal Zone at Bottom (CTT)	=	$\phi * \beta n * A_{node} * 0.85 * f'_c$
	=	153.0 kN

5.7.7.2 Top Chord

βs for Top Strut	=	1.00
Capacity of Strut at Top	=	$\phi * \beta s * A_{strut} * 0.85 * f'_c$
= 216.8 kN		
βn for Top Nodal Zone (CCT)	=	0.80
Capacity of Nodal Zone at Top (CCT)	=	$\phi * \beta n * A_{node} * 0.85\ f'_c$
	=	173.4 kN

5.7.7.3 Vertical Members

Area of Vertical member As	=	201.06 mm2
Capacity of Vertical member ϕ *fy*As	=	62.6 kN
βn for Bottom Nodal Zone (CTT)	=	0.60
Capacity of Nodal Zone at Bottom (CTT)	=	$\phi * \beta n * A_{node} * 0.85 * f'_c$
	=	306.0 kN

5.7.7.4 Diagonal Members

βs for Inclined Strut (With stirrup reinforcement)	=	0.75

Capacity of Inclined Strut = $\phi * \beta s * A_{strut} * 0.85 * f'_c$

= 210.3 kN

βn for Bottom Nodal Zone (CTT) = 0.60

Capacity of Nodal Zone at Bottom (CTT) = $\phi * \beta n * A_{node} * 0.85 * f'_c$

= 168.2 kN

5.7.7.5 Bracing Members

βs for Bracing = 1.00

Capacity of Bracing = $\phi * \beta s * A_{strut} * 0.85 * f'_c$

= 216.4 kN

5.7.8 Results and Prediction of Mode of Failure

Table 5.2 shows the Factored forces from STAAD out put, the allowable strength calculated as per ACI provisions and the stress ratio for various elements and nodal zones. For bottom nodal zones the ultimate force for the design is the difference between forces in adjacent ties as per ACI.

The output shows the stress ratio of bottom reinforcement as 0.98 which is very close to 1.0 and stress ratios for all other elements are less which indicates the mode of failure under overloading of the slab as flexural failure which is the desired behavior.

TABLE 5.2: Forces, Strength and Stress Ratios of Elements and Nodes

	Bottom Tie		Top Strut		Inclined-Strut		Vertical Tie	
	Member	Node	Member	Node	Member	Node	Member	Node
Axial Force (kN)	240.5	99.9	75.4	75.4	111.2	111.2	32.4	32.4
Allowable Capacity (kN)	244.5	153.0	216.8	173.4	210.3	168.2	62.6	306.0
Stress Ratio	0.98	0.65	0.35	0.44	0.53	0.66	0.52	0.11

CHAPTER 6

PROPOSED STM VERSUS OTHER DESIGN METHODS FOR WAFFLE SLABS

Design of a 9m * 9m simply supported slab was done using different design methods to compare the results. The design was done using "SAFE" program, which designs the slab using ACI methods. Also orthotropic plate theory was used to design the waffle slab manually. Finally the design was carried out using Strut-and-tie method using STWAF.

6.1 DETAILS OF THE 9M * 9M SLAB USED FOR COMPARISON OF DESIGN METHODS

Span in X and Y directions are 9m. All four edges are simply supported and corner lifting allowed. Grade of concrete considered as 20 MPa and grade of reinforcement as 415 Mpa. The details of the waffle slabs are shown in Fig 6.1. Slab is designed for a uniformly distributed live load of 7.0 kN/m^2. Self weight, of the slab is calculated as 5.846 kN/m^2.

Effective Cover in mm	Overall depth in mm	Slab Thickness in mm	Rib thickness in mm	Rib Spacing in mm
50	500	60	200	900

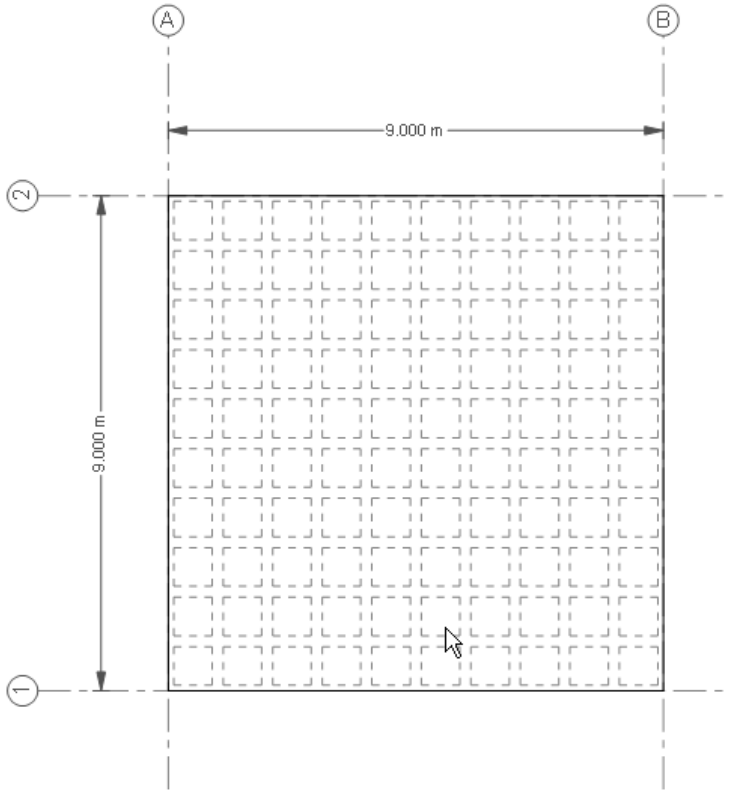

Figure 6.1: Arrangement of Ribs- 9m * 9m slab

6.2 DESIGN OF 9M * 9M WAFFLE SLAB BY STRUT-AND-TIE METHOD USING STWAF

STWAF is used for the design of the slab with strut-and-tie method. Figure 6.2 shows the strut-and-tie model of the 9m * 9m waffle slab generated by STWAF.

The depth of compression block is considered as 25mm which is less than the slab thickness of 60 mm and is sufficient to avoid failure of top strut and nodal zones. Figure 6.3 shows the calculation of strut sizes and Figure 6.4 shows properties of the elements of the truss model calculated by STWAF.

Figure 6.5 to 6.11 shows the design of each type of elements and nodal zones of the model. Strut-and-tie design provisions of ACI-318 are followed by STWAF.

Figure 6.12 shows the summary of the design which shows stress ratios of all types of elements. The stress ratio of bottom chord (reinforcement) is the maximum and is the governing element which restricts strength of the waffle slab. This means that the mode of failure expected is flexural failure which is the desired mode of failure in case of overloading. Also stress ratios of all other element are well within limits.

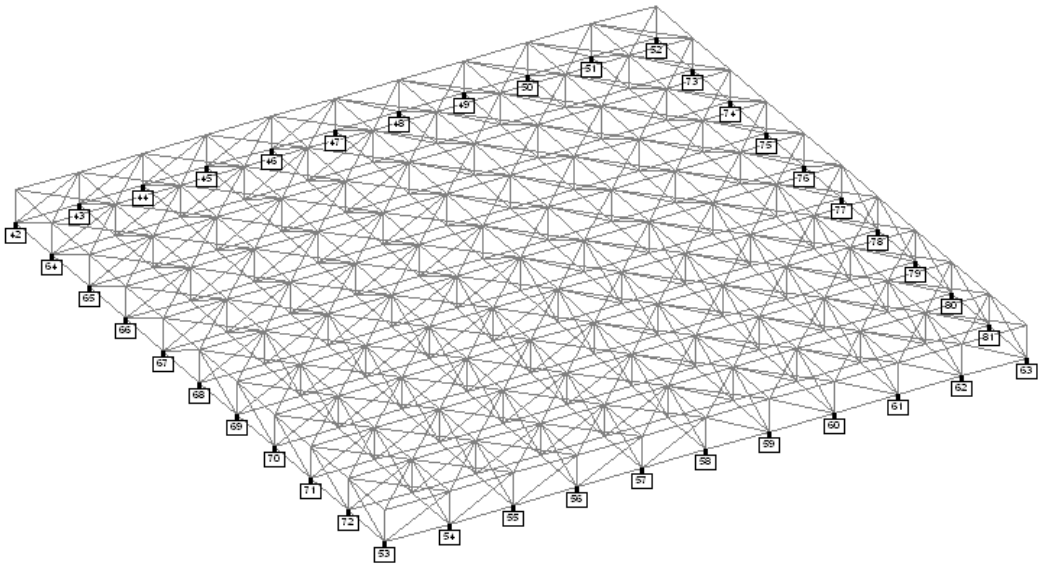

Figure 6.2: Strut-and-Tie Model for 9m * 9m Slab

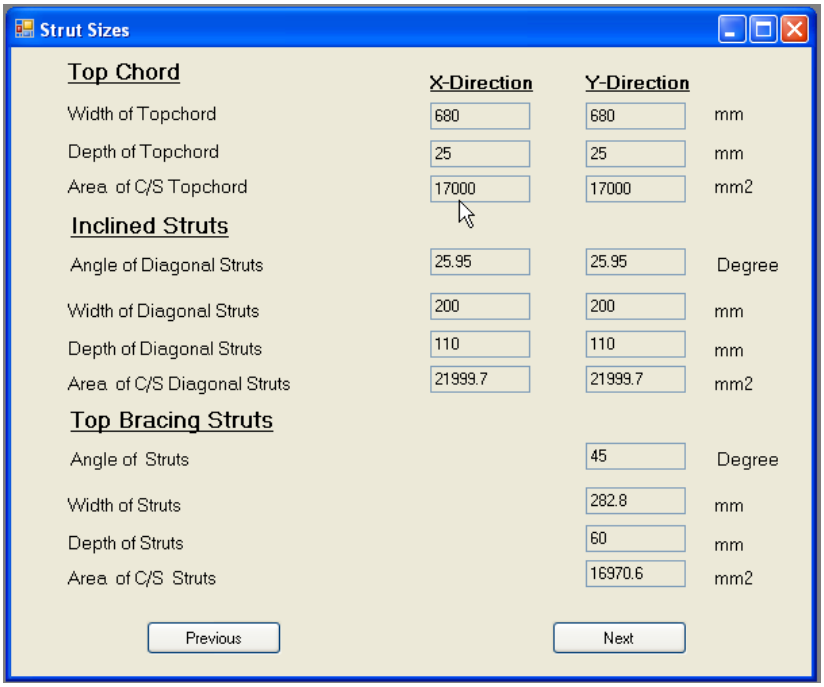

Figure 6.3: Size of struts-Strut-and-Tie method for 9m * 9m Slab

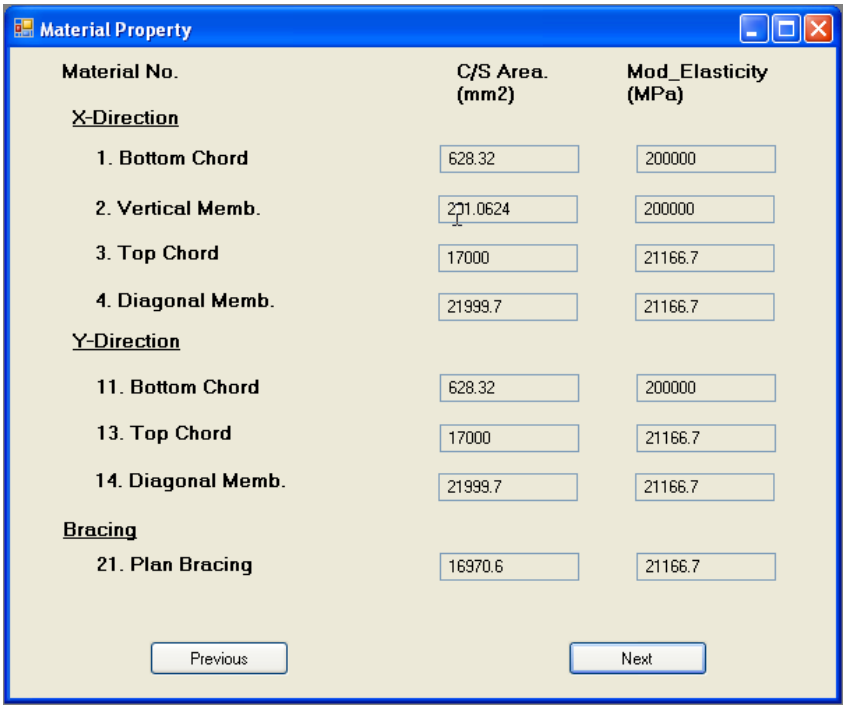

Figure 6.4: Properties of elements-Strut-and-Tie method for 9m * 9m Slab

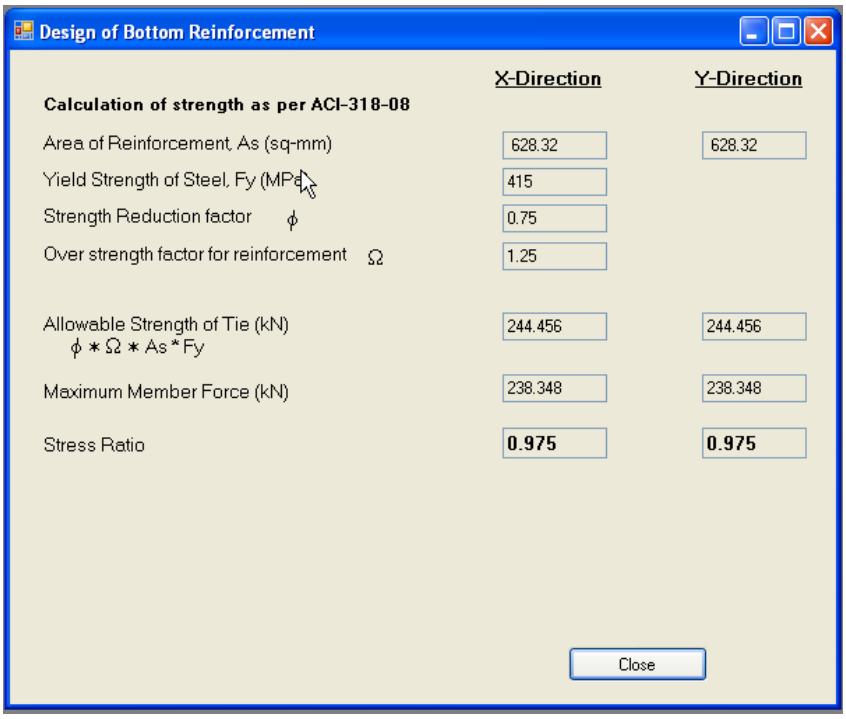

Figure 6.5: Design of Bottom Chord-Strut-and-Tie method

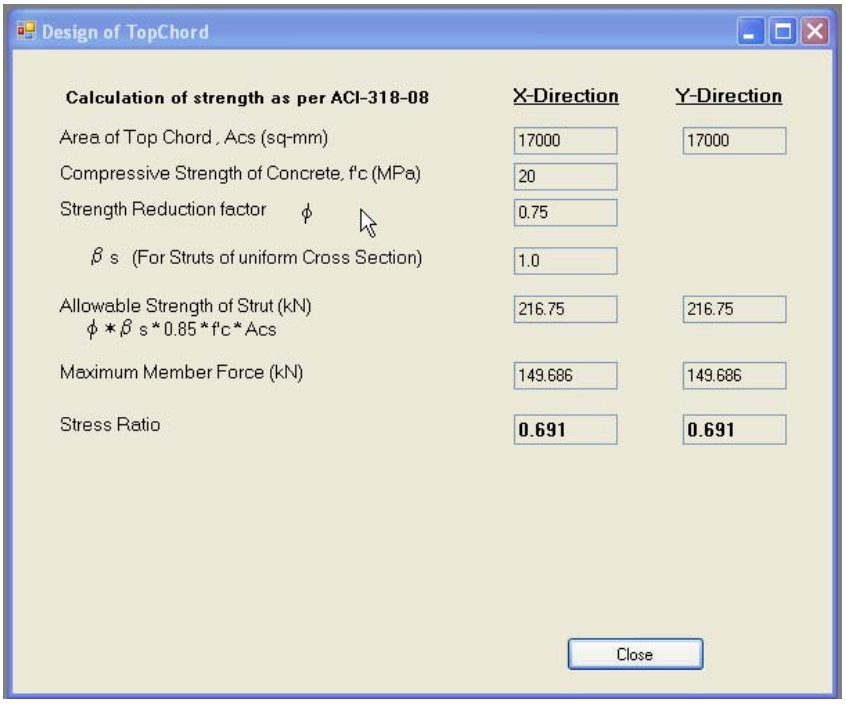

Figure 6.6: Design of Top Chord-Strut-and-Tie method

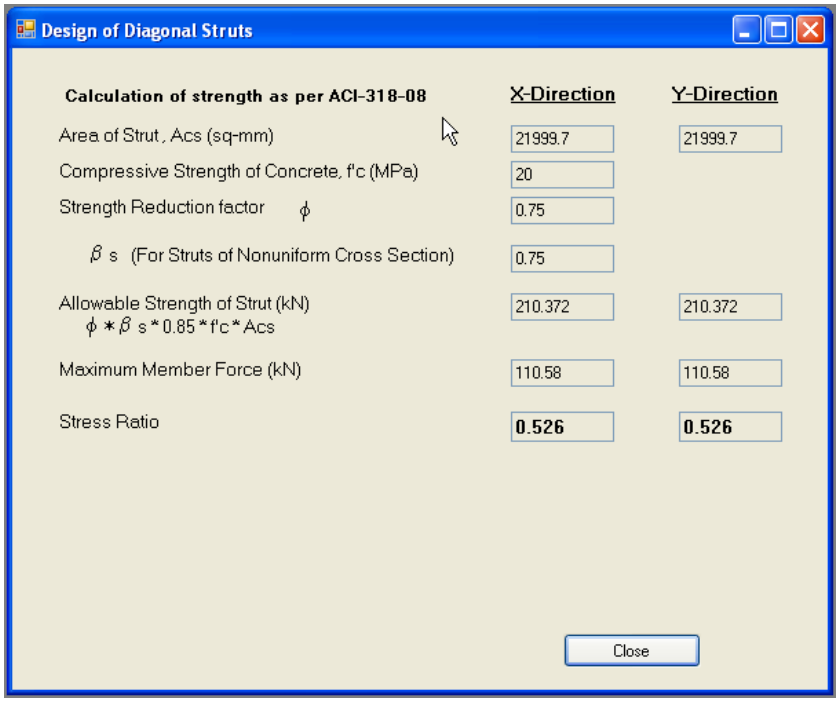

Figure 6.7: Design of Diagonal Strut-Strut-and-Tie method

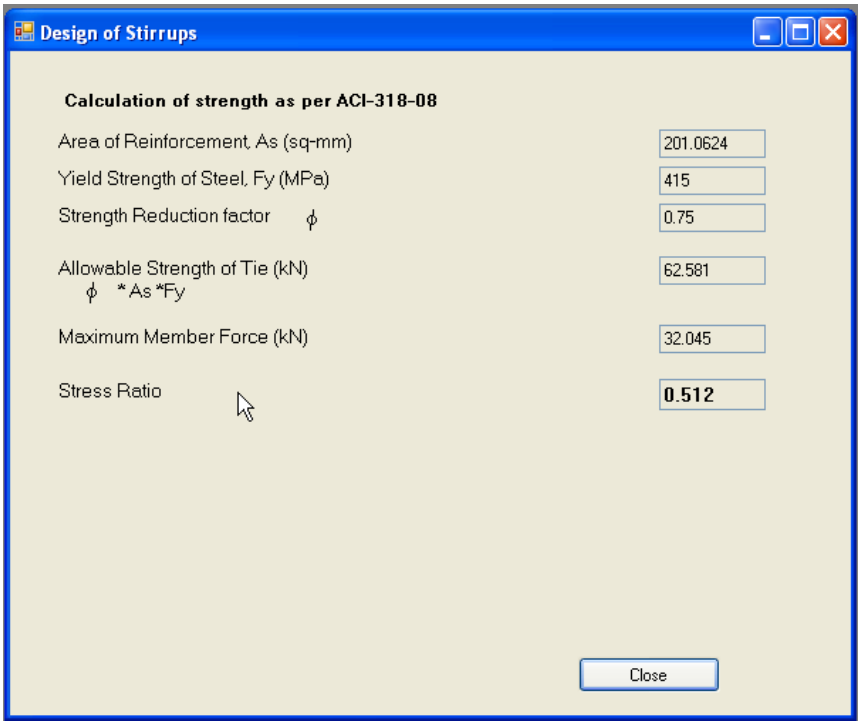

Figure 6.8: Design of Vertical Tie-Strut-and-Tie method

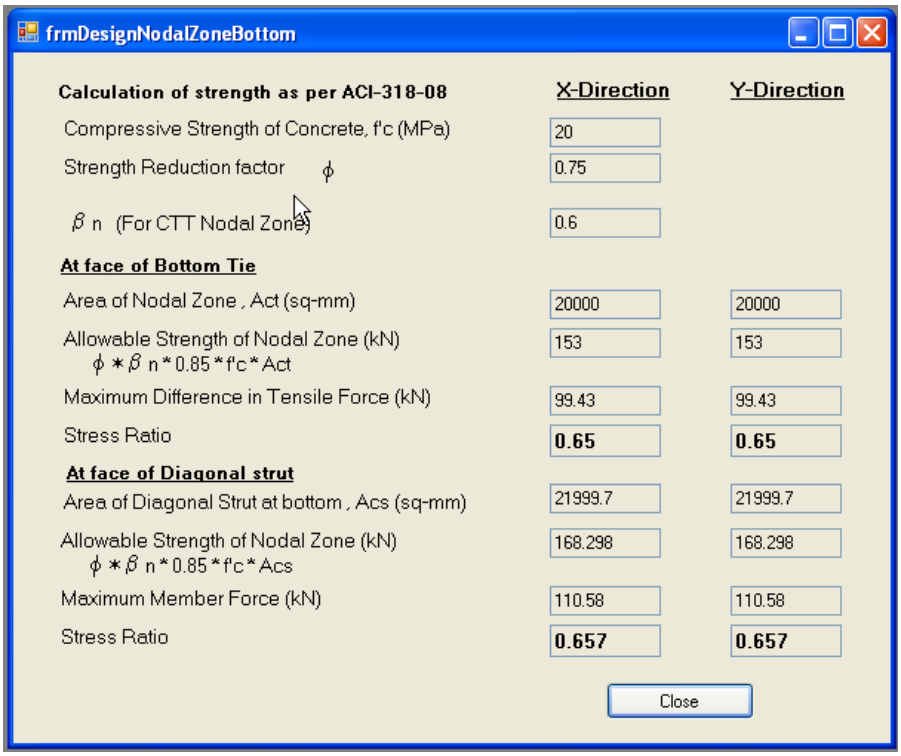

Figure 6.9: Design of Node at Bottom-Strut-and-Tie method

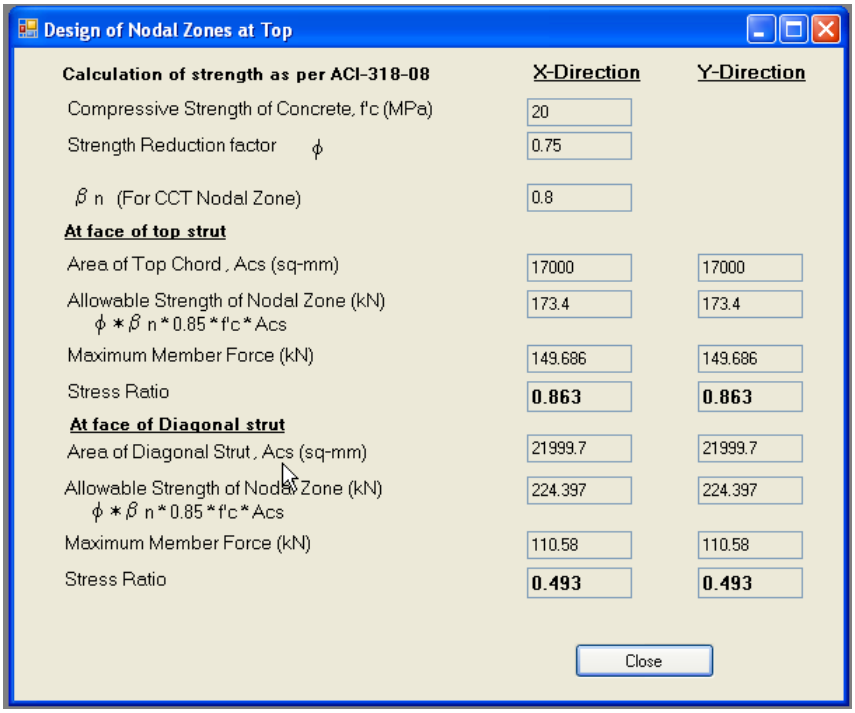

Figure 6.10: Design of Node at Top-Strut-and-Tie method

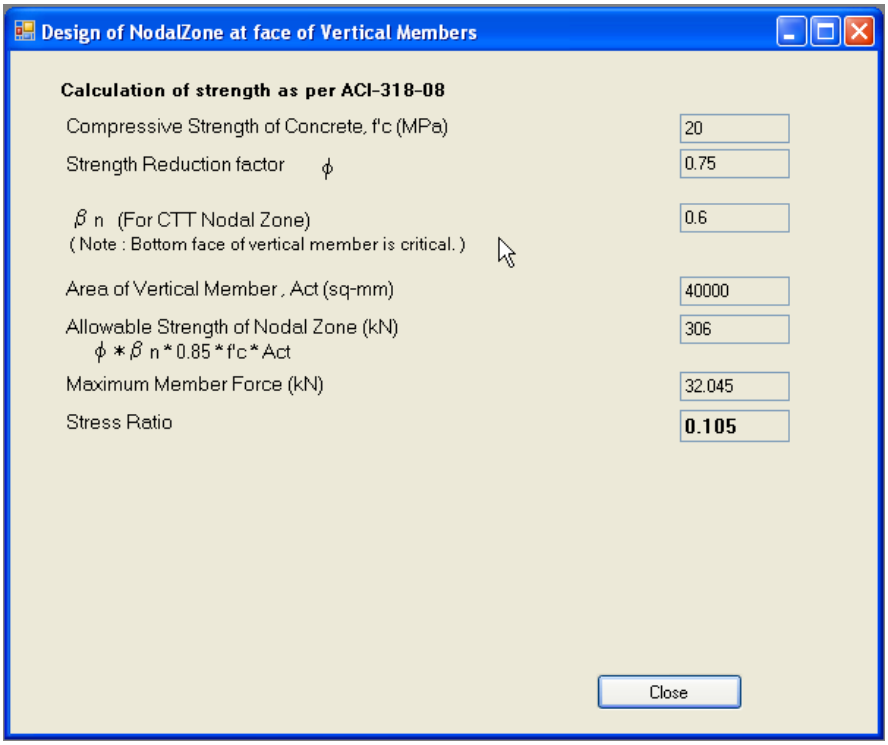

Figure 6.11: Design of Node for Vertical Member-Strut-and-Tie Method

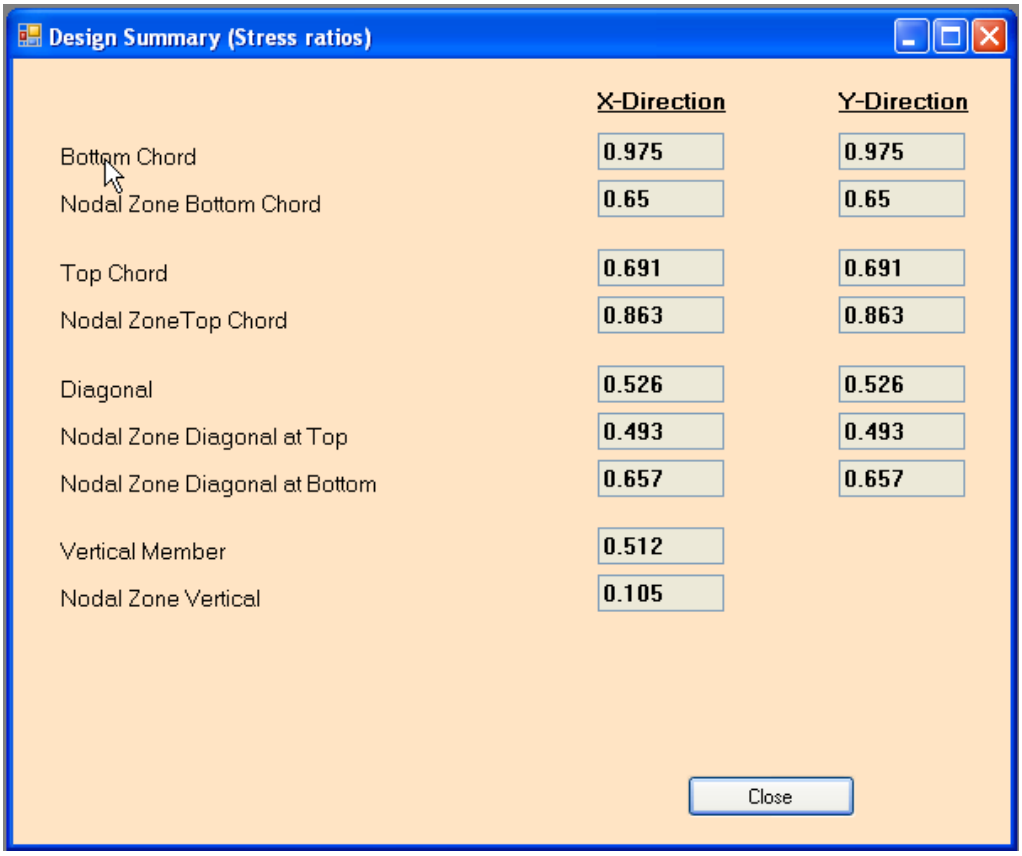

Figure 6.12: Design Summary Strut-and-Tie method for 9mx9m Slab

6.3 DESIGN OF 9M * 9M WAFFLE SLAB WITH SAFE PROGRAM

SAFE (Slab Analysis by Finite Element method) is a program developed by Computers and Structures, Inc. SAFE design waffle slabs using the methods recommended by ACI-318.

The deflected shape of the slab is shown in Fig 6.13. Maximum deflection under service loads is 6.33mm at center. The distribution of bending moment per meter width is shown in Fig 6.14. Maximum bending moment per meter width is 107.5 kNm. Since the rib spacing is 900mm, the bending moment per rib is 96.75 kNm. The distribution of required reinforcement per meter width is shown in Fig 6.15. Maximum reinforcement per meter width is 709.1 mm2. Maximum reinforcement required per rib is 638.2 mm2.

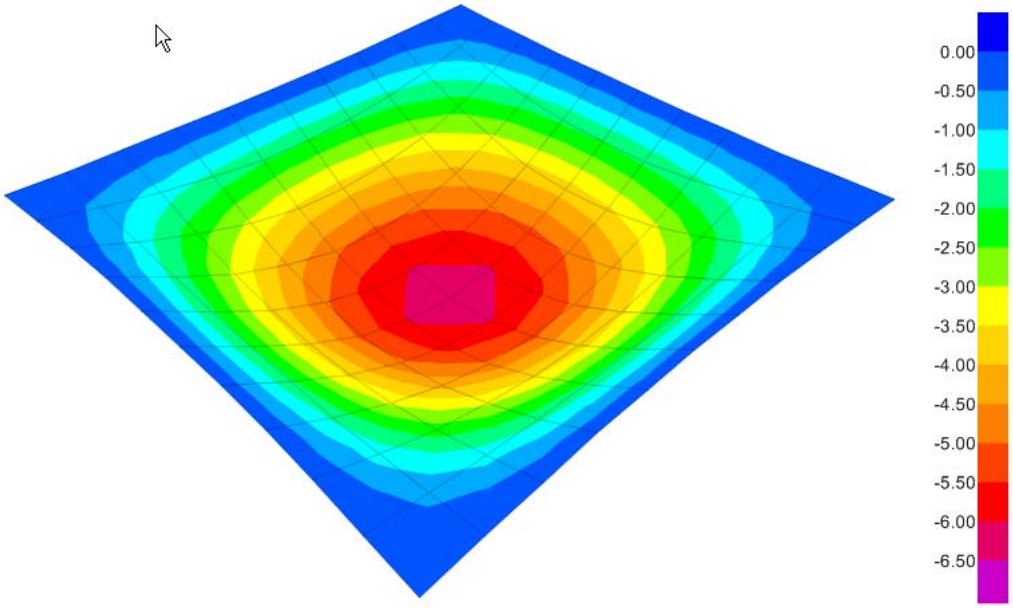

Figure 6.13: Deflected Shape by SAFE

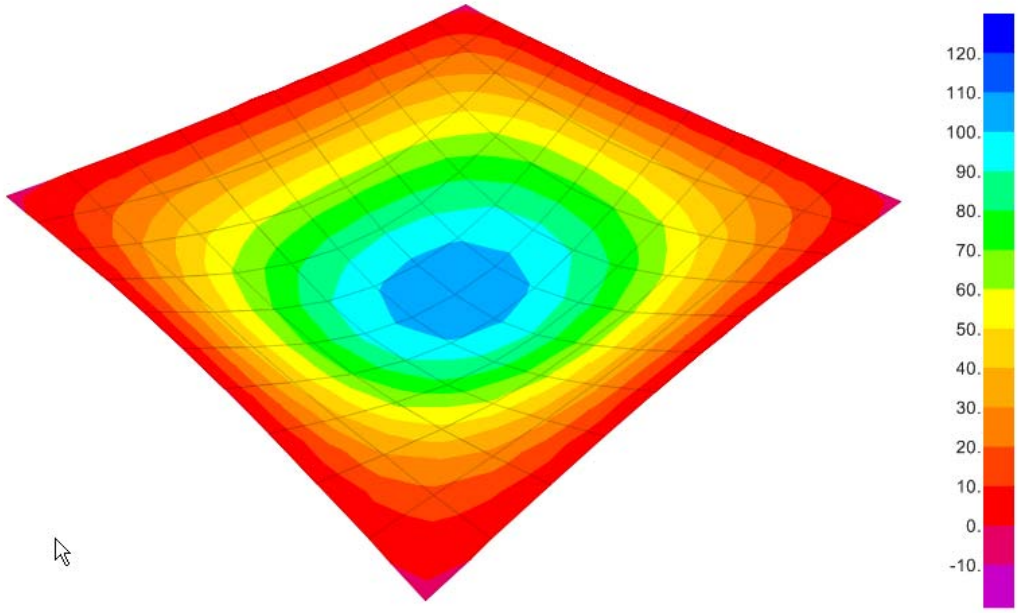

Figure 6.14: Bending Moment/meter by SAFE

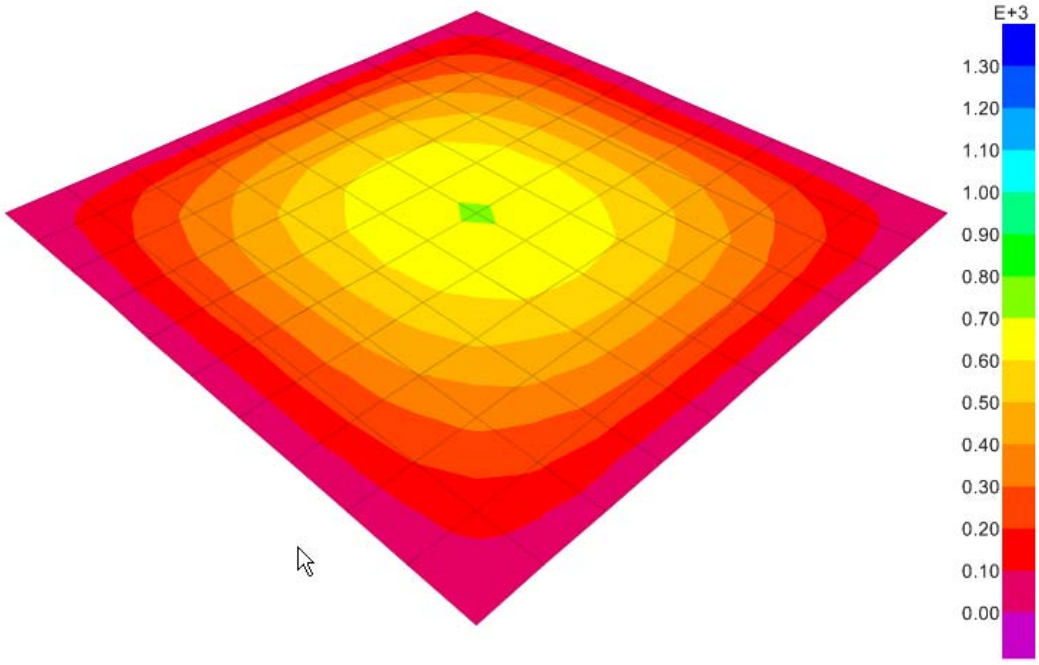

Figure 6.15: Reinforcement in mm2/meter by SAFE

6.4 DESIGN OF 9M * 9M WAFFLE SLAB BY ORTHOTROPIC PLATE

THEORY

Orthotropic plate theory uses differential equation solutions for the design of simply supported waffle slab. General differential equation for Orthotropic plate is given by,

$$D_X \frac{\partial^4 \omega}{\partial x^4} + 2H \frac{\partial^4 \omega}{\partial x^2 \partial y^2} + D_Y \frac{\partial^4 \omega}{\partial y^4} = q$$

Defining:

q = Load per unit area

ω = Deflection of the slab at any point

Δ = Deflection of the slab at center

a, b = Length of plate in X and Y directions respectively

D_X, D_Y = Flexural rigidity EI of beams in X and Y directions per unit width

D_1, D_2 = Coupling rigidities in X and Y directions per unit width

$$= \frac{\upsilon}{1-\upsilon^2} \text{ EI}$$

C_X, C_Y = Torsional rigidity of beams parallel to X and Y directions per unit width

$$2H = \frac{C_1}{b_1} + \frac{C_2}{a_1}$$

Deflection at Center of slab is given by,

$$\Delta = \frac{16q}{\pi^6\left(\frac{D_x}{a^4} + \frac{2H}{a^2 b^2} + \frac{D_y}{b^4}\right)} \sin\frac{\pi x}{a} \sin\frac{\pi y}{b}$$ Where, x = a/2 and y = a/2

The bending moments in X and Y directions are computed as follows:

$$M_X = D_X \frac{\partial^2 \omega}{\partial x^2} + D_1 \frac{\partial^2 \omega}{\partial y^2}$$

$$= \quad -D_X \left(\frac{\pi}{a}\right)^2 \Delta \sin \frac{\pi x}{a} \sin \frac{\pi y}{b} - D_1 \left(\frac{\pi}{b}\right)^2 \Delta \sin \frac{\pi x}{a} \sin \frac{\pi y}{b}$$

$M_Y = D_Y \frac{\partial^2 \omega}{\partial y^2} + D_2 \frac{\partial^2 \omega}{\partial x^2}$

$$= \quad -D_Y \left(\frac{\pi}{b}\right)^2 \Delta \sin \frac{\pi x}{a} \sin \frac{\pi y}{b} - D_2 \left(\frac{\pi}{a}\right)^2 \Delta \sin \frac{\pi x}{a} \sin \frac{\pi y}{b}$$

The Torsional moments in X and Y directions are computed as follows:

$M_{XY} = C_X \frac{\partial^2 \omega}{\partial x \partial y} = C_X \frac{\pi^2}{ab} \Delta \cos \frac{\pi x}{a} \cos \frac{\pi y}{b}$

$M_{YX} = -C_Y \frac{\partial^2 \omega}{\partial x \partial y} = -C_Y \frac{\pi^2}{ab} \Delta \cos \frac{\pi x}{a} \cos \frac{\pi y}{b}$

The Shear in X and Y directions are computed as follows:

$Q_X = \frac{\partial}{\partial x}\left[D_X \frac{\partial^2 \omega}{\partial x^2} + C_Y \frac{\partial^2 \omega}{\partial y^2}\right]$

$$= \quad -\Delta \left[D_X \left(\frac{\pi}{a}\right)^3 + C_Y \left(\frac{\pi^3}{ab^2}\right)\right] \cos \frac{\pi x}{a} \sin \frac{\pi y}{b}$$

$Q_Y = \frac{\partial}{\partial y}\left[D_Y \frac{\partial^2 \omega}{\partial y^2} + C_X \frac{\partial^2 \omega}{\partial x^2}\right]$

$$= \quad -\Delta \left[D_Y \left(\frac{\pi}{a}\right)^3 + C_X \left(\frac{\pi^3}{a^2 b}\right)\right] \sin \frac{\pi x}{a} \cos \frac{\pi y}{b}$$

For the 9m*9m slab, Forces are calculated as follows:

Compressive strength of concrete, f'_c = 20 MPa = 2901 psi

Yield Strength of Steel reinforcement, F_y = 415 MPa = 60189 psi

Elasticity of concrete as per ACI-318-8.5.1,

Ec = $57000*(f'_c)^{1/2}$ = 21167 MPa = 3070 ksi

Poisson's ratio for concrete, υ = 0.2

Elasticity of Steel reinforcement, Es = 199955MPa = 29000 ksi

Span in X-direction	=	9000	mm	=	354.33	in
Spacing of waffles	=	900	mm	=	35.43	in
Span in Y-direction	=	9000	mm	=	354.33	in
Spacing of waffles	=	900	mm			
Thickness of slab (t)	=	60	mm	=	2.36	in
Overall depth of waffle slab (h)	=	500	mm	=	19.69	in
Depth of ribs	=	440	mm			
Thickness of waffle ribs (b_w)	=	200	mm	=	7.87	in
Diameter of Bottom bar-X direction	=	20	mm	=	0.79	in
Diameter of Bottom bar-Y direction	=	20	mm	=	0.79	in
Effective depth	=	450	mm	=	17.72	in
Dead Load including self weight	=	5.846	kN/m^2			
Live Load	=	7.00	kN/m^2			
Factored Load (1.2 DL+1.6 LL)	=	18.2152	kN/m^2			
Service Loads (1.0 DL+1.0 LL)	=	12.846	kN/m^2			

Moment of Inertia of a flange beam about it's own centroidal axis is calculated as:

$I = \frac{k * b_w * h^3}{12}$ Where,

$k = \frac{1+(Q-1)P(4-6P+4P^2+(Q-1)P^3)}{1+(Q-1)P}$

P = t/h , Q = b_E/b_w

b_E is the effective width of flange calculated as per ACI-318

b_E	=	680	mm

P = t/h = 0.120

Q = b_E/b_w = 3.4

k = $\frac{1+(Q-1)P(4-6P+4P^2+(Q-1)P^3)}{1+(Q-1)P}$ = 1.52

I = $k*b_w*h^3/12$

= $3174*10^6$ mm^4

If I_1 and I_2 are second moment of area of the T-section about the centroidal axis in the X and Y directions,

$D_x = E*I_1$

$D_y = E*I_2$

Here $I_1 = I_2 = I$ and

a1, b1 = Spacing of ribs in X and Y directions respectively

$a_1 = b_1$ = 900 mm

$D_x = D_y$ = $3.527 *10^{-3} * E$

$D_1 = D_2$ = $(\upsilon/(1-\upsilon^2))EI = 0.208\ EI$

= $0.7336 *10^{-3} * E$

The Torsional Rigidity in X and Y directions are given by

J = $\Sigma (1-0.63*x/y)*(x^3*y/3)$ = $1026* 10^6$ mm^4

	x_1	y_1	x_2	y_2	J
Case1)	60	680	200	440	$883*10^6$
Case2)	60	240	200	500	$1026*10^6$

C1 = C2 = J*G = J * (E/(2*(1+υ)) = 427.69 *10^6 * E mm^4

= 0. 42769 *10^{-3} * E m^4

2*H = $\frac{C_1}{b_1} + \frac{C_2}{a_1}$ = 0. 950417 *10^{-3} *E

Deflection at Center of slab for Service Loads is given by,

$\Delta = \frac{16q}{\pi^6\left(\frac{D_x}{a^4}+\frac{2H}{a^2b^2}+\frac{D_y}{b^4}\right)} \sin\frac{\pi x}{a} \sin\frac{\pi y}{b}$ Where, x = a/2 and y = a/2

q = 12.846 kN/m2

E = 21167 MPa = 21167*10^3 kN/m^2

Dx/a^4 = 5.37555*10^{-07} *E = 11.378

Dy/b^4 = 5.37555 *10^{-07} *E = 11.378

2H/(a^{2}b^2) = 1.44859 *10^{-07} *E = 3.066

Deflection at center of plate = 0.0083 m (at x = a/2 and y = b/2)

= 8.3 mm

Assuming creep coefficient as 2.0, E_{ce} = E_c / 3

Long term Deflection = 24.9 mm

Allowable Deflection = Short Span / 250

= 36 mm > 24.9 mm

Design moments and shear are calculated as follows using factored loads:

$\Delta = \frac{16q}{\pi^6\left(\frac{D_x}{a^4}+\frac{2H}{a^2b^2}+\frac{D_y}{b^4}\right)} \sin\frac{\pi x}{a} \sin\frac{\pi y}{b}$ Where, x = a/2 and y = a/2

Where, q = 18.2152 kN/m2

Δ_{ult} = 0.0118 m

The bending moment, torsional moments and shear at various salient points are computed as follows

$M_X = D_X \frac{\partial^2 \omega}{\partial x^2} + D_1 \frac{\partial^2 \omega}{\partial y^2}$

$= -D_X \left(\frac{\pi}{a}\right)^2 \Delta \sin \frac{\pi x}{a} \sin \frac{\pi y}{b} - D_1 \left(\frac{\pi}{b}\right)^2 \Delta \sin \frac{\pi x}{a} \sin \frac{\pi y}{b}$

$= 129.15 * \sin \frac{\pi x}{a} \sin \frac{\pi y}{b}$

$M_Y = D_Y \frac{\partial^2 \omega}{\partial y^2} + D_2 \frac{\partial^2 \omega}{\partial x^2}$

$= -D_Y \left(\frac{\pi}{b}\right)^2 \Delta \sin \frac{\pi x}{a} \sin \frac{\pi y}{b} - D_2 \left(\frac{\pi}{a}\right)^2 \Delta \sin \frac{\pi x}{a} \sin \frac{\pi y}{b}$

$= 129.15 * \sin \frac{\pi x}{a} \sin \frac{\pi y}{b}$

$M_{XY} = C_X \frac{\partial^2 \omega}{\partial x \partial y} = C_X \frac{\pi^2}{ab} \Delta \cos \frac{\pi x}{a} \cos \frac{\pi y}{b}$

$= -14.40 * \cos \frac{\pi x}{a} \cos \frac{\pi y}{b}$

$M_{YX} = -C_Y \frac{\partial^2 \omega}{\partial x \partial y} = -C_Y \frac{\pi^2}{ab} \Delta \cos \frac{\pi x}{a} \cos \frac{\pi y}{b}$

$= -14.40 * \cos \frac{\pi x}{a} \cos \frac{\pi y}{b}$

$Q_X = \frac{\partial}{\partial x}\left[D_X \frac{\partial^2 \omega}{\partial x^2} + C_Y \frac{\partial^2 \omega}{\partial y^2}\right]$

$= -\Delta \left[D_X \left(\frac{\pi}{a}\right)^3 + C_Y \left(\frac{\pi^3}{ab^2}\right)\right] \cos \frac{\pi x}{a} \sin \frac{\pi y}{b}$

$= -42.35 * \cos \frac{\pi x}{a} \sin \frac{\pi y}{b}$

$Q_Y = \frac{\partial}{\partial y}\left[D_Y \frac{\partial^2 \omega}{\partial y^2} + C_X \frac{\partial^2 \omega}{\partial x^2}\right]$

$$= \quad -\Delta \left[D_Y \left(\frac{\pi}{a}\right)^3 + C_X \left(\frac{\pi^3}{a^2 b}\right) \right] \sin \frac{\pi x}{a} \cos \frac{\pi y}{b}$$

$$= \quad -42.35 * \sin \frac{\pi x}{a} \cos \frac{\pi y}{b}$$

a = b = 9 m

Factored Moments at center = 129.15 kNm / meter width

Waffle spacing = 0.9 m

Factored Moment per waffle spacing

Mu = Mx*Waffle spacing = 116.23 kNm

ϕ = 0.9

Required Nominal Moment capacity, M_n = 129.15 kNm = 95.21 k-ft

T section with effective width, be is considered as per ACI-318.

b_e = 680 mm = 26.77 in

d = 17.72 in

a = 1.121 in

Area of reinforcement per rib required,

As = M/(ϕ*fy*(d-a/2))

= 1.229 in^2

= 793.2 mm^2

6.5 COMPARISON OF MAIN REINFORCEMENT FOR DIFFERENT METHODS

Table 6.1 shows the comparison of main reinforcement required for the ribs. Required reinforcement is more or less same between SAFE and STWAF with Ω =1.25.

TABLE 6.1: Comparison of Main Reinforcement for Different Methods

As by SAFE (mm^2)	As by Plate Theory (mm^2)	As by STWAF(mm^2) Ω =1.25	As by STWAF(mm^2) Ω =1.00
639	793	629	770

Required reinforcement in the ribs is calculated without considering over strength factor also in a similar way using STWAF, as shown in Table 6.1. It matches with reinforcement calculated using orthotropic plate theory. However in this case the reinforcement required is more than the conventional methods which consider distribution of reinforcement over the entire strip.

As per ACI, ultimate moment is calculated for a strip of slab, consisting of many ribs, and the moment is distributed equally for all the ribs at center. It is a reasonable assumption since waffle slab consists of ribs at close spacing and loads are well distributed due to inter connected ribs in both directions. To account for this distribution, the over strength factor of 1.25 is applied to the design of bottom reinforcement. Since this is applied along with strength design factor of 0.75, the total stress in reinforcement at the center rib will be 0.94 times yield stress which is still less than the yield strength.

CHAPTER 7

PARAMETRIC STUDY OF ACI PROVISIONS FOR WAFFLE SLABS USING STWAF

A 10m * 10m simply supported slab was selected to study the effect of rib spacing, depth of rib, thickness of rib and reinforcement cover on the strength and mode of failure of waffle slab. The design was carried out using strut-and-tie simulation in STWAF environment.

7.1 DETAILS OF THE 10M * 10M SLAB USED FOR PARAMETRIC STUDY

Span in X and Y directions are 10m. All four edges are simply supported and corner lifting allowed. Grade of concrete considered as 20 MPa and grade of reinforcement as 415 Mpa. Self weight is calculated and applied by STWAF. Live loads applied as uniformly distributed loads. In each slab the additional live load capacity of the slab is calculated.

7.2 EFFECT OF RIB SPACING

For the waffle slab used to study the effect of rib spacing, a slab thickness of 75 mm considered and the overall depth of all slabs kept as 600mm. Rib thickness considered is 200mm and an effective cover of 50mm was used for all slabs. Area of main reinforcement at bottom of rib is 942.48 mm^2 and area of stirrups used is 100.53 mm^2.

The slab is designed with 12 equal rib spacings to 5 equal rib spacings, keeping all other parameters same and the additional live load carrying capacity is calculated and reported, as shown in Figure 7.1.

As the rib spacing increases, moment of inertia and strength reduces as shown in Figure 7.1. Table 7.1 shows the stress ratios of various elements of the strut-and-tie model. For closer spacing of ribs, the bottom chord element, which is the reinforcement, is the critical element that fails first, if the load is further increased. This means that mode of failure is flexural failure and is due to yielding of reinforcement. A further increase in rib spacing will make bottom nodal zone critical which results a slip bond failure. A large spacing of ribs makes diagonal member fail which is a sudden punching shear failure.

Closer spacing of ribs is recommended since it makes flexural failure under overloading. ACI recommends a maximum clear spacing of ribs as 30 inch. Only slabs 1 and 2 meets this criteria. For these two slabs, the mode of failure is flexural and ACI recommendation is in line with behavior predicted by strut-and-tie method.

The nodal zone for bottom chord for all these specimens are seen with higher stress ratios and this can be avoided by increasing the concrete cover. To have sufficient warning under overloading, stress ratios of all elements and nodal zones other than bottom reinforcement should be kept as low as possible.

Slab No	Rib Spacing mm	Self weight kN/m^2	Angle of Strut	Live Load kN/m^2
1	833	7.419	32.21	12.60
2	909	7.015	30.01	11.60
3	1000	6.600	27.70	9.60
4	1111	6.175	25.29	8.20
5	1250	5.739	22.78	5.80
6	1429	5.293	20.18	4.55
7	1667	4.836	17.48	2.70
8	2000	4.369	14.71	1.55

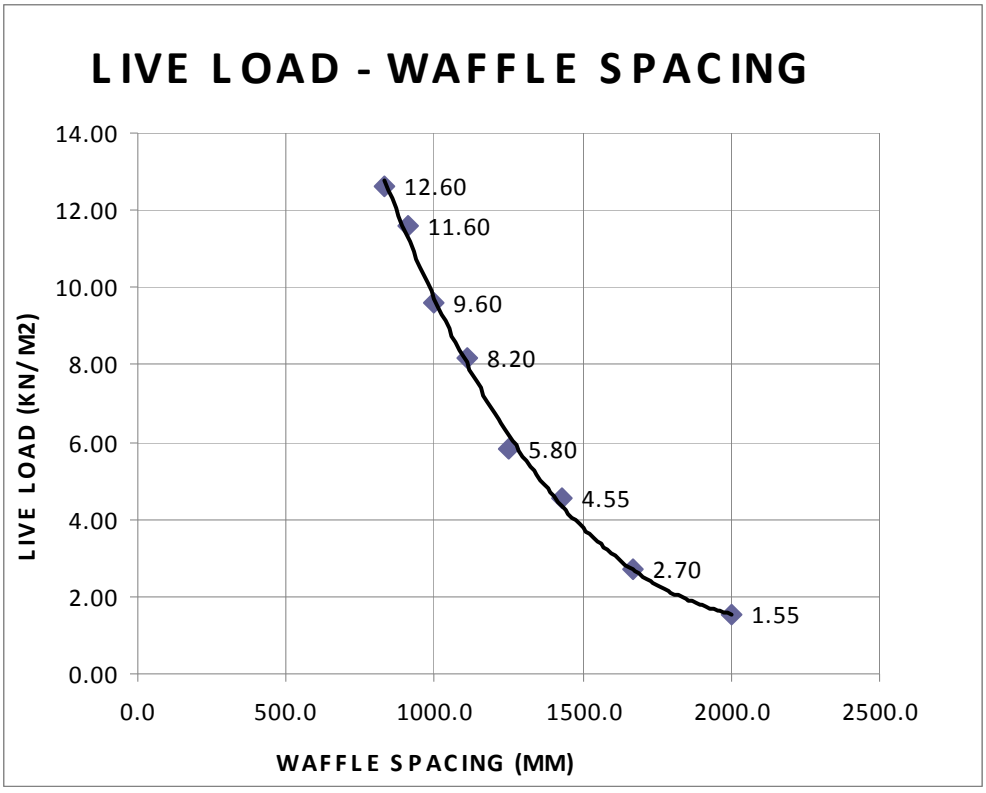

Figure 7.1: Effect of Rib Spacing on the Load Carrying Capacity

TABLE 7.1: Effect of Rib Spacing - Stress Ratios of Various Elements of the Model

Slab No	Bottom Chord		Top Chord		Diagonal Member			Vertical Member	
	Element	Node	Element	Node	Element	Node Top	Node Bottom	Element	Node
1	**0.992**	0.947	0.504	0.630	0.602	0.564	0.752	0.871	0.178
2	**0.991**	0.939	0.480	0.600	0.606	0.568	0.757	0.883	0.181
3	**0.953**	**0.998**	0.481	0.602	0.657	0.616	0.821	0.781	0.160
4	**0.908**	**0.991**	0.430	0.537	0.671	0.629	0.839	0.730	0.149
5	0.824	**0.990**	0.411	0.514	0.695	0.652	0.869	0.596	0.122
6	0.752	**0.994**	0.350	0.438	0.731	0.685	**0.914**	0.504	0.103
7	0.682	**0.994**	0.331	0.413	0.774	0.725	**0.967**	0.380	0.078
8	0.556	**0.949**	0.279	0.349	0.792	0.742	**0.990**	0.263	0.054

7.3 EFFECT OF RIB DEPTH

For the waffle slab used to study the effect of rib depth, a slab thickness of 75 mm considered and the rib spacing of all slabs kept as 833mm. Rib thickness considered is 200mm and an effective cover of 50mm used for all slabs. Area of main reinforcement at bottom of rib is 942.48 mm^2 and area of stirrups used is 100.53 mm^2.

The slab is designed with overall depth of slab from 1100 to 400 mm, keeping all other parameters same and the additional live load carrying capacity is calculated and reported, as shown in Figure 7.2.

As the depth of waffle slab increases from 400 to 700 mm, moment of inertia and strength increases as shown in Figure 7.2. However a further increase in depth is not contributing much to the additional live carrying capacity. Even it has a negative impact due to increase in self weight after a depth of 800 mm. Table 7.2 shows the stress ratios

of various elements of the strut-and-tie model. For smaller depth of waffle slab, the bottom chord element, which is the reinforcement, is the critical element that fails first, under overloading of the slabs. This means mode of failure is flexural failure and is due to yielding of reinforcement. A further increase in depth will make bottom nodal zone fail and diagonal member fail which results in a slip bond failure and a sudden punching shear failure, respectively.

Smaller depth of rib is recommended since it leads to the desired flexural failure under overloading. ACI recommends a maximum depth of rib as 3.5 times the rib thickness. Only slab numbers 5 to 8 meet these criteria. For slabs with depth less than 700 mm, the mode of failure is flexural.

For the slab number 5 with 700 mm depth, since bottom nodal zone and diagonal members are also equally critical, it will not give warning under overloading and is not recommended. However 700 mm depth can be used with higher thickness of rib, which makes the bottom nodal zone and diagonal member less critical and result in a flexural failure under overloading.

Slab No	Overall Depth mm	Self weight kN/m^2	Angle of Strut	Live Load kN/m^2
1	1100	12.699	50.89	15.10
2	1000	11.643	47.99	15.30
3	900	10.587	44.71	15.40
4	800	9.531	41.02	15.40
5	700	8.475	36.87	14.70
6	600	7.419	32.21	12.60
7	500	6.363	27.02	10.00
8	400	5.307	21.31	7.20

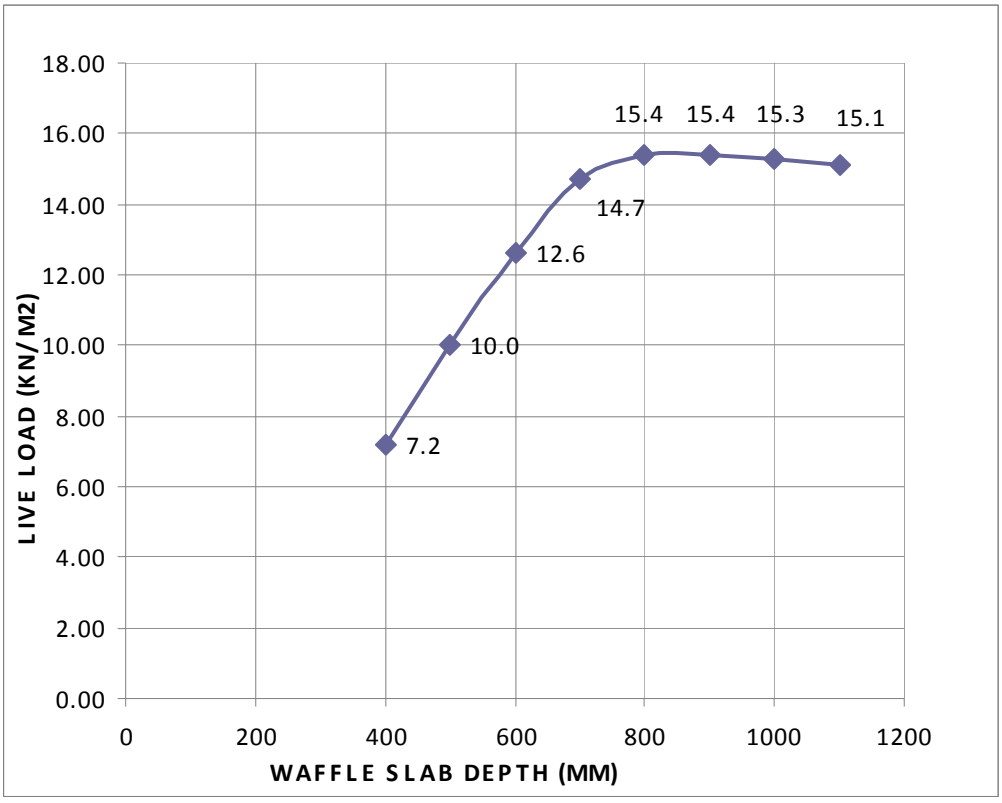

Figure 7.2: Effect of Rib Depth on the Load Carrying Capacity

TABLE 7.2: Effect of Rib Depth - Stress Ratios of Various Elements of the Model

Slab No	Bottom Chord		Top Chord		Diagonal Member			Vertical Member	
	Element	Node	Element	Node	Element	Node Top	Node Bottom	Element	Node
1	0.748	0.954	0.360	0.450	0.648	0.607	0.810	0.992	0.203
2	0.790	0.965	0.386	0.482	0.633	0.594	0.792	0.991	0.203
3	0.842	0.977	0.416	0.520	0.624	0.585	0.780	0.992	0.203
4	0.910	0.996	0.455	0.569	0.625	0.586	0.781	0.995	0.203
5	0.973	0.997	0.491	0.614	0.623	0.584	0.779	0.969	0.198
6	0.992	0.947	0.504	0.630	0.602	0.564	0.752	0.871	0.178
7	0.992	0.887	0.507	0.634	0.588	0.552	0.735	0.735	0.150
8	0.981	0.831	0.503	0.628	0.598	0.561	0.748	0.572	0.117

7.4 EFFECT OF RIB THICKNESS

For the waffle slab used to study the effect of rib thickness, a slab thickness of 75 mm was considered and the overall depth of all slabs was kept as 600mm. Rib spacing of all slabs was kept as 833mm and an effective cover of 50mm was used for all slabs. Area of main reinforcement at bottom of rib was 942.48 mm^2 and area of stirrups used was 100.53 mm^2.

The slab is designed with a rib thickness from 100mm to 250mm, keeping all other parameters same and the additional live load carrying capacity is calculated and reported, as shown in Figure 7.3.

As the rib thickness increases from 100 to 200 mm, moment of inertia and strength increases as shown in Figure 7.3. However a further increase in rib thickness has a marginal negative impact on the additional live load carrying capacity due to increase in

self weight after a thickness of 200 mm. A thickness of 200 mm is sufficient to avoid concrete failure in the structure.

Table 7.3 shows the stress ratios of various elements of the strut-and-tie model. For thickness of ribs greater than or equal to 200mm, the bottom chord element, which is the reinforcement, is the critical element that fails first, under overloading of the slabs. This means mode of failure is flexural failure and is due to yielding of reinforcement. A reduction in thickness of rib will make bottom nodal zone or diagonal member fail which results in a slip bond failure or a sudden punching shear failure which is not a recommended mode of failure.

An increased rib thickness will avoid concrete failure in structure. ACI recommends a minimum rib thickness of 200 mm. Only slab numbers 1 and 2 meet this criteria. For these two slabs, the mode of failure is flexural and ACI recommendation is in line with behavior predicted by strut-and-tie method. However for waffle slabs with larger span and loads, minimum rib thickness of 200 mm as recommended by ACI will not be enough to avoid shear failure.

Slab No	Rib Thickness mm	Self weight kN/m^2	Angle of Strut	Live Load kN/m^2
1	250	8.569	32.21	11.80
2	200	7.419	32.21	12.60
3	150	6.175	32.21	10.00
4	100	4.836	32.21	4.30

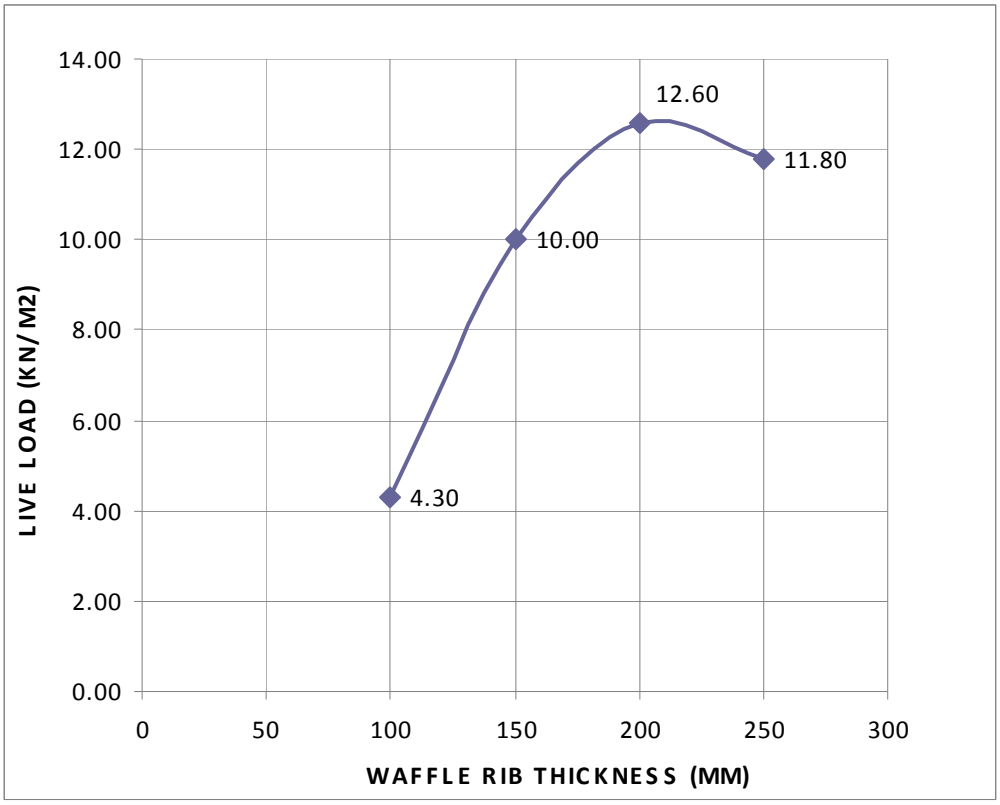

Figure 7.3: Effect of Rib Thickness on the Load Carrying Capacity

TABLE 7.3: Rib Thickness - Stress Ratios of Various Elements of the Truss Model

Slab No	Bottom Chord		Top Chord		Diagonal Member			Vertical Member	
	Element	Node	Element	Node	Element	Node Top	Node Bottom	Element	Node
1	**0.995**	0.770	0.490	0.613	0.415	0.389	0.518	0.864	0.113
2	**0.992**	0.947	0.504	0.630	0.602	0.564	0.752	0.871	0.178
3	0.798	**0.998**	0.426	0.533	0.772	0.724	**0.965**	0.714	0.259
4	0.432	0.788	0.243	0.304	0.779	0.730	**0.974**	0.394	0.323

7.5 EFFECT OF EFFECTIVE COVER

For the waffle slab used to study the effect of effective cover for main reinforcement, a slab thickness of 75 mm was considered and the overall depth of all slabs was kept as 600mm. Rib thickness considered was 200mm and rib spacing of all slabs was kept as 833mm. Area of main reinforcement at bottom of rib was 942.48 mm^2 and area of stirrups used was 100.53 mm^2.

The slab is designed with an effective concrete cover from 30mm to 60mm, keeping all other parameters same and the additional live load carrying capacity is calculated and reported, as shown in Figure 7.4

As the effective cover increases from 30 to 50 mm, strength increases dramatically as shown in Figure 7.4. This is due to the slip bond failure at bottom of the ribs due to less concrete cover in ribs (as in the case of 30mm cover). The nodal zone for bottom reinforcement has lesser area than required to transfer the tensile force in reinforcement to the structure.

However a further increase in concrete cover has a marginal negative impact on the additional live load carrying capacity due to reduction in effective depth. An effective cover of 50 mm is sufficient for this configuration of waffle slab. This study shows the importance of concrete cover for waffle slab and strut-and-tie method can find the optimum cover.

Table 7.4 shows the stress ratios of various elements of the strut-and-tie model. For effective concrete cover greater than or equal to 50mm, the bottom chord element, which is the reinforcement, is the critical element that fails first, under overloading of the slabs. This means mode of failure is flexural failure and is due to yielding of reinforcement. A reduction in concrete cover will make bottom nodal zone fail which results in a slip bond failure.

Minimum clear concrete cover specified by ACI for slabs and joists not exposed to weather or not in contact with ground is only 0.75 inch (19mm) for bar diameter #11 (36mm) or less and 1.5 inch (38mm) for bar diameter #14 (43mm) and #18(57mm). ACI specifies more cover only for structures exposed to weather or in contact with ground.

However strut-and-tie method proposes more concrete cover for all cases and concrete cover is not just for the protection of steel reinforcement. It considers the load transfer from reinforcement to the concrete. Basically strut-and-tie method defines a load path and checks all elements and joints for the safe flow of stresses. It considers even the detailing aspect of the waffle slab from the model itself.

Slab No	Effective cover mm	Self weight kN/m^2	Angle of Strut	Live Load kN/m^2
1	60	7.419	31.72	12.40
2	50	7.419	32.21	12.60
3	40	7.419	32.70	9.80
4	30	7.419	33.19	6.00

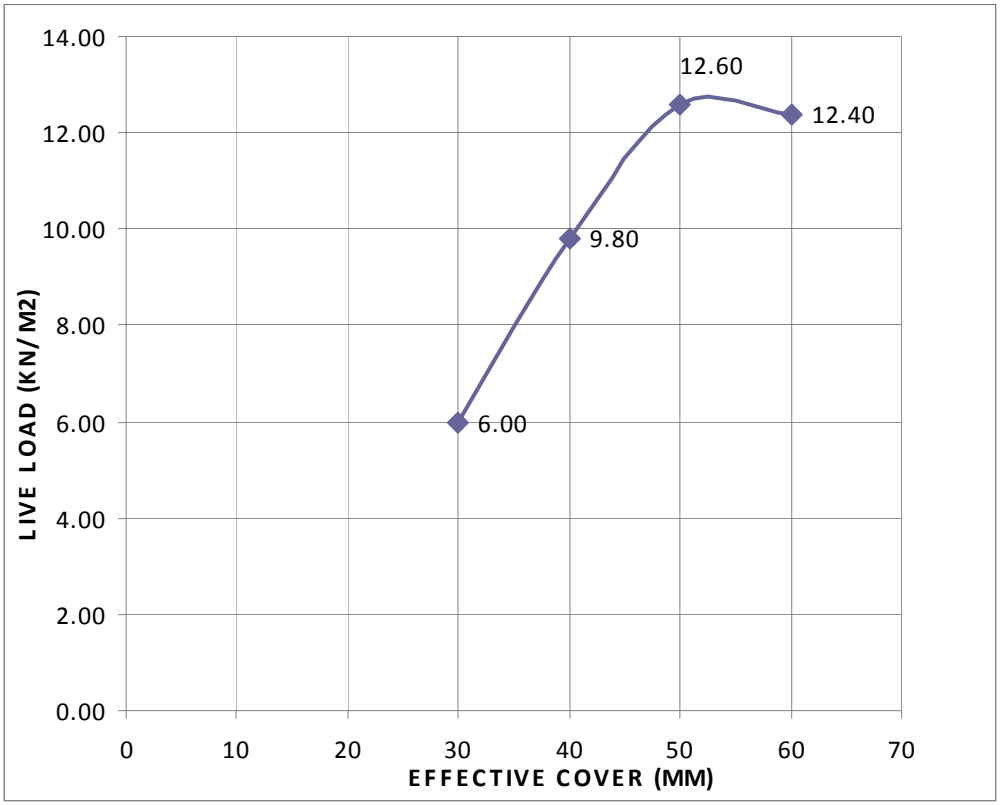

Figure 7.4: Effect of Concrete Cover on the Load Carrying Capacity

TABLE 7.4: Effective Cover - Stress Ratios of Various Elements of the Model

Slab No	Bottom Chord		Top Chord		Diagonal Member			Vertical Member	
	Element	Node	Element	Node	Element	Node Top	Node Bottom	Element	Node
1	**0.999**	0.790	0.508	0.635	0.604	0.566	0.755	0.865	0.177
2	**0.992**	0.947	0.504	0.630	0.602	0.564	0.752	0.871	0.178
3	0.824	**0.990**	0.418	0.523	0.502	0.470	0.627	0.734	0.150
4	0.609	**0.983**	0.309	0.386	0.373	0.349	0.466	0.550	0.113

CHAPTER 8

SUMMARY, CONCLUSIONS AND RECOMMENDATIONS

8.1 SUMMARY

Strut-and-tie method for simply supported waffle slabs is developed and proposed for design of waffle slab. A user friendly design tool STWAF is developed for automatic generation of the Strut-and-tie model. The method provides great flexibility to the designer in terms rib spacing and rib dimensions.

Mode of failure can be predicted by the STM model. The type of member which is critical will predict the mode of failure. If the bottom reinforcement is critical, the mode of failure is flexural failure. If the diagonal strut near the support fails first, it is a flexural shear failure. The failure of diagonal struts, near the concentrated load results in a sudden punching shear failure. The bottom nodal zone failure causes slip-bond failure.

Based on the proposed STM model, out of the 6 experimental specimens (S1 to S6) used in this study, 3 slabs (S1, S2 and S5) failed under pure flexure, one slab (S4) failed under punching shear under the concentrated load. Slabs S3 and S6 failed mainly due to flexure, but with punching shear cracks under the load.

8.2 CONCLUSIONS

Based on the study, the following conclusions can be drawn:

- Strut-and-tie method is an excellent method for design of waffle slabs and handles major modes of failure like shear critical, bending critical and even consider local failure due to large concentrated loads.
- A linear Strut-and-tie model as per ACI Strut-and-tie provisions is sufficient for design of waffle slabs. However it cannot predict the ultimate load carrying capacity of the slab since analysis is limited till the reinforcement in center rib reaches a stress level of 0.75 times the yield stress. It gives an indication of the mode of failure.
- A non linear Strut-and-tie model can very well predict the ultimate strength and mode of failure of waffle slabs. The redistribution of forces after yielding of reinforcement is well described in ANSYS nonlinear model and hence the results are very close to experimental results and are conservative.
- Based on the study an over strength factor of 1.25 is found appropriate for the design of bottom reinforcement considering the capacity of the slab to redistribute the forces between interconnected ribs.
- Based on the experimental data, the efficiency factor of 0.6 used for diagonal struts without stirrup reinforcement and for nodal zones at bottom, as per ACI provisions is found to be conservative. A factor of 0.7 is found more appropriate to predict mode of failure.

- Since STM is a method which consider an internal mechanism to take loads at the ultimate stage and ignores the contribution of cracked concrete on the stiffness of the waffle slab, STM cannot predict deflections accurately. Code based design provisions for STM only address ultimate limit state requirements. Hence Orthotropic plate theory is used for calculating deflections of simply supported waffle slabs in STWAF.
- Based on the parametric study, it is clear that ACI recommendation on the size and spacing of ribs is done in such a way that the slab fails under flexure in case of overloading for normal range of spans from 6 to 12m. However the concrete cover and thickness of ribs may not be sufficient for larger spans.

8.3 RECOMMENDATIONS FOR FUTURE STUDY

Based on the study, the following recommendations are made for future study:

- Strut-and-tie model is developed for simply supported waffle slabs with corner lifting allowed. Future study is recommended for slabs without corner lifting and can be extended to multi-span cases as well. Since strut-and-tie method can handle shear critical structure, the punching shear at column locations can be effectively handled by this method. However since the top chord near columns will be subjected to tensile stresses, fixing the type of element needs multiple iterations.
- Currently all ribs are considered with equal sizes in both directions. Future study is recommended to include wider beams along column lines and at periphery.
- Experimental study need to be conducted on a large scale to evaluate the efficiency factors for struts and nodal zones which play an important role in evaluating the allowable strength.
- Study on STM for waffle slabs need to be conducted to predict deflections under service loads considering nonlinear material model and the effect of cracked concrete on the stiffness of the model.

REFERENCES

1. Building Code Requirements for Structural Concrete-ACI 318 -08 and Commentary, American concrete institute, Farmington Hills, Michigan, 2008.

2. Schlaich, J., Schafer, K. and Jennewein, M., "Toward a Consistent Design of Structural Concrete," Prestressed Concrete Institute Journal, Vol. 32, No. 3, May 1987, pp. 74-150.

3. Timoshenko, S., and Woinowsky-Krieger, S. (1959). Theory of plates and shells, 2nd Ed., McGraw-Hill, New York, 364–377.

4. Bares, R., and Massonnet, C. (1966). Analysis of beam grids and ortho-tropic plates. Lockwood, London, 241–256.

5. Tebbett, I. E., and Harrop, J. (1979). ''Analytical design of ribbed flat slabs.'' The Struct. Engr., London, 57(7), 223–230.

6. Cusens, A. R., and Pama, R. P. (1975). Bridge deck analysis, 1st Ed., Wiley, England, 29–111.

7. Kennedy, J. B., and Iyengar, K. J. (1982). ''Rigidities of non-orthogonally shaped waffle slabs.'' J. Struct. Div., ASCE, 108(10), 2263–2278

8. Magura, D. D., and Corley, W. G. ''Tests to destruction of multi-panel waffle slab structure—1964–1965 New York World's Fair.'' ACI Journal, 68(9), 699–703, September 1, 1971.

9. Donald D. Magura and W. Gene Corlet, " Test to destruction of a Multi panel waffle slab structure – 1964-1965 New York's World Fair '', ACI Journal Proceedings , 68(9). Sept. 1971.

10. Ji, X., Chen, S., Huang, T., and Lu, L. (1986). ''Deflection of waffle slabs under gravity and in-plane loads.'' American Concrete Institute, Detroit, 283–294.
11. Ajdukiewicz, A. B., and Kliszczewicz, A. T. (1986). ''Experimental analysis of limit states in a six panel waffle flat-plate structure.'' ACI Journal, 83(6), 909–915.

12. Mario E. Rodriguez, Jacketing and Sergio A. Santiago, "Simulated Seismic Load Tests on Two –Story Waffle Flat Plate structure Rehabilitated." ACI Structural Journal, 95(2).

13. Hashim M.S. Abdul-Wahab and Mohammad H. Khalil, "Rigidity and strength of orthotropic reinforced concrete waffle slabs", Journal of Structural Engineering, February- 2000, Pages 219-227.

14. J. Prasad, S. Chander and A.K. Ahuja , Department of Civil Engineering, I.I.T.R., Roorkee, India. "Optimum Dimensions of Waffle slab for Medium Size Floors", Asian Journal of Civil Engineering (Building and Housing) Vol.6, No.3 (2005), Pages 183-197.

15. P. F. Schwetz, F. P. S. L. Gastal and L. C. P. Silva on "Numerical and experimental study of real scale waffle slab" , IBRACON Structures and Materials Journal,Volume 2, Number 4 (December, 2009) p. 380 – 403.

16. Anis Mohamad Ali, B.J. Farid and A.I.M. Al-Janabi, " Stress-Strain Relationship for Concrete in Compression Made of Local Materials", Civil Engineering Department, University of Basrah, Iraq, Eng. Sci. Vol.2. pp 183-194, 1990.

17. Ken Watanabe, Junichiro Niwa, Hiroshi Yokota and Mitsuyasu Iwanami. "An experimental study on stress-strain curve of concrete considering localized failure in compression", Journal of Advanced Concrete Technology Vol.2, No.3,395-407, October 2004.

18. Jung-woong Park and Daniel Kuchma., "Strut-and-tie Model Analysis for Strength Prediction of Deep beams", ACI Structural Journal, Vol. 104, No.6, 2007. pp. 657-666.

19. A. Arabzadeh, A.R. Rahaie and R.Aghayari, "A Simple Strut-and-tie Model for prediction of Ultimate Shear Strength of RC Deep beams", International Journal of Civil Engineering. Vol.7, No.3, September 2009.

20. ASTM A615, "Standard Specification for Deformed and Plain Billet Steel bars for concrete reinforcement" American Society for Testing and Materials.

21. Javier Malvar and John E. Crawford, " Dynamic Increase Factors for Steel reinforcing Bars", Twenty-Eighth DDESB Seminar, Orlando, FL, August 1998.

22. Mirza S.A., MacGregor J.G., "Variability of Mechanical properties of Reinforcing Bars", Journal of Structural Division, Vol. 105, No.ST5, May 1979. pp. 921-937.

23. Cowell W.L., "Dynamic Tests on High Strength Steels", Technical report N-427, Naval Civil Engineering laboratory, Port Hueneme, CA, February 1962, 17 pp.

24. MacGregor, J.G., "Reinforced Concrete-Mechanics and Design," 3rd edition, Prentice Hal, 1997.

25. Ritter, W. "The Hennebique Design Method (Die Bauweise Hennebique)," 1899.

26. Marti, P., "Truss Model in Detailing," Concrete International, December, 1985, pp 66-73.

27. Vecchio, F.J. and Collins, M.P., "Compression Response of Cracked Reinforced Concrete," Journal of Structural Engineering, Dec., 1986, pp. 3590-3611.

28. Collins, M.P. , Mitchell, D., Adebat, p. and Vecchio, F.J. "A General Shear Design Method," ACI Structural Journal , January-Febraury, 1996,pp36-45.

29. AASHTO, "LRFD Bridge Design Specifications," 2nd ed., American Association of State Highway and Transportation Officials, Washington, D.C., 2005.

30. Nielson, M.P., Limit Analysis and Concrete Plasticity, 2nd Edition, CRC Press, 1998.

31. Schlaich, J. and Anagnostou, G., "Stress Fields for Nodes of Strut-and-Tie Models," Journal of Structural Engineering, ASCE, Vol.116, No.1, January, 1990, pp. 13-23.

32. Schlaich, J. and Weischede, D., "Detailing Reinforced Concrete Structures," Canadian Structural Concrete Conference, Department of Civil Engineering, University of Toronto, Toronto, 1981, pp. 171-198.

33. Hwang, S.J., Fang, W.H., Lee, H.J., and Yu, H.W., "Analytical Model for Predicting Shear Strength of Squat Walls," Journal of Structural Engineering, Vol. 127, No. 1, 2001, pp. 43-50.

34. Tan, K.H., Tong, K., and Tang, C.Y., "Direct Strut-and-tie Model for Prestressed Deep Beams," Journal of Structural Engineering, Vol. 127, No. 9, 2001, pp. 1076-1084.

35. Tan, K.H., Tang, C.Y., and Tong, K., "A Direct Method for Deep Beams with Web Reinforcement," Magazine of Concrete Research, Vol. 55, No. 1, 2003, pp. 53-63.

36. Nielson, M.P., Braestrup, M.W., and Bach, F., "Rational Analysis of Shear in Reinforced Concrete Beams," LABSE Periodic, Proceedings, P-15/78, No. 2, May 1978, p. 18.

37. Bakir, P.G. and Boduroglu, H.M., "Mechanical Behavior and Non-linear Analysis of Short Beams Using Softened Truss and Direct Strut and Tie Models," Engineering Structure Journal, Vol. 27, 2005, pp. 639-651.

38. Young, M.Y., "Computer Graphics for Nonlinear Strut-Tie Model Approach," Computing in Civil Engineering Journal, Vol. 14, No. 2, April 2000, pp. 127-133.

39. Tjhin, T.S. and Kuchma, D.A. "Computer-Based Tools for Design by Strut-Tie Method: Advances and Challenges," ACI Structural Journal, September-October, 2002, pp. 586-594.

40. Hyo-Gyoung, K. and Sang-Hoon, N., "Determination of Strut-and-tie Models Using Evolutionary Structural Optimization", Engineering Structures Journal, Vol. 28, 2006, pp. 1440-1449.

41. Alshegeir, A., Ramirez, J., "Computer Graphics in Detailing Strut-Tie Models," Computing in Civil Engineering Journal, Vol. 6, No. 1, April 1992, pp. 220-231.

42. Liang, J.L., Chang, W.H., Chuin, S.C., and Ying, P.L., "Strut-and-tie Design Methodology for Three-Dimensional Reinforced Concrete Structures," Structural Engineering Journal, Vol. 132, No. 6, 2006, pp. 929-938.

43. Chun, S.C., "Three-Dimensional Strut-and-tie Analysis for Footing Rehabilitation," Structural Engineering Journal, Vol. 7, No. 2, Feb. 2002, pp. 14-25.

44. Richard, W., "Strut-and-tie Model for Punching Shear of Concrete Slabs," M.S. Thesis, Civil Engineering Dept., University of Newfoundland, Aug. 1995.

45. Richard W.Tiller. "Strut-and-tie model for punching shear of concrete slabs", thesis report submitted to Memorial University of Newfoundland, August 1995.

46. Tjen N. Tjhin , "Analysis and Design Tools for Structural Concrete Using Strut-and-tie Models". Dissertation submitted to University of Illinois, 2004.

47. Tjen N. Tjhin, Daniel A. Kuchma, " Integrated Analysis and Design Tool for the Strut-and-tie Method", Engineering Structures 29 (2007), 3042-3052.

48. ANSYS version-11, *ANSYS Inc*., Global Headquarters, South Pointe, 275 Technology Drive, Canonsburg, PA

VITA

NAME : **Sunil Kumar G Pillai**
ADDRESS : Shaleena, Kaduvinal P.O.,
Vallikunnam, Alappuzha Dist,
Kerala, India
E-MAIL : sunilkumargpillai@rediffmail.com /
sunilpillai@zamilsteel.com

EDUCATIONAL QUALIFICATIONS

M.S Civil Engineering – Structures (April 2011)

King Fahd University of Petroleum and Minerals
Dhahran, Saudi Arabia

B.Tech. -Civil Engineering (October 1995)

T.K.M. College of Engineering
Kerala University,
Kollam, Kerala, India

OTHER ACHIEVEMENTS

- Attended courses in C- programming and Visual Basic (VB.net)
- Published paper in SEMC – South Africa on "Design of Waffle slabs using Strut-and-tie Method".

WORK EXPERIENCE

Currently working as Lead Structural engineer for one of the engineering groups, Engineering department, Pre-Engineered Building Division (PEB), Zamil Steel, Dammam, KSA since August 2009.

The past experience includes:

- Engineering Supervisor, in Engineering Department, United Steel Buildings, Al-Shuwayer group, Cochin, India, from August 2008 to June 2009.
- Senior Design Engineer and Design Checker in Engineering Department, Pre-Engineered Building Division (PEB), Zamil Steel, Dammam, KSA from September 1999 to August 2008.

- Assistant Engineer in Civil / Structural Engineering Department, Kvaerner Process India Limited, Bangalore, India from April 1997 to September 1999.
- Design Engineer (Structural), Silpi Design and Engineering Pvt. Ltd., Bangalore, India from December 1995 to April 1997.

Work includes analysis, design and checking of various onshore and offshore steel structures. The experience includes design and checking of Pre-Engineered buildings as per international design codes such as AISC, BS, Euro code etc. and Loading codes like ASCE, MBMA, UBC, IBC, BS 6399, IS codes etc. Conversant with structural analysis programs like STAAD III, SAP, ANSIS and X-STEEL. The experience includes design of concrete buildings as well. Familiar with American, European and Indian design requirements and codes of practices.

The work also includes recruitment and training of design engineers, developing engineering standards, manuals and Design Tables. As part of the work, developed a number of engineering tools using Microsoft excel and Visual Basic.net.

Major Projects Involved

As part of the work in Zamil Steel, designed more than 200 steel buildings, for various countries and checked the design for more than 100 buildings. A few are mentioned below:

- Yarmouq Mall (Riyadh , KSA)
- Dywidag Saudi Arabia Co. Ltd. (Jubail , KSA , Client – Unicoil)
- Villagio (Doha , Qatar)
- Al-Hokhair (Riyadh , KSA)

The major projects handled before joining Zamil includes:

- BHN Revamp project , Bombay High, India , Client – ONGC
- DHDS project, Vizag Refinery, Client – HPCL, Contractor : Larsen and Toubro Limited, Harp, Baroda, India
- Bayer Chlor-Alkali Project, Client - Kvaerner John Brown, Houston, Texas, USA
- ARCO EB-1 New Front Project, Client – ARCO Chemical Company, Channelview, Texas, USA
- Indo-gulf Copper Project, Client : MECON, Bangalore, India